UNIVERSITÉ DU QUÉBEC À MONTRÉAL

ORIGINE ET QUANTIFICATION DE L'HÉTÉROGÉNÉITÉ DU SIGNAL ISOTOPIQUE DES PRÉCIPITATIONS EN MILIEU URBAIN

THÈSE

PRÉSENTÉE

COMME EXIGENCE PARTIELLE

DOCTORAT EN SCIENCES DE LA TERRE ET DE L'ATMOSPHÈRE

PAR

CÉCILE CARTON

AVRIL 2026

UNIVERSITÉ DU QUÉBEC À MONTRÉAL
Service des bibliothèques

Avertissement

La diffusion de cette thèse se fait dans le respect des droits de son auteur, qui a signé le formulaire *Autorisation de reproduire et de diffuser un travail de recherche de cycles supérieurs* (SDU-522 – Rév.12-2023). Cette autorisation stipule que «conformément à l'article 11 du Règlement no 8 des études de cycles supérieurs, [l'auteur] concède à l'Université du Québec à Montréal une licence non exclusive d'utilisation et de publication de la totalité ou d'une partie importante de [son] travail de recherche pour des fins pédagogiques et non commerciales. Plus précisément, [l'auteur] autorise l'Université du Québec à Montréal à reproduire, diffuser, prêter, distribuer ou vendre des copies de [son] travail de recherche à des fins non commerciales sur quelque support que ce soit, y compris l'Internet. Cette licence et cette autorisation n'entraînent pas une renonciation de [la] part [de l'auteur] à [ses] droits moraux ni à [ses] droits de propriété intellectuelle. Sauf entente contraire, [l'auteur] conserve la liberté de diffuser et de commercialiser ou non ce travail dont [il] possède un exemplaire.»

REMERCIEMENTS

Un doctorat est une sacrée aventure, et pour la réussir, il vaut mieux être bien accompagné !

Mes premiers remerciements vont naturellement à mes co-encadrant·e·s, Florent Barbecot, Jean-François Hélie et Jean Birks, pour leur encadrement humain et leurs si précieux conseils tout au long de ce projet. Merci en particulier à Florent de m'avoir offert cette si belle opportunité, et à Jean-François pour son soutien constant. Je remercie également les membres du jury, Philippe Lucas-Picher et Nils Michelsen, pour leurs questions et commentaires pertinents, qui m'ont ouvert de nouvelles pistes de réflexion autour de ce travail.

Merci à toutes les citoyennes et tous les citoyens du Grand Montréal qui ont volontairement participé au réseau d'échantillonnage Collect'O UQAM, et sans qui cette aventure aurait été bien différente. Merci pour votre engagement et votre patience depuis le début de ce projet.

Merci à Viorel Horoi, pour son aide inestimable lors de l'étape de conception des collecteurs, mais aussi à l'équipe HydroSciences UQAM-ÉTS (tout particulièrement aux Zozotopes !), et à mes collègues du Geotop, de l'UQAM, de Polytechnique Montréal, qui ont rendu cette expérience humaine encore plus enrichissante et mémorable.

Merci à toutes celles et tous ceux qui ont facilité ce doctorat d'une manière ou d'une autre : la Faculté des Sciences et le département des sciences de la Terre et de l'atmosphère de l'UQAM ; les différents médias qui ont participé à la diffusion de ce projet ; René Audet pour son œil critique sur l'enquête sociale du chapitre 6 ; le Fonds de recherche du Québec et le centre de recherche Geotop pour avoir financé et soutenu ce projet ; mais aussi le Coeur des Sciences pour m'avoir permis de m'investir plus encore dans des projets de vulgarisation scientifique en parallèle de ma thèse.

Sur un plan plus personnel, je tiens à remercier mon conjoint Marouane, qui m'a permis de braver la tempête finale par son amour et m'a inspirée par sa propre persévérance. Merci à lui et à ma belle-fille Camélia pour toute la joie qu'ils m'apportent au quotidien. Merci aussi à ma chère petite famille, mon Papa, ma sœur Anaëlle, et Mamilou, qui m'ont toujours soutenue, jusque dans les moments de doute les plus forts. Je vous aime.

Merci aussi à toutes celles et tous ceux qui ne sont plus physiquement présent·e·s dans ce monde mais qui continuent à vivre à travers moi. En tout premier lieu à ma petite lumière, ma merveilleuse Maman, et mes grands-parents Mati et Titi. Mulțumesc pentru tot, vă iubesc din toată inima mea.

Merci à ma famille choisie, les Nanas, avec qui j'ai grandi et qui continuent de me supporter depuis maintenant deux décennies. Merci pour votre amitié inconditionnelle et cette tendresse radicale qui m'ont tellement apporté dans la vie.

Je ne peux raisonnablement pas nommer tout le monde, je finirai donc par remercier infiniment toutes les autres personnes de mon entourage, ma famille et mes ami·e·s, au Québec comme outre-Atlantique, de Montréal, Brest, Crégy-lès-Meaux, Dieppe, Salé, El Jadida, et j'en passe ! Je ne vous oublie pas.

Merci à toutes celles et tous ceux qui font partie de mon histoire. Je suis infiniment reconnaissante de tout ce qui m'a été offert dans la vie, et en particulier d'avoir eu la grande chance de vous y compter. Je vous dédie cet accomplissement.

TABLE DES MATIÈRES

LISTE DES FIGURES

LISTE DES TABLEAUX

RÉSUMÉ

La croissance démographique mondiale entraîne l'accroissement et la densification des zones urbaines. Le climat et en particulier la dynamique des précipitations en ville en sont modifiés. Cela a des conséquences directes sur la qualité de vie des citoyen·ne·s, car les précipitations permettent de réduire la pollution atmosphérique et de limiter l'amplitude des vagues de chaleur en ville. Cependant, la haute hétérogénéité spatiale et temporelle d'un tel environnement a rendu difficile l'identification et la généralisation des processus impliqués dans les modifications des précipitations urbaines par la seule utilisation des outils météorologiques traditionnels. En parallèle, les isotopes stables de la molécule d'eau ont prouvé être des traceurs exceptionnels de la dynamique des précipitations à grande échelle régionale, mais leur utilisation a encore été très peu considérée pour l'étude des précipitations urbaines. Cette thèse cherche à évaluer comment l'analyse isotopique des précipitations urbaines à haute résolution spatiale et temporelle peut aider à améliorer la compréhension des processus à l'origine de la modification des précipitations en milieu urbain.

Atteindre une haute résolution d'échantillonnage pour étude isotopique a nécessité le développement d'une méthodologie adaptée, partagée avec la communauté scientifique afin de rendre ce type d'analyse reproductible pour d'autres contextes. En particulier, des collecteurs événementiels et intra-événementiels de pluie et de neige à moindre coût ont été développés afin de conserver les signatures isotopiques des précipitations après échantillonnage, tout en maintenant un budget réduit afin d'augmenter le nombre de stations. Le premier réseau participatif d'échantillonnage pour étude isotopique des précipitations urbaines a ensuite été développé à l'échelle du Grand Montréal. Ce site d'étude a été choisi car le climat de Montréal s'est révélé être particulièrement affecté par l'environnement urbain. En effet, entre 2013 et 2017, un phénomène d'îlot de chaleur urbain (ICU) de plus en plus marqué y a été observé, avec des températures minimales quotidiennes en moyenne 2°C plus élevées dans la ville que dans ses environs. De plus, les précipitations sont devenues plus rares en ville par rapport à la région (- 4 % en moyenne).

Entre septembre 2021 et octobre 2022, une cinquantaine de participant·e·s a ainsi collecté simultanément 20 épisodes de pluie et de neige depuis leur domicile. Les résultats ont montré une importante variabilité isotopique (jusqu'à 8‰ en $\delta^{18}O$) entre toutes les stations pour chaque événement échantillonné, qui n'avait jamais été considérée à une telle échelle. Contre-intuitivement, l'évaporation des précipitations lors de leur chute vers le sol ne semblait pas être la principale cause de cette importante variabilité. Cependant, l'étude statistique de ces événements et l'échantillonnage de deux événements subséquents ont permis de déterminer que la variabilité observée sur chaque événement est directement corrélée avec le temps écoulé depuis les plus récentes précipitations. Le recyclage des précipitations, favorisé par l'îlot de chaleur urbain,

semble ainsi à l'origine de la variabilité isotopique observée, et le temps de résidence des précipitations en ville a pu être estimé à 2 jours. De plus, les signatures isotopiques ont permis de calculer que l'eau de combustion issue des transports et du chauffage des bâtiments représente jusqu'à 5 % de l'eau retrouvée dans les précipitations. Ces résultats montrent la valeur ajoutée de l'étude isotopique des précipitations à haute résolution spatiale et temporelle pour l'identification de processus subtils à l'origine de la modification des précipitations urbaines.

En parallèle de ces avancées scientifiques, les dimensions sociales de cette thèse n'avaient pas été anticipées lors de sa conception. Ce projet multidisciplinaire a représenté une opportunité unique d'impliquer et sensibiliser la communauté montréalaise à la compréhension des changements climatiques liés aux précipitations urbaines. Notamment, les résultats montrent clairement que les précipitations permettent de réduire les concentrations de particules fines atmosphériques et de limiter l'amplitude des vagues de chaleur par ré-évaporation jusqu'à plusieurs jours suivant un événement. Ce travail met ainsi en évidence la nécessité d'adapter les villes aux modifications actuelles et futures des précipitations afin de protéger les citoyen·ne·s les plus vulnérables, notamment en accordant une attention particulière aux techniques de stockage permettant de conserver l'eau de pluie en ville (telles que la végétalisation), afin de maintenir l'effet de climatisation naturelle de la ville durant les journées les plus sèches. Ce message a été largement diffusé auprès des participant·e·s du réseau, et la portée de sensibilisation de la population montréalaise par ce biais a été investiguée grâce à la contribution des participant·e·s, dans l'espoir d'aider de futurs projets similaires dans cet effort. À l'heure où les réseaux participatifs suscitent une attention grandissante en hydrologie, une telle démarche de sensibilisation apparaît comme un tremplin fort pour favoriser l'action collective.

Mots-clés : précipitations, isotopes, ville, climat urbain, réseau participatif

ABSTRACT

Global population growth is leading to the expansion and densification of urban areas. These changes are altering the climate and, in particular, precipitation patterns in cities. Citizens' quality of life is directly impacted, as precipitation helps to reduce air pollution and limits the severity of heat waves in cities. However, the high spatial and temporal heterogeneity of such an environment has made it difficult to identify and generalize the processes involved in urban precipitation changes using traditional meteorological tools alone. At the same time, stable isotopes of water molecules have proven to be exceptional tracers of large-scale regional precipitation dynamics, but their use has been largely overlooked in the study of urban precipitation. This thesis seeks to evaluate how high-resolution spatial and temporal isotopic analysis of urban precipitation can help to improve our understanding of the processes impacting precipitation in urban areas.

Achieving high sampling resolution for isotopic analysis required the development of a suitable methodology, which was shared with the scientific community to make this type of analysis reproducible in other contexts. In particular, low-cost event and intra-event rain and snow collectors were developed to preserve the isotopic signatures of precipitation after sampling, while keeping costs low and increasing the number of stations. The first participatory sampling network for isotopic studies of urban precipitation was then developed across the Greater Montreal. This study site was chosen because Montreal's climate was found to be particularly affected by the urban environment. Indeed, between 2013 and 2017, an increasingly pronounced urban heat island (UHI) phenomenon was observed, with average daily minimum temperatures 2°C higher in the city than in its surroundings. In addition, precipitation became scarcer in the city compared to the surrounding region (- 4 % on average).

Thus, between September 2021 and October 2022, around 50 participants simultaneously collected 20 episodes of rain and snow from their homes. The results showed significant isotopic variability (up to 8‰ in $\delta^{18}O$) between all stations for each sampled event, which had never been considered on such a scale before. Counter-intuitively, sub-cloud evaporation linked to the UHI did not seem to be the main cause for this important variability. However, statistical analysis of these events and sampling of two subsequent events determined that the variability observed in each event is directly correlated with the time spanned since the previous precipitation. Precipitation recycling, promoted by the UHI effect, thus appears to be the cause of the observed isotopic variability, and the residence time of precipitation was estimated at 2 days. In addition, isotopic signatures were used to find that combustion water from transportation and residential heating accounts for up to 5 % of the water in precipitation. These results demonstrate the added value of

high spatial and temporal resolution isotopic precipitation studies in identifying the subtle processes that cause changes in urban precipitation.

Alongside these scientific advances, the social dimensions of this thesis were not anticipated when it was first conceived. Indeed, this multidisciplinary project represented a unique opportunity to involve and raise awareness among the Montreal community about climate change related to urban precipitation. In particular, the results clearly show that precipitation reduces concentrations of fine atmospheric particles and limits the amplitude of heat waves by reevaporation for up to several days following an event. This work highlights the need to adapt cities to current and future changes in precipitation to protect the most vulnerable citizens, in particular by paying special attention to storage techniques that enable the conservation of rainwater in cities (such as greening), to maintain the city's natural cooling effect during the driest days. This message was widely disseminated among network participants, and its extent in raising awareness among the Montreal population was investigated with the help of participants, in the hope of assisting future similar projects in this effort. At a time when participatory networks are attracting growing attention in hydrology, such an awareness-raising approach can be a powerful tool to promote collective action.

Keywords: precipitation, isotopes, city, urban climate, participative network

INTRODUCTION GÉNÉRALE

Bien qu'ayant été tardivement abordé, le changement climatique mondial est aujourd'hui largement étudié et documenté, et constitue un excellent exemple de l'impact involontaire des activités humaines sur l'environnement. Les villes, qui concentrent à elles seules plus de la moitié de la population humaine (United Nations, Department of Economic and Social Affairs, Population Division, 2019), contribuent aux changements du climat et de la composition de l'atmosphère à différentes échelles temporelles et spatiales. À une échelle plus locale, les activités urbaines impactent également les climats propres aux villes, et notamment les précipitations. Bien que ce phénomène soit largement moins discuté, il revêt toute son importance dans le contexte d'urbanisation croissante que nous vivons actuellement, alors que 2 habitants sur 3 résideront en ville d'ici 2050 (United Nations, Department of Economic and Social Affairs, Population Division, 2019), et que nous n'avons pas d'autre choix que d'étendre et densifier nos villes pour contenir ces populations grandissantes.

C'est en 1818 que Luke Howard documente pour la première fois à Londres l'existence de températures plus élevées à l'intérieur des villes qu'à leurs alentours, un phénomène qu'on appelle maintenant îlot de chaleur urbain (ICU). Ce phénomène est depuis ce jour resté l'objet le plus étudié dans la recherche sur les climats urbains. C'est en effet un sujet de grande envergure pour les villes, en premier lieu pour des questions de rendement énergétique, mais également pour la santé des citadin·e·s les plus vulnérables, notamment durant les vagues de chaleur. En effet, les îlots de chaleur urbains accentuent le stress thermique perçu en ville lors des vagues de chaleur extrêmes de plus en plus fréquentes provoquées par le réchauffement climatique (Roberge et Sushama, 2018).

En parallèle des températures, c'est en 1892 que Hellmann rapporte pour la première fois la modification des précipitations dans la ville de Berlin (Oke *et al.*, 2017). Depuis ce jour, les études se sont multipliées afin de démontrer l'impact de nombreuses villes du monde sur les précipitations locales en termes de quantités et de fréquence. En particulier depuis les années 1960, de nouveaux instruments et de nouvelles techniques ont été mis au point pour mesurer les précipitations et les processus hydrologiques à haute résolution (Oke *et al.*, 2017). Ce type d'études a beaucoup apporté à la climatologie urbaine telle que nous la connaissons aujourd'hui. Les études ont démontré que la modification locale des nuages et des précipitations peut être due à une grande variété d'interactions physiques, liées notamment aux influences de l'ICU, de la rugosité de la surface et des émissions anthropiques telles que chaleur, vapeur d'eau et aérosols.

Cependant, les recherches menées jusqu'à présent ont montré qu'il est très difficile d'acquérir des mesures suffisamment représentatives de la façon dont les précipitations sont modifiées dans les zones urbaines. L'origine, la localisation et l'intensité de l'impact des villes sur les précipitations urbaines varient selon les études et sont restées extrêmement difficiles à généraliser (Liu et Niyogi, 2019). En cause, l'hétérogénéité à la fois temporelle et spatiale des villes. En effet, la grande variabilité de la distribution des précipitations dans la couche superficielle de l'atmosphère, causée par la forte turbulence locale et la distorsion de l'écoulement de l'air, est la principale raison pour laquelle notre connaissance des climats urbains est encore limitée (Maier *et al.*, 2020). Dans les zones densément urbanisées, il est difficile de trouver des emplacements représentatifs pour installer des pluviomètres sans l'influence de bâtiments ou d'autres obstacles. Les réseaux de stations météorologiques ne répondent généralement pas à des normes de mesure suffisamment représentatives des zones urbaines, et il est donc difficile de caractériser les différents processus en jeu (Maier *et al.*, 2020). Les données radars, si elles sont disponibles, peuvent permettre de mieux estimer la variabilité spatiale et temporelle des précipitations (Berenguer *et al.*, 2005). Mais si le radar se trouve trop loin de la ville, le signal risque d'être atténué. Même s'il se trouve au cœur de la ville, les échos réfléchis par les surfaces urbaines entraînent des erreurs dans l'interprétation des données mesurées. Les radars situés au-dessus de la canopée urbaine ne fournissent de toute façon pas d'informations sur les précipitations au sol, ce qui complique encore l'analyse des effets des surfaces urbaines sur les précipitations.

L'étude directe des quantités de précipitations ne s'est donc pas révélée une manière idéale de comprendre comment les précipitations sont modifiées en milieu urbain. Alors que notre siècle est marqué par des taux d'urbanisation encore inégalés dans l'histoire, nous peinons encore à comprendre l'impact que nous avons sur notre environnement local, et les effets sur notre santé. Tout comme les îlots de chaleur urbains, la modification des précipitations urbaines a également une grande influence sur la qualité de vie des citadins. Les précipitations permettent non seulement de lessiver l'atmosphère des polluants particulièrement présents dans l'environnement urbain, mais jouent également un rôle dans la climatisation naturelle de la ville. Pendant les vagues de chaleur, les effets de refroidissement par évaporation peuvent réduire la température jusqu'à plusieurs jours après un événement pluvieux (Starke *et al.*, 2010).

En outre, dans ces zones où les matériaux imperméables remplacent les surfaces absorbantes, la fréquence et la quantité des précipitations sont immédiatement liées à l'occurrence des inondations, particulièrement dans un contexte de changement climatique où les événements météorologiques se font de plus en plus extrêmes et fréquents (Tabari, 2020). Avec un ruissellement plus rapide et une capacité de stockage de l'eau limitée, non seulement la hauteur et le débit des cours d'eau urbains augmentent plus rapidement que ceux

des cours d'eau ruraux, mais le système de collecte des eaux est également rapidement débordé. Cela entraîne une probabilité accrue et des périodes de retour réduites des inondations (Kirchmeier-Young et Zhang, 2020), ainsi qu'un volume total d'eau déversé plus important.

En plus de structures urbaines en constante évolution, l'urbanisation est susceptible d'augmenter les apports de chaleur, de vapeur d'eau et de polluants provenant des transports, et du chauffage et de la climatisation des habitations. Pour augmenter notre résilience à ces aléas, il est impératif et urgent de comprendre comment les précipitations sont modifiées en milieu urbain. En répondant à cette question, nous pourrons ainsi mieux concevoir comment adapter nos villes à ces changements.

Cette thèse de doctorat propose d'investiguer une méthode encore peu explorée pour améliorer la compréhension de l'impact de l'urbanisation sur les précipitations urbaines. Cette méthode repose sur l'utilisation des isotopes stables de la molécule d'eau comme traceurs des processus impactant ces précipitations.

Au cours des deux dernières décennies, les isotopes stables de la molécule d'eau se sont imposés comme des traceurs puissants qui ont transformé notre compréhension du cycle hydrologique à différentes échelles spatiales et temporelles (Leibundgut *et al.*, 2009a). Leur utilisation en tant que traceurs repose sur le comportement différent des isotopes stables légers (^{1}H et ^{16}O) par rapport aux isotopes stables les plus lourds (^{2}H et ^{18}O). Les isotopes légers s'évaporent préférentiellement et restent plus facilement dans la phase vapeur lors de la condensation et la formation des précipitations. L'abondance relative des isotopes stables (rapports $^{2}H/^{1}H$ et $^{18}O/^{16}O$) dans les molécules d'eau agit donc comme un témoin de l'histoire de l'eau et des différents processus physiques et chimiques qu'elle a subis lors de son parcours.

Étant donné que les variations naturelles des rapports isotopiques R (Équation 1) restent très faibles, il est difficile de mesurer les rapports isotopiques absolus sans un degré élevé d'incertitude analytique. Pour y remédier, les rapports isotopiques des échantillons sont normalisés par rapport à des normes internes de laboratoire, retraçables à une échelle de référence internationale connue sous le nom d'échelle VSMOW-SLAP (Camin *et al.*, 2025). Cette normalisation permet de comparer les résultats entre laboratoires.

Équation 1

$$R = \frac{[isotope\ lourd]}{[isotope\ léger]}$$

La notation δ, exprimée en pour mille (‰), exprime ainsi la différence relative entre le rapport isotopique de l'échantillon et celui de la norme internationale Vienna Standard Mean Ocean Water (VSMOW) (Équation 2).

Équation 2

$$\delta = \left(\frac{R_{échantillon}}{R_{VSMOW}} - 1\right)$$

En plus de δ^2H et δ^{18}O, l'excès en deutérium (d-excess), défini comme d = δ^2H – 8 × δ^{18}O (Dansgaard, 1964), permet une bonne représentation des processus impliqués dans la formation des gouttelettes et des divers échanges ayant lieu durant leur chute vers le sol (Merlivat et Jouzel, 1979). L'évaporation de la pluie sous le nuage se traduit par une diminution du d-excess, tandis qu'une augmentation du d-excess représente généralement un apport en vapeur d'eau dans le nuage.

Plusieurs études isotopiques ont déjà pu montrer la modification des précipitations urbaines de différentes villes du monde. À Bologne, en Italie, quatre années d'échantillonnage mensuel des précipitations sur un site urbain ont mis en évidence une évaporation secondaire des précipitations lors de leur chute à travers l'atmosphère. Ce phénomène s'est traduit par une ordonnée à l'origine plus basse et un d-excess plus faible sur le site urbain par rapport au site suburbain (Cortecci *et al.*, 2008).

Des résultats similaires ont été obtenus dans le cadre d'une étude menée à Pékin, en Chine, où la composition isotopique de l'eau de pluie au sol, ainsi que la température et l'humidité, ont été intégrées à un modèle d'évaporation sous-nuageux afin de calculer les valeurs $\Delta\delta^{18}$O et $\Delta\delta^2$H (différences entre les compositions isotopiques au sol et dans les nuages). Cette approche a permis de déterminer que les précipitations s'évaporaient jusqu'à 23 % lors de leur chute vers le sol. Étant donné que les valeurs $\Delta\delta^{18}$O et $\Delta\delta^2$H présentaient une corrélation significative avec les concentrations de particules fines de diamètre inférieur ou égal à 2.5 microns (PM2.5), cette étude suggère que l'activité urbaine, représentée par les concentrations de PM2.5, contribue à l'évaporation sous les nuages dans l'eau de pluie (Zhu *et al.*, 2024).

À l'inverse, dans une étude menée à Chengdu, en Chine, les précipitations mensuelles enregistrées sur un site urbain et dans une zone rurale voisine (située à 148 km) ne présentaient aucune différence significative au niveau des valeurs de δ^{18}O (Zhao *et al.*, 2023). Cependant, la zone rurale affichait un d-excess significativement plus élevé que la zone urbaine, ce qui a été interprété comme un indicateur d'un flux d'évapotranspiration plus important dans la zone rurale.

Dans un exemple tiré de Tokyo, au Japon, la convection ascendante provoquée par l'îlot de chaleur urbain a donné lieu à des épisodes de pluies intenses typiques des environnements urbains (Uchiyama *et al.*, 2017). Cette étude a montré que ces épisodes présentaient des compositions isotopiques nettement plus faibles que d'autres événements pluvieux estivaux de quantités de pluie comparables (Uchiyama *et al.*, 2017). L'hypothèse avancée était que la réévaporation des molécules plus légères induite par l'effet d'îlot de chaleur urbain entraîne une diminution des valeurs de $\delta^{18}O$ et $\delta^{2}H$ dans l'eau des nuages. À l'aide de cartes radar, cette étude a également montré que le $\delta^{18}O$ pouvait constituer un bon indicateur de la distance par rapport à la zone de formation de ce type de précipitations (Uchiyama *et al.*, 2017).

Les signatures isotopiques peuvent également fournir des informations précieuses sur les sources de vapeur d'eau anthropiques et servir à quantifier leur contribution aux précipitations enregistrées dans les zones urbaines. Dans une étude menée à Salt Lake City, la composition isotopique de l'eau de combustion de gaz pour le chauffage et d'essence pour les transports a été estimée théoriquement ; les résultats suggèrent que la vapeur d'eau issue de tels processus de combustion présente un marquage isotopique très distinct, caractérisé par des valeurs de $\delta^{18}O$ extrêmement élevées et de $\delta^{2}H$ extrêmement faibles, ce qui n'est pas possible avec les sources naturelles de vapeur d'eau présentes dans une atmosphère « propre » (Gorski *et al.*, 2015). Lorsque des conditions d'inversion de subsidence se sont produites au-dessus de Salt Lake City, c'est-à-dire lorsque de l'air chaud a agi comme un couvercle sur l'air plus froid près du sol, la composition isotopique de la vapeur d'eau atmosphérique mesurée a été utilisée pour quantifier le mélange entre les sources de vapeur d'eau d'origine naturelle et celles issues de la combustion. Dans de telles conditions, la vapeur d'eau issue de la combustion représentait jusqu'à 13 % de la vapeur d'eau atmosphérique mesurée (Gorski *et al.*, 2015). De même, dans une étude menée dans le nord-ouest de la Chine, la composition isotopique des précipitations a permis de déterminer que la vapeur d'eau issue de la combustion représentait jusqu'à 6 % de l'humidité atmosphérique hivernale et présentait une corrélation positive avec les concentrations de PM2.5 (Xing *et al.*, 2020).

Ces travaux indiquent que l'étude des facteurs contrôlant le comportement de ces traceurs environnementaux présente un grand potentiel pour retracer les processus à l'origine de la modification des précipitations urbaines (Uchiyama *et al.*, 2017), et devrait améliorer notre capacité à comprendre l'ampleur des effets de l'urbanisation sur le cycle de l'eau. Toutefois, l'étude isotopique des précipitations urbaines est un domaine de recherche encore vierge, et le peu d'études menées jusqu'à présent n'analysait pour la plupart que des données ponctuelles ou mensuelles. À notre connaissance, aucune étude ne s'est penchée sur les variations isotopiques des précipitations urbaines à haute résolution spatiale et temporelle, ce qui limite la compréhension des processus urbains à l'origine de la modification des précipitations dans un

environnement aussi hétérogène que la ville, tant dans l'espace que dans le temps. L'identification de variations spatiales et temporelles intra-urbaines du signal isotopique pourrait fournir des éléments clés pour affiner notre compréhension des interactions entre la ville et son climat local.

C'est pourquoi cette thèse de doctorat se propose de répondre à la question de recherche « Quelle est la valeur ajoutée de l'étude isotopique des précipitations à haute résolution spatiale et temporelle pour la détermination de l'impact des villes sur les précipitations urbaines ? ». Pour répondre à cette question, il nous était nécessaire de développer une méthodologie adaptée, du choix du terrain d'étude jusqu'au protocole d'échantillonnage isotopique à haute résolution. Nous partageons dans ce manuscrit l'implémentation d'une telle méthodologie, les leçons scientifiques tirées d'un tel projet, et les perspectives de recherche associées. Ce manuscrit de thèse est divisé en quatre parties qui correspondent chacune à l'un des sous-objectifs visés par ce travail de recherche :

1) Discuter les climats urbains de l'Est canadien

Le but est ici de déterminer si les quatre plus grandes villes de l'Est du Canada (Toronto, Ottawa, Montréal et la ville de Québec) montrent des microclimats affectés par les infrastructures urbaines, et donc de déterminer si l'une de ces villes serait adaptée à l'étude isotopique des processus à l'origine de ces changements. Cette partie est présentée sous la forme d'un article publié en janvier 2024 dans la revue *Urban Climate.*

2) Développer une méthode d'échantillonnage adaptée à l'étude isotopique des précipitations urbaines à haute résolution spatiale et temporelle

Pour répondre au défi posé par l'étude isotopique des précipitations urbaines à haute résolution spatiale et temporelle tout en maintenant un budget et des ressources limités, nous avons développé toute une méthodologie, en commençant par la création de collecteurs à bas coût adaptés à l'échantillonnage événementiel et intra-événementiel de pluie pour étude isotopique. Nous avons également créé Collect'O, le premier réseau participatif dédié à la collecte d'échantillons de précipitations (pluie et neige) pour étude isotopique des précipitations urbaines. Cette dimension méthodologique est le cœur du travail réalisé pour ce projet et s'articule en trois parties, comprenant notamment deux articles parus en février 2024 et mars 2025 dans la revue *Rapid Communications in Mass Spectrometry.*

3) Analyser les informations apportées par la signature isotopique des précipitations urbaines

Dans cette partie, nous analysons les informations apportées par le signal isotopique des précipitations urbaines à haute résolution spatiale et temporelle, et les processus urbains à l'origine de la modification des précipitations ainsi identifiés. Interpréter les résultats d'échantillonnages ponctuels dans un système où le régime des précipitations est hautement variable s'est avéré des plus complexe. Cela nous a conduits à proposer une analyse des capacités du réseau à montrer certains processus qui sont propres aux précipitations urbaines. Nous évaluons et partageons la valeur scientifique ajoutée d'une telle approche, ainsi que les perspectives de recherche associées. Les données sont présentées sous la forme d'un article soumis en août 2025 à la revue *Urban Climate*.

4) Évaluation sociale du réseau Collect'O

En parallèle d'une résolution d'échantillonnage bonifiée, nous nous sommes aperçus au cours du projet que le réseau participatif Collect'O a inclus une dimension sociale non négligeable, dont il nous a paru nécessaire d'investiguer la plus-value. Dans un contexte où les changements climatiques sont intrinsèquement liés à la prise de conscience publique, nous avons cherché à analyser les réussites et limites de ce projet quant à la portée de sensibilisation des participant·e·s et de leur entourage, dans le but d'aider à la mise en place et au rayonnement de réseaux participatifs environnementaux futurs. Le dernier sous-objectif de cette thèse est ainsi dédié au retour d'expérience des participant·e·s du réseau participatif Collect'O.

Note : Les signatures isotopiques des précipitations sont déjà intégrées à certains modèles de circulation générale atmosphérique et modèles climatiques régionaux (Xi, 2014). Cependant, à notre connaissance aucune initiative n'a encore été prise pour modéliser la signature isotopique des précipitations en milieu urbain en intégrant des modules de canopée urbaine comme certains modèles atmosphériques à fine échelle (Nogueira *et al.*, 2022 ; Roberge et Sushama, 2018). Il est important de souligner que bien que ce ne soit pas ici l'objet de ce travail, la recherche en hydrologie urbaine gagnerait à explorer le couplage entre signatures isotopiques et modélisation des précipitations à l'échelle urbaine dans de futurs travaux.

CHAPITRE 1 :
CHOIX DU SITE D'ÉTUDE

1.1 Mise en contexte de l'article A

Comme les différentes études menées jusqu'à présent ne concordent pas pour déterminer quel est l'impact des différents processus urbains sur la modification des précipitations urbaines, nous ne savons pas non plus si toutes les villes sont touchées par ce phénomène.

Dans ce chapitre, nous cherchons à évaluer si les climats urbains des quatre plus grandes villes de l'Est canadien (Montréal, Québec, Ottawa et Toronto) ont été modifiés par l'urbanisation. L'objectif est de déterminer si l'une de ces villes serait un site d'étude approprié pour étudier les processus physiques et chimiques à l'origine de la modification éventuelle de la signature isotopique des précipitations urbaines.

Les stations météorologiques ne sont pas suffisamment bien réparties autour des villes, et n'enregistrent pas continuellement les données, ce qui rend difficile une étude à l'échelle climatologique. Comme alternative, nous avons donc fait le choix d'utiliser des données interpolées. Nous utilisons les grilles climatiques quotidiennes du Programme de surveillance du climat du Québec (Bergeron, 2016), qui fournissent des données journalières de températures minimales et maximales ainsi que de quantités de précipitations. Nous comparons les tendances climatologiques entre les zones urbanisées et les zones moins urbanisées de ces quatre villes sur la période 1988-2017.

Il est à noter que les villes de Toronto et Ottawa sont situées à l'extérieur de la province de Québec, et les stations météorologiques utilisées pour cette base de données sont donc très rares par rapport à Montréal et Québec. Les estimations de Toronto et Ottawa sont donc de moins bonne qualité, car elles sont extrapolées au point de grille, toutefois nous avons fait le choix de conserver ces deux villes à des fins de comparaison dans notre analyse. Cette particularité doit être gardée à l'esprit lors de la lecture de ce chapitre.

Improved understanding of the impact of urbanization on the temperature, precipitation, and air quality of major eastern Canadian cities (Article A)

Published in Urban Climate (January 2024)

Cécile Carton [a], Florent Barbecot [a], Jean Birks [b], Jean-François Hélie [a]

[a] Geotop - Université du Québec à Montréal, Department of Earth and atmospheric sciences, Canada
[b] University of Calgary, Department of Geosciences, Canada

1.2 Abstract

Purpose: This study aims at identifying the impact of urbanization on urban climates of Eastern Canada.

Methods: Gridded climate data were used over the 1988–2017 period to investigate inter and intra-annual trends of daily minimum and maximum temperatures and precipitation, within and outside the four largest cities of Eastern Canada (Montreal, Ottawa, Quebec City and Toronto).

Results: Montreal was identified as the city where urbanization impacted temperature and precipitation the most. An urban heat island is particularly visible at night in summer and winter and has increased over the period. Urban precipitation has become less frequent and intense in the city compared to its rural surroundings, particularly during summer. The reduced capacity of cooling by precipitation reevaporation, and a modified albedo during winter, may have reinforced the urban heat island. Both rain and snow have a major impact on PM2.5 concentrations, particularly on the day following the meteorological event.

Significance: Better awareness of the impact of urbanization on urban temperature and precipitation will improve our ability to predict the consequences of its acceleration on citizens' health, and to adapt our cities accordingly. To the best of our knowledge, no such study has yet been conducted in the region.

1.3 Introduction

Global population growth coupled with rapid urbanization is leading to the exponential expansion of urban areas. Today, more than half of the world's population lives in cities (United Nations, Department of Economic and Social Affairs, Population Division, 2019).

Cities contribute to changes in climatic and atmospheric conditions at different temporal and spatial scales. Global climate change is a prime example of urban modification – the unintended impact of human activities on the environment. Human influence has already statistically contributed to an increase in the frequency and intensity of regional precipitation extremes in North America (Singh *et al.*, 2020). But these interactions can also result in changes in the processes controlling the climate at the local scale. Here the focus is made on urban microclimates experienced by cities.

First, to accommodate this growing population, urban areas are spreading, and there are major differences between the composition of surfaces in urban and rural areas. The materials used for built surfaces can have a wide range of albedos, but the convoluted shape of buildings in cities traps solar radiation directed towards the surface. The surfaces absorb a total of 15–30% more solar radiation during the day than rural areas (Chen *et al.*, 2012 ; Dixon et Mote, 2003 ; Middel *et al.*, 2014 ; Oke *et al.*, 2017 ; Tabeaud, 2010). The re-emission of these higher amounts of energy absorbed during the day is also inhibited, due to infrared radiation trapping by the urban canopy during the night.

Cities are complex environments that are challenging to characterize with physical parameters (Oke *et al.*, 2017). Within the same city and over very short distances (less than 500 m), significant temperature variations can be recorded. Heterogeneities are driven by spatial and temporal variations in human activities, such as the release of heat from the heating and cooling of buildings, industrial processes, and transportation (Schatz et Kucharik, 2014). In Montreal's metropolitan area, a strong increase in heat islands has been observed in certain neighbourhoods (Cavayas et Baudouin, 2008), with the downtown area, industrial and commercial zones, large parking lots, and major traffic routes being the most susceptible to heat islands formation. Moreover, due to anthropogenic pollution, particulate matter is often at least 10 times more abundant over urban areas than rural ones, thus cooling the city by reducing up to 30% of incoming solar radiation (Kamsali *et al.*, 2011). However, this cooling effect is small in comparison to the increased heating caused by urban processes such as solar and infrared radiation trapping, and indoor heating and air conditioning. As a result, cities constitute Urban Heat Islands (UHI) (Roberge et Sushama, 2018) with higher average minimum temperatures than in adjoining rural regions. For the rest of this article, UHIs will be defined as city-size UHIs, meaning the spatially averaged temperature of the city is higher than that of the surroundings of the city.

In the past decades, climate research in built-up areas has mainly focused on UHIs (Arnfield, 2003). But significant changes in precipitation patterns and trajectories have also been identified in urban areas. The urban effect on clouds and precipitation is due to a variety of physical effects, that can broadly be combined in the influence of the UHI, surface roughness and anthropogenic emissions (Figure 1.1).

Figure 1.1: Physical controls on urban precipitation

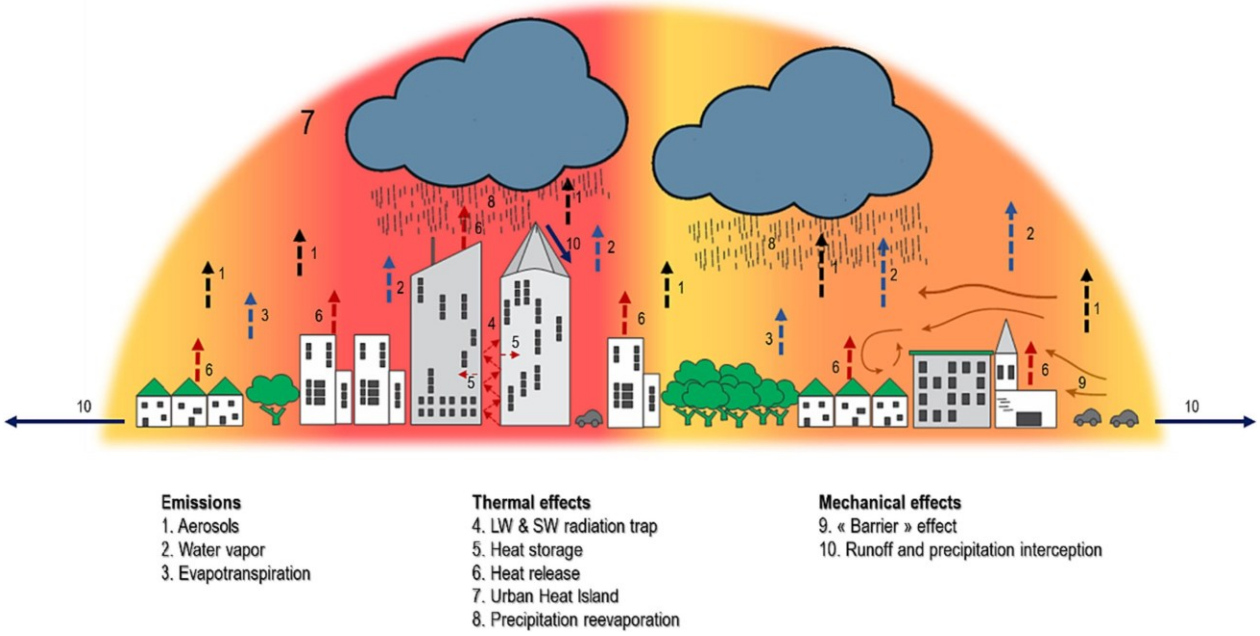

Previous studies have identified several potential alterations to precipitation patterns in urban areas including:

- The uplift caused by both city-size UHI and roughness enhances cloud formation and precipitation. Under calm or light wind conditions, the UHI appears to be the most important cause of uplift. It can lead to the initiation and/or enhancement of precipitation over and downwind of the city (Lorenz *et al.*, 2019).
- Due to the UHI, the sub-cloud evaporation of precipitation is boosted, reducing precipitation amounts, and the frequency of freezing rain and snow in the city (Oke *et al.*, 2017).
- During synoptic-scale events, urban effects are weaker and more difficult to detect. The “barrier” effect caused by the convergence of winds at the entrance of cities is particularly important in the tallest (ex: skyscrapers) and densest urban areas. The bifurcation or split of regional storms on either side of the city causes a decrease in precipitation over the city centre, and an increase on the lateral and downwind sides of the city (Hass *et al.*, 1967 ; McLeod *et al.*, 2017 ; Niyogi *et al.*, 2017).
- On one hand, aerosols have been shown to modify the formation of precipitation within convective clouds. The rise of condensation nuclei density decreases the size of droplets formed, delays collision and coalescence processes, and thus the droplets growth. On the other hand, paradoxically, aerosols cause more intense and more frequent localised showers in the vicinity of cities, particularly on their downwind side (Rosenfeld *et al.*, 2008).

- Additions of water vapor from combustion heating systems can locally slightly increase clouds and precipitation (Oke *et al.*, 2017).

While these individual effects have been observed, interactions between all the processes involved remain poorly understood, mainly because the spatial and temporal heterogeneity of cities, and lack of spatial coverage of meteorological stations, make it difficult to acquire measurements representative enough of this environment, where precipitation amounts are not affected by the influence of buildings or other obstacles (Oke *et al.*, 2017). Even if the link between urban climates and meteorology has raised increased interest since the 1960s, the location and intensity of the impact of cities on urban precipitation is still unclear and varies between studies (Liu et Niyogi, 2019).

In the meantime, these modifications are of major interest for the strategic management of water resources, which is important for the future of the global economy (McDonald *et al.*, 2014), but also for health and safety aspects:

1. During heat waves, cooling effects by evaporative heat loss can improve the city's climate even several days after rain events (Starke *et al.*, 2010). A reduced precipitation amount, associated with the reduction in absorptive surfaces, trees, and vegetation, that temporarily store water, leads to a reduced capacity of air cooling by evaporation in cities. As climate projections suggest significant increases in temperatures for both urban and nonurban regions, this phenomenon will enhance the heat stress experienced in cities during these increasingly frequent heat waves (Roberge et Sushama, 2018).
2. Air pollutants such as PM10, SO_2, NO_2, and CO show statistically significant negative correlations between their concentrations and rain intensity due to the washout effect (Rosenfeld *et al.*, 2007 ; Yoo *et al.*, 2014). Precipitation has a strong impact on the quality of air breathed by citizens.
3. The replacement of vegetated areas by buildings and less permeable materials in urbanized watersheds fundamentally alters the natural water budget (Starke *et al.*, 2010). Urban infiltration is strongly reduced by both surface imperviousness and the decrease in frequency of rains of lower intensities, and surface runoff becomes the dominant process. The quantity of rainwater stored in urban infrastructures is significantly reduced. With less storage capacity for water and more rapid runoff, urban streams rise more quickly during storms and have higher peak discharge rates than rural streams, leading to an increased probability (and reduced return periods) of flooding events (Kirchmeier-Young et Zhang, 2020 ; Singh *et al.*, 2020), as well as a larger total volume of water

discharged. This phenomenon requires ensuring that stormwater management systems are adaptable to these changes.

The urban influence on precipitation is likely to impact human health as much as UHIs do (Heaviside *et al.*, 2017). In the coming years, the constant urbanization phenomenon we are facing may furthermore increase the climate change already experienced in cities. In addition to modifications in urban geometric structures and therefore altered air circulation patterns, urbanization is likely to increase inputs of heat, aerosols, and water vapor from housing and transport. It is becoming imperative to better understand the consequences that these changes will have on precipitation received in cities, to be able to support the adaptation (adjustments of practices and developments) of the urban hydrological cycle. Monitoring and understanding the evolution of urban precipitation are among the most challenging tasks of the 21st century.

In Eastern Canada, several models and reanalyses at a fine grid resolution from 250 m to 1 km have been used to bring significant content to the discussion of the impact of cities on the local climate (Gaur *et al.*, 2021 ; Lauer *et al.*, 2023 ; Leroyer *et al.*, 2022 ; Shu *et al.*, 2022, 2023). However, such a high spatial resolution simulation requires important computing resources, and these studies only had the opportunity to focus on meteorological events. To our knowledge it has not yet been possible to proceed to such a study over a climatological scale, that is required to assess the impact of urbanization on cities' temperature and precipitation through years.

Coarser grid resolutions are inappropriate for representing the highly heterogeneous urban environments and their meteorological processes (Nogueira *et al.*, 2022), and until now, urban structures have remained poorly represented in these models.

The goal of this study is to compare urban and rural temperature and precipitation over a period long enough to identify the impact of urbanization on the urban microclimates of Toronto, Ottawa, Montreal, and Quebec City, and discuss the interactions of these variables in a mid-latitude, North American context. For that, we use daily climatic grids computed by the Quebec Climate Monitoring Program, interpolated from meteorological stations data at an 11 km resolution (Bergeron, 2016 ; MELCCFP, 2022). To the best of our knowledge, no such study has yet been conducted in the region.

1.4 Materials and methods

1.4.1 Study area

Like many metropolitan areas, urbanization is a major issue faced by the cities of Toronto, Ottawa, Montreal, and Quebec City, the most populated cities of Eastern Canada. In only 5 years, their populations have respectively increased by 2.3, 8.9, 3.2, and 3.3% (Table 1.1). To contain this growing population, the number of building permits has doubled between 2001 and 2018 in Montreal (source: Statistics Canada). Previous studies have already shown the presence of a city-size UHI (Roberge et Sushama, 2018 ; Touchaei et Wang, 2015), and localised heat islands increasingly marked in some neighbourhoods of Montreal (Cavayas et Baudouin, 2008).

Table 1.1: 2021 census of population geographic summary (source: Statistics Canada, 2021 census of population)

	Toronto	Ottawa	Montreal	Quebec City
Population, 2021	2 794 356	1 017 449	2 004 265	588 777
Population percentage change, 2016 to 2021	2.3%	8.9%	3.2%	3.3%
Population density per square kilometre	4 427	364	4 022	1 075

These cities all belong to the Great Lakes and St. Lawrence Valley region, made up of fertile plains, rolling hills, large freshwater bodies to the west and river valleys to the east. This region represents more than 20% of the world's supply of surface freshwater and about 84% of freshwater in North America, providing drinking water to over 8.5 million Canadians.

According to Köppen's climate classification, the Great Lakes and St. Lawrence Valley region is located in the climate type Dfb, a climate fully humid, marked by large seasonal variations in temperature, with snow in winter and warm summers (Kottek *et al.*, 2006). Precipitation is well distributed throughout the year, which favours abundant forests and prosperous cropland. It is one of the most densely populated, prosperous, and productive regions in Canada.

As is common for mid-latitudes, different air masses influence the weather in Eastern Canada, and three of them are dominant in the region, with relative importance varying throughout the year (Lutgens *et al.*, 2019). Polar continental air masses, formed above 45° N, produce very cold, dry and stable weather. They are responsible for the extreme cold of the Canadian winter, and some heat waves relief in summer. Polar maritime air masses warm up and are destabilized while gathering moisture as they pass over the Atlantic Ocean, bringing rain, fog, and snow to the Atlantic coast. In summer, the Azores anticyclone allows the

tropical maritime air mass from the Gulf of Mexico to move up the East of America, bringing the great heat and humidity in the region that can occur at this period of the year.

Ottawa, Montreal, and Quebec City are located in the St. Lawrence Valley, while Toronto belongs to the Great Lakes basin (Figure 1.2). In the St. Lawrence Valley, the southwest to northeast orientation of the river valley exerts a significant influence on the trajectory of low-pressure systems, therefore preferentially having a southwest to northeast trajectory (Milrad *et al.*, 2013). In Toronto, the presence of Lake Ontario influences the local climate of the city. Land and lake breezes reduce the amplitude of daily climate variations and favour the formation of convective clouds.

Figure 1.2: Location of Toronto, Ottawa, Montreal, and Quebec City in Eastern Canada (shaded grey), and the stations monitoring concentrations of particulate matter of diameter inferior or equal to 2.5 µm (PM2.5) (blue)

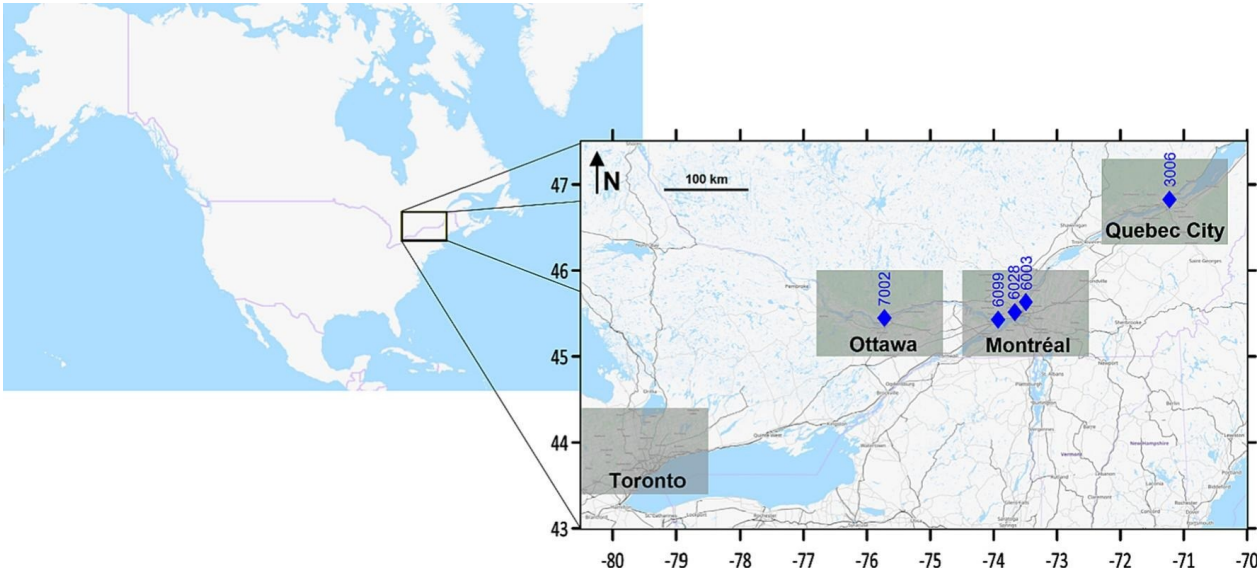

1.4.2 Data

The daily climatic grids computed by the Quebec Climate Monitoring Program (Bergeron, 2016 ; MELCCFP, 2022) were used to compare temperatures and precipitation over a period long enough to identify the impact of urbanization on the urban microclimates of Toronto, Ottawa, Montreal, and Quebec City.

This data includes daily minimum and maximum temperatures, and total daily precipitation (solid and liquid), interpolated by a kriging method at a spatial resolution of 0.1° (~11 km). Measurements taken at meteorological stations were used as observational data for the interpolation. For minimum and maximum temperature and total precipitation measured at stations below the 50th parallel, the estimates are of better

quality due to the high density of the station network. For these variables, the estimates show respectively a mean error (ME) of less than ± 0.1 °C, ± 0.1 °C, and ± 0.1 mm in almost all cases, and a root mean square error (RMSE) and interpolation variance generally lower than 3 °C, 2 °C, and 4 mm. The estimates are of lower quality in the area outside of the province of Quebec, because they are extrapolated to the grid point (Bergeron, 2016).

The daily gridded data were used to study climatic patterns in Toronto, Ottawa, Montreal and Quebec City. As the UHI is primarily a nighttime phenomenon (Oke *et al.*, 2017) it is expected to be the most intense for lower temperatures and negligible for higher temperatures. For this reason, mean daily temperatures were not investigated as this parameter would only blur the signal. Moreover, the data used in this study only included minimum and maximum temperatures. Estimating the daily mean temperature would induce a bias.

Monthly temperature and precipitation are calculated over 30 years, between 1988 and 2017. Precipitation frequencies are calculated monthly, by selecting days when daily precipitation amounts were greater than 1 mm, to avoid trace precipitation. To better understand the evolution of the impact of urbanization on the climate for both urban and rural areas, each grid cell within the study area was characterized as either urban or rural, using the limits of the city (Figure 1.3). Spatial averages could be made for both zones, for each one of the meteorological variables considered. The same nodes were used for both temperature and precipitation data. The results for the UHI - calculated as the difference between the average temperature of urban areas, and the average temperature of rural areas - and the urban-rural differences in precipitation amounts and frequencies, will be discussed in the following sections.

Figure 1.3: Selection of nodes for urban (red) and rural (green) areas

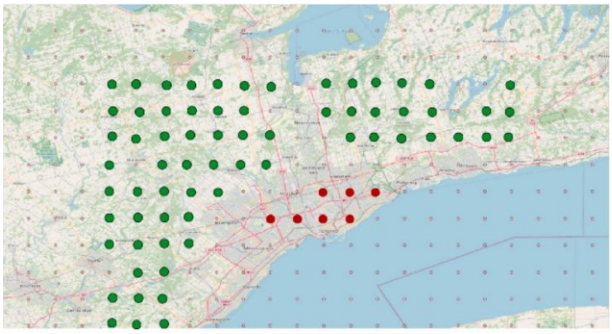

Toronto

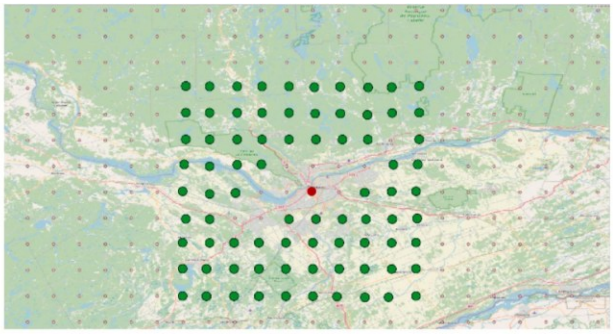

Ottawa

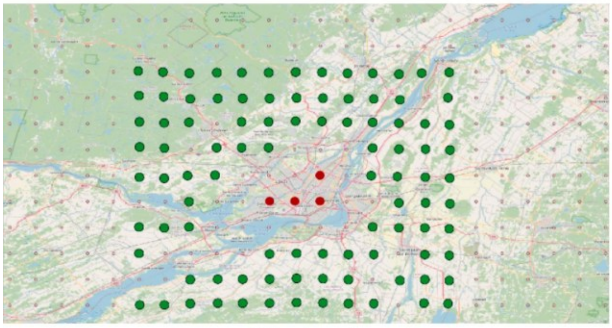

Montreal

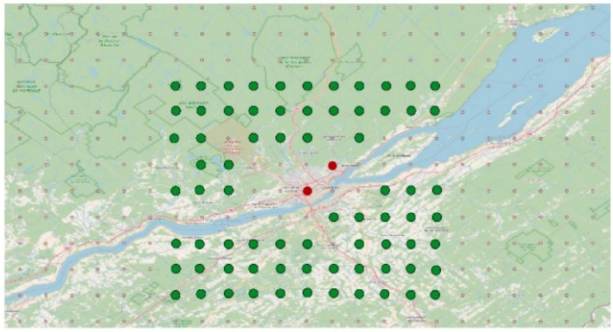

Quebec City

It should be noted that the surface of the study site is not the same for each city considered. For the cities of Toronto, Ottawa, Montreal, and Quebec, 7, 1, 4, and 1 grid nodes were respectively considered for the representation of the urban zone (Figure 1.3). Rural areas were visually selected using OpenStreetMap, as the nodes belonging to the surrounding areas that are the freest of housing and industrial areas. For each one of the cities considered, peri-urban areas (transition zones between urban and rural areas) and surface water areas were excluded from calculations. The number of rural nodes was arbitrarily defined to find a compromise between having a surface large enough to be representative of all rural areas surrounding each city, but not too important to observe a latitudinal effect on temperature.

To enrich the discussion, hourly temperature data from Montreal's airport weather station (courtesy of Environment and Climate Change Canada) were used to investigate the monthly-averaged proportion of days when the hour at which the minimum temperature measured was comprised between sunset and sunrise. Finally, the air quality data was used to determine Montreal's precipitation impact on concentrations of particulate matter of diameter inferior or equal to 2.5 μm (PM2.5) (MELCCFP, 2023). For Montreal, these concentrations are calculated as the average of the data measured at the monitoring stations 6003, 6028, and 6099, all located on the Island of Montreal, from 2015 to 2017 (Figure 1.2). The monitoring stations 3006 and 7002 were also used to study PM2.5 concentrations in the cities of Quebec and Ottawa respectively.

For better visualization, daily data underwent a moving average of 365 days (Figure 1.4 a, b, Figure 1.5 a, b, Figure 1.6 a, b, Figure 1.10 a, b, Figure 1.12 a, Figure 1.14 a), while monthly data underwent a moving average of 30 days (Figure 1.5 c, d, Figure 1.6 c, d, Figure 1.10 c, d), so both types of data would be representative of the evolution over a year, and a month, respectively.

Figure 1.4: 365 days moving average of daily minimum temperatures (a) and maximum temperatures (b) for Toronto (black), Ottawa (red), Montreal (blue) and Quebec City (green)

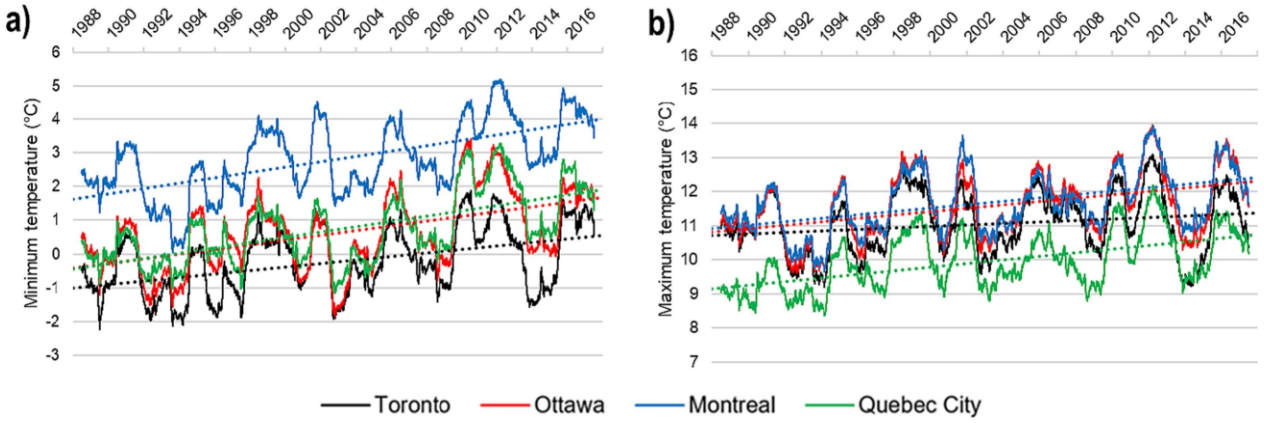

Figure 1.5: 365 days moving average of daily precipitation amounts (a) and frequencies (b) and 30 days moving average of daily precipitation amounts (c) and frequencies (d) averaged over 30 years for Toronto (black), Ottawa (red), Montreal (blue) and Quebec City (green)

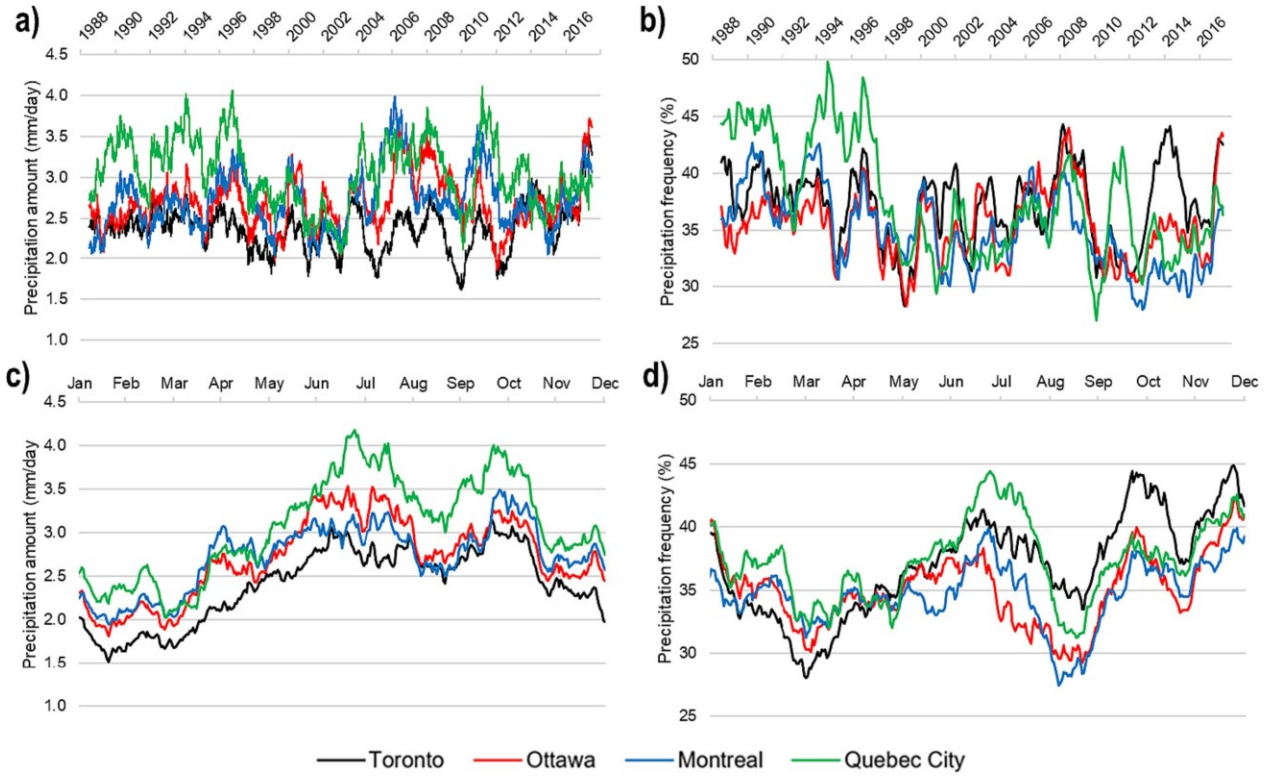

Figure 1.6: 365 days moving average of urban-rural differences in daily minimum temperatures (a) and maximum temperatures (b) and 30 days moving average of Urban-Rural differences in daily minimum temperatures (c) and maximum temperatures (d) averaged over 30 years for Toronto (black), Ottawa (red), Montreal (blue) and Quebec City (green)

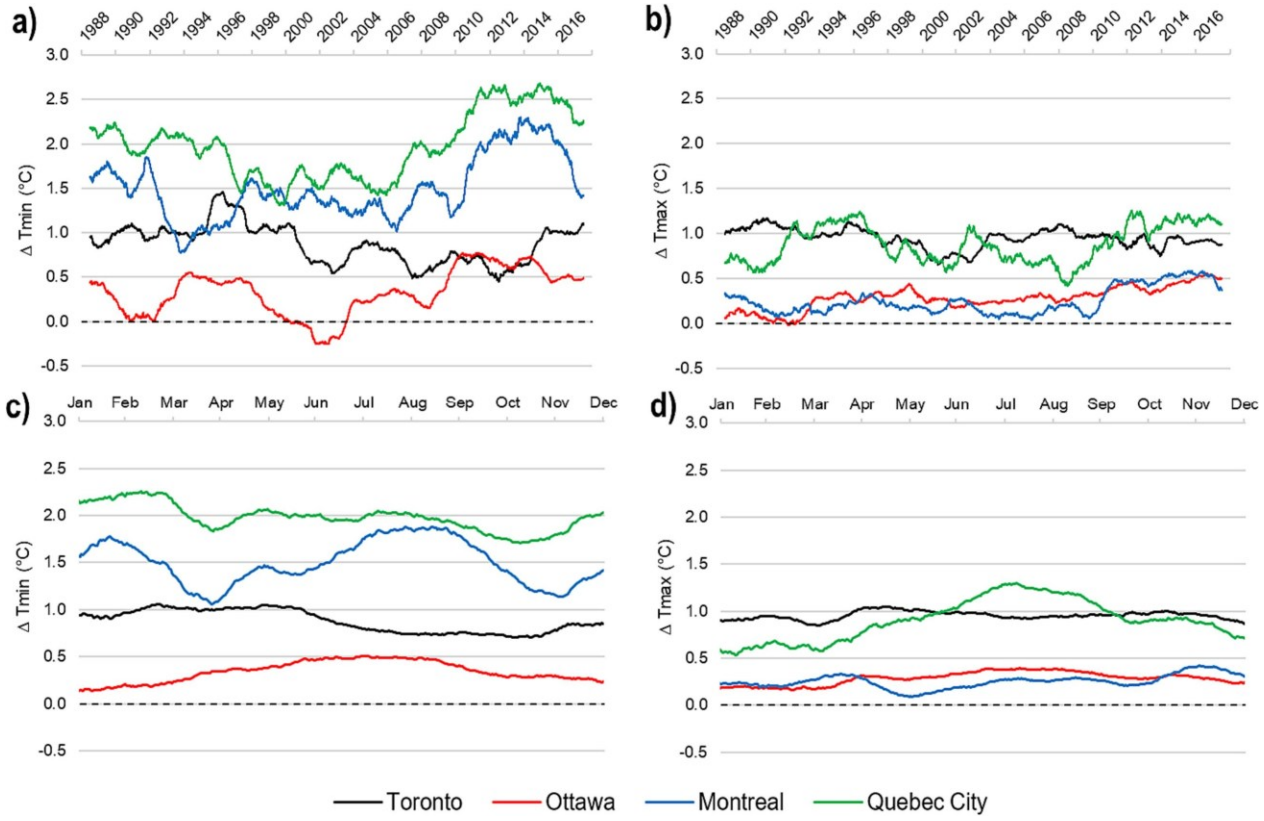

The timeframe 1988–2017 is used to investigate the evolution of temperature and precipitation over 30 years. Table 1.3, Figure 1.7 and Figure 1.11 also show data averaged over the last 5 years of the period (2013–2017). This was done so that the result would be representative of the magnitude of the effect of urbanization in the last years, and would not be weakened by the beginning of the period, when the signal was less intense. As for cross-correlations between the minimum temperature UHI and precipitation, and PM2.5 concentrations, the period 2015–2017 was chosen to have consistency and avoid monitoring gaps in PM2.5 concentration measured at the different monitoring stations.

Figure 1.7: 2013–2017 averaged daily minimum temperatures, interpolated from daily climatic grids computed by the Quebec climate monitoring program. Contours are represented every 0.3 °C

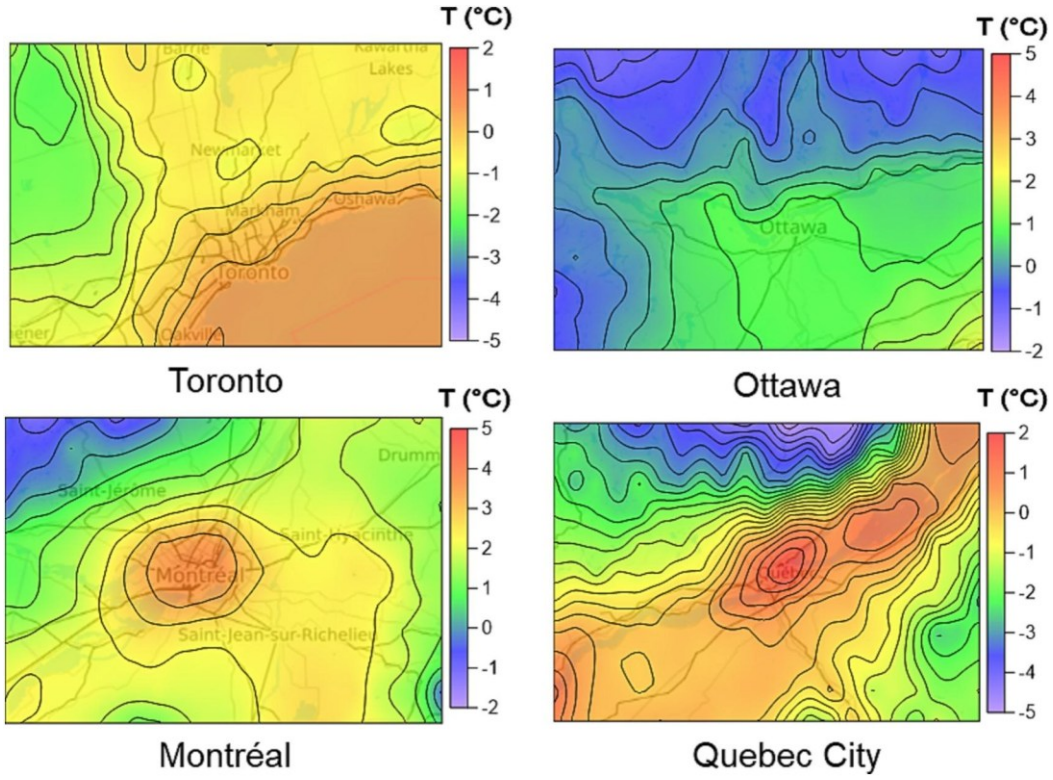

1.5 Results & discussion

1.5.1 Regional patterns

Variations in daily minimum and maximum temperatures are similar for all cities and thus representative of the synoptic pattern impacting the region. In particular, there is a large seasonal amplitude in temperatures, with daily minimum temperatures reaching a minimum average of around −15 °C in winter and a maximum of 15 °C in summer for all cities. Daily maximum temperatures reach a minimum average of around −5 °C in winter and a maximum of around 25 °C in summer (not shown here).

Between 1988 and 2017, an increase in both minimum and maximum temperatures can be observed, for all sites, with a maximum of +2.4 °C in daily minimum temperatures in Montreal (Figure 1.4 a, b and Table 1.2), highlighting the global warming of the region. A previous report (Bush et Lemmen, 2019), was showing that between 1948 and 2016, the best estimate of mean annual temperature increase is 1.7 °C for Canada as a whole. This increasing trend seems to be even more important in Eastern Canadian cities.

Table 1.2: Difference in average daily minimum and maximum temperatures between 1988 and 2017, calculated as the difference in values of the dashed linear trendlines from Figure 1.4, between the end and the beginning of the period

	Daily minimum temperatures	Daily maximum temperatures
Toronto	1.6 °C	0.6 °C
Ottawa	2.1 °C	1.5 °C
Montreal	2.4 °C	1.5 °C
Quebec City	2.3 °C	1.6 °C

In this region, the North Atlantic Oscillation causes changes in the intensity and location of the North Atlantic jet stream and storm tracks, and thus large-scale variations of the heat and moisture transport (Hurrell, 2003). This can induce considerable interseasonal and interannual variability in temperature and precipitation in eastern North America, especially in winter (Chartrand et Pausata, 2020). A synchronous oscillation can be observed in temperatures of all cities, with the same frequency (Figure 1.4), and is thus representative of the regional atmospheric circulation. However, no statistical correlation could be observed between the data used in this study and the NAO index, highlighting the complexity of controls on climatic variations in the region.

No significant trends in daily average precipitation amount can be observed over the study period (Figure 1.5 a). What can be observed however is that the return period and inter-annual variability have increased in the last years. In the meantime, precipitation has significantly decreased in frequency in all cities over the past 30 years, and more importantly in Montreal and Quebec City (Figure 1.5 b), with respectively −7% and − 11% of rainy and snowy days yearly. All cities show the same seasonal pattern in precipitation amounts and frequencies (Figure 1.5 c and d), seemingly the result of the synoptic atmospheric circulation.

While precipitation amounts have remained quite constant, precipitation frequencies have decreased, meaning more intense precipitation events in the region. Previous studies have shown an increase in extreme precipitation events related to global warming, and that urbanization itself might be the cause of more extreme precipitation found in the vicinity of cities (Kirchmeier-Young et Zhang, 2020 ; Seneviratne *et al.*, 2012 ; Singh *et al.*, 2020). Seasonally, the pattern is the same for all cities, with twice higher precipitation amounts in summer than in fall (+2 mm/day on average, between the minimum in March and the maximum in July). That can be the result of tropical maritime air masses bringing more water vapor at this time of the year, as well as convection due to solar radiation. For all months, precipitation amounts seem greater for Quebec City, which could reflect the impact of the Saint-Lawrence Valley on the formation of precipitation. The storms having a preferential south-east to north-west direction would have the opportunity to recharge

in water vapor during their transport over the St-Lawrence River. Moreover, the passage over the city of Montreal can act as a supplier of condensation nuclei in the form of particulate matter from anthropogenic pollution. These combined effects have the potential to initiate increasingly intense precipitation along the St-Lawrence Valley.

1.5.2 Comparison between urban and rural climates

While for Ottawa and Toronto both minimum and maximum temperature UHIs seem weak, UHIs are stronger for daily minimum temperatures than for daily maximum temperatures in Montreal and Quebec City, and have increased to reach respectively 2.0 and 2.5 °C in the 2013–2017 period (Figure 1.6 a, b, and Table 1.3). For comparison, New York City, located only 500 km from Montreal, had an average nighttime UHI intensity of 3.51 °C between 2006 and 2013 (Hardin *et al.*, 2018). New York's UHI is the third largest UHI out of American cities with UHI data (Climate Central, 2021).

Table 1.3: Urban – rural differences in daily minimum and maximum temperatures for the period 1988–2017 and 2013–2017

	$\Delta_{urban-rural}$ daily minimum temperatures		$\Delta_{urban-rural}$ daily maximum temperatures	
	1988-2017	2013-2017	1988-2017	2013-2017
Toronto	0.9 °C	0.9 °C	0.9 °C	0.9 °C
Ottawa	0.3 °C	0.6 °C	0.3 °C	0.5 °C
Montreal	1.5 °C	2.0 °C	0.3 °C	0.5 °C
Quebec City	2.0 °C	2.5 °C	0.9 °C	1.1 °C

The average over the 2013–2017 period of daily minimum temperatures for each grid point in the region illustrates a significant temperature anomaly consistent with a UHI phenomenon in Montreal and Quebec City (Figure 1.7), that was not present in Toronto or Ottawa. This effect shows a seasonal pattern in Montreal, with Montreal's UHI being most important in February and August (Figure 1.6 c), with average values of respectively 1.7 °C and 1.8 °C, compared to a minimum of 1.1 °C and 1.2 °C in April and December.

1.5.3 Factors behind the urban-rural differences observed

1.5.3.1 Sensible heat

Several phenomena may be responsible for Montreal and Quebec City having such strong UHIs for minimum temperatures but not for maximum temperatures. Overall, a very large proportion of daily minimum temperatures seems to happen at night, with a higher ratio found during the end of summer and

beginning of fall (97%, compared to a minimum of 81% in winter) (Figure 1.8). Hence, the hypothesis is made that in the data used for this study, minimum temperatures are statistically measured at night, and the strong UHI previously observed is thus representative of a nighttime UHI. With a non-significative UHI observed for daylight hours, the UHI is higher at night than during the day. Even though that might be counter-intuitive, this result is consistent with previous research conducted in Vancouver (Oke, 1982) showing that at night, the cooling rate is higher in rural areas than in urban areas. First, the thermal admittance is smaller in soils than in urban surface materials, especially if they are dry. Soils emit more rapidly the energy they have stored from solar radiation during the day into the atmosphere (Oke *et al.*, 2017), which is even more compounded by their more favourable sky view factor. In cities, all vertical surfaces trap the re-emission of energy absorbed during the day, increasing the UHI which is thus more subject to be higher during the night (Chen *et al.*, 2012 ; Christen et Vogt, 2004 ; Middel *et al.*, 2014). During the day, the high thermal admittance of urban materials and the shading caused by high buildings significantly reduce the UHI, if not inverses it (Oke *et al.*, 2017).

Figure 1.8: Frequency at which minimum temperatures are measured at night between 1988 and 2017

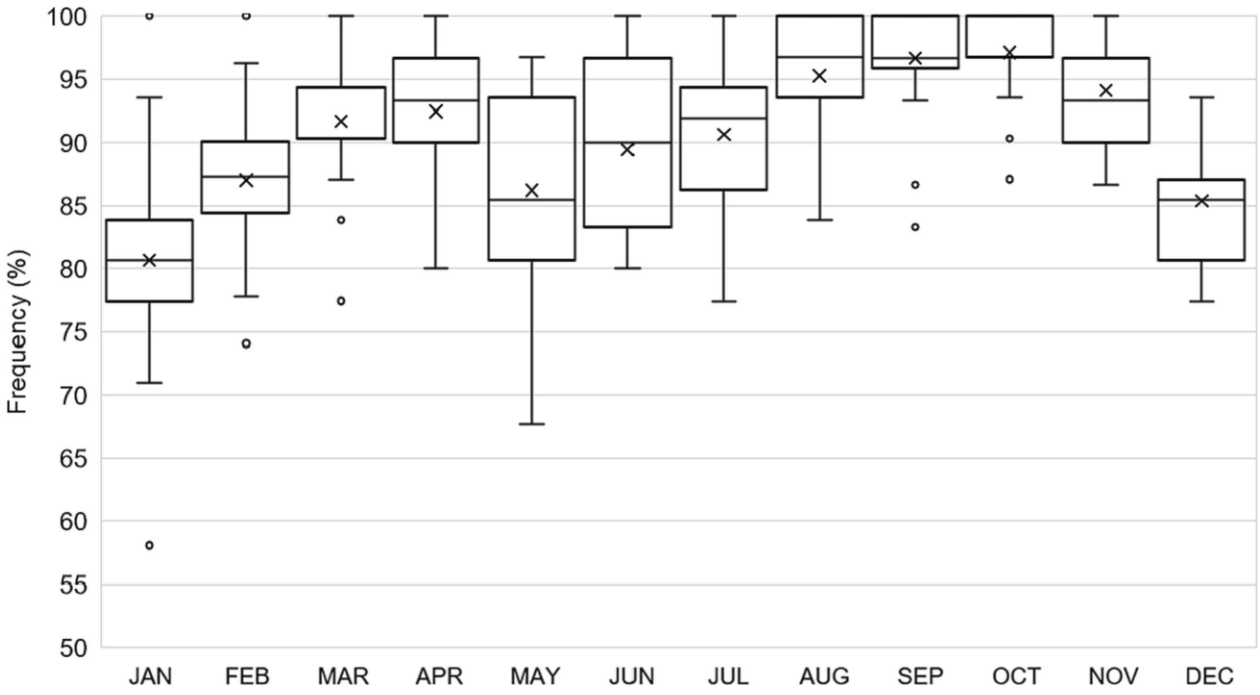

In Montreal, it was observed that the UHI is particularly important for minimum temperatures, for any of the months considered, but especially during the summer months, and in the middle of winter (Figure 1.6 c). The first period might be partly representative of a stronger daily solar radiation, increasing the trapping phenomenon described above, as well as a stronger anthropogenic heat release, caused by the air conditioning in response to the higher temperatures observed during these months. The second is probably

due to the presence of snow, which is usually abundant in Eastern Canada. Snow has indeed a strong impact on the albedo surface. While less-urbanized areas have a strong albedo due to the untouched snow covering the ground, in cities snow undergoes several alterations, such as snow clearance, soiling/tracking by cars and snow piles, snow removal on main roads, and the difficulty for it to aggregate on walls and pitched roofs (Oke *et al.*, 2017). As the albedo is lessened in cities, they absorb more solar radiation than less-urbanized areas, amplifying the UHI. With snow, the albedo difference between urban and rural areas can be as high as 0.11 to 0.55 (Oke *et al.*, 2017). However, this difference can change significantly between cities, depending on their practices. During the winter 2016–2017, the albedo difference between urban and rural areas appears to be much more important for Toronto and Montreal than for Ottawa and Quebec City (Figure 1.9), explaining in part why no seasonal variation could be observed in the Quebec City's UHI. Finally, with the very low temperatures that can be found in Eastern Canada in winter, the anthropogenic heat source is more intense due to indoor heating. With this seasonality, Montreal seems to be the city of Eastern Canada whose climate is the most clearly impacted by urban practices.

Figure 1.9: Landsat 8 aerial photographs taken over Toronto, Ottawa, Montreal and Quebec City during winter 2016–2017, to assess the albedo difference between urban and rural areas after a snow event. Data available from the U.S. Geological Survey

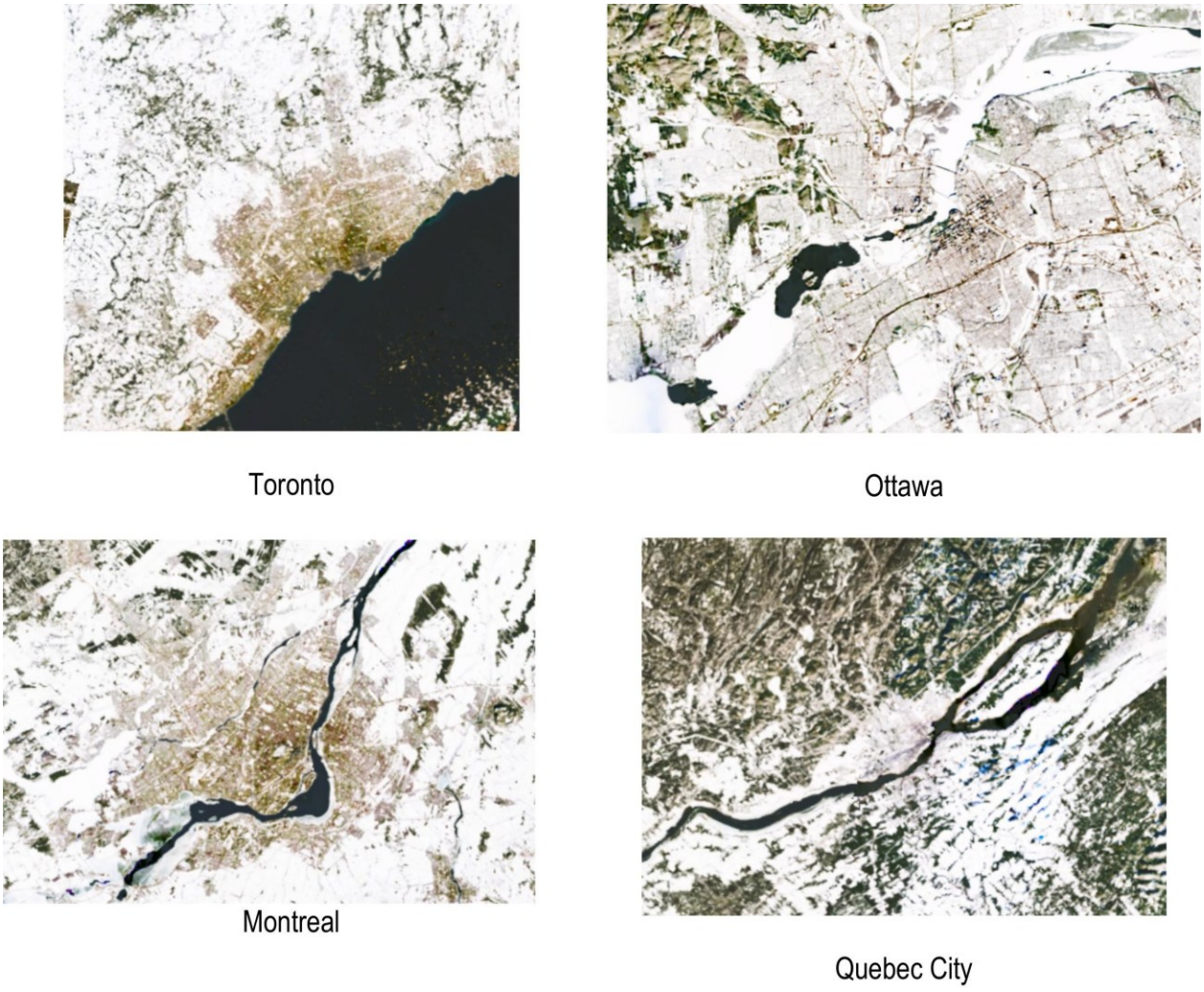

1.5.3.2 Latent heat

While there is no significant difference between urban and rural precipitation for Ottawa and Toronto, precipitation amounts have become less important in the cities of Montreal and Quebec City, with respectively −0.2 mm/day and − 0.6 mm/day (Figure 1.10 a). Again, Montreal shows a seasonal pattern that cannot be seen in Quebec City, with an Urban-Rural difference that is the most important during summer months (−0.5 mm/day in June, no difference from November to April) (Figure 1.10 c).

Figure 1.10: 365 days moving average of urban-rural differences in daily precipitation amounts (a) and frequencies (b) and 30 days moving average of urban-rural differences in daily precipitation amounts (c) and frequencies (d) averaged over 30 years for Toronto (black), Ottawa (red), Montreal (blue) and Quebec City (green)

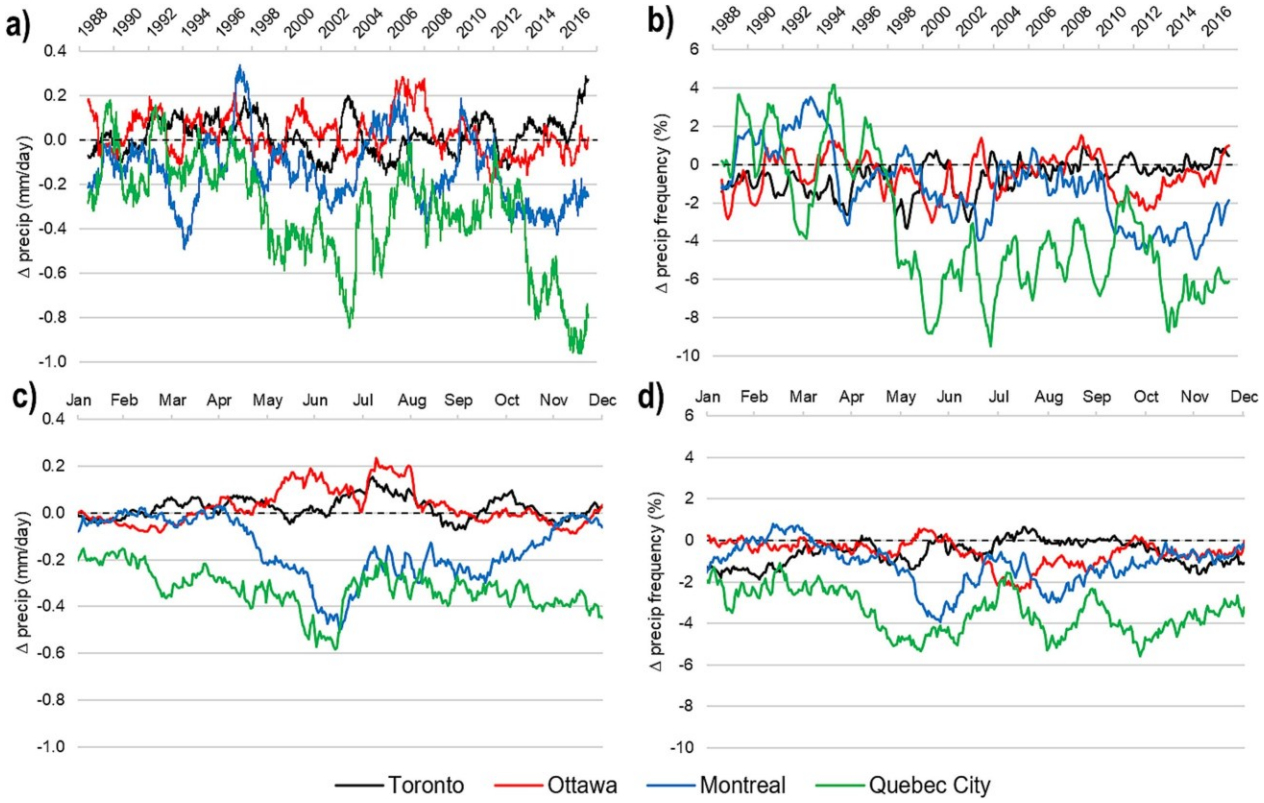

Moreover, precipitation frequency is dropping faster in urbanized areas in Montreal and Quebec City (Figure 1.10 b and Figure 1.11). Between 1988 and 2017, the difference in annual rainy and snowy days between urban and rural areas has increased by respectively 5.2% in Montreal and 8.4% in Quebec City (Figure 1.10 b). While precipitation was more frequent in the city at the beginning of the 30 years period, possibly a result of the local topography, it has now become more frequent in rural areas (+3.7% in Montreal, +7.6% in Quebec City).

Figure 1.11: Monthly averaged urban-rural differences in precipitation intensities and frequencies between 1988 and 1997 (blue) and between 2013 and 2017 (orange). Squares represent the mean of each series

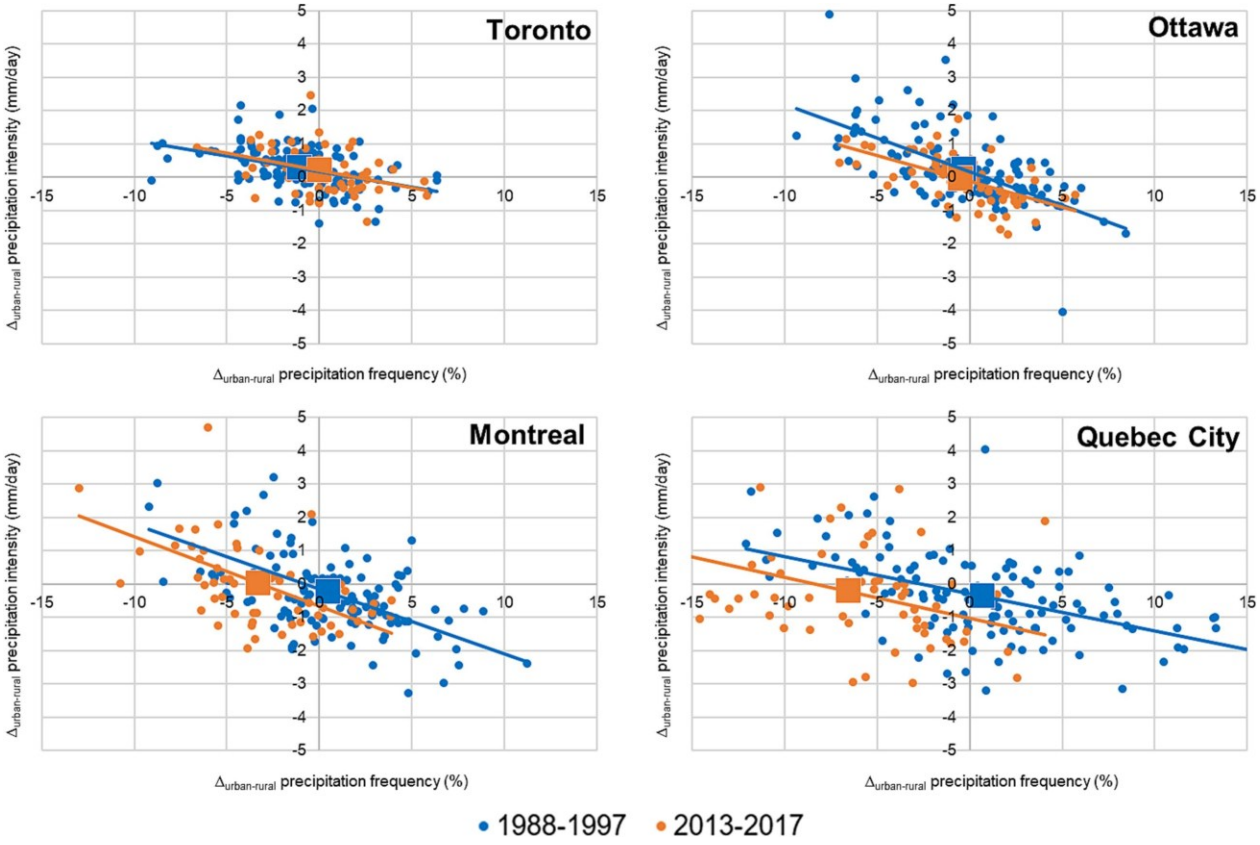

Several mechanisms could cause the decreased frequency of precipitation in urban areas. First, it could be reflecting the increase in building density and thus an enhanced roughness and barrier effect. However, an increase in aerosols and vapor emissions linked to urbanization is more likely to have been significant during this relatively short period. As it has been discussed, these emissions allow clouds to grow further before breaking into showers. Whether these showers tend to happen more readily inside the city or while the cloud is already outside of it (and the associated distance linked to it), is still poorly understood (Liu et Niyogi, 2019).

Finally, there seems to be no difference in precipitation amounts and frequencies in Montreal's urban and rural areas in winter, but in summer and especially in June precipitation is less intense (−0.5 mm/day) and frequent (−4% of rainy days) in urban areas than in rural areas (Figure 1.10 c and d). The increasing difference observed in precipitation amount and frequency between urban and rural areas would thus mainly be due to a process taking place in summer. As these results could indicate that solid precipitation is less likely to be affected by anthropogenic emissions and the city roughness, this may also show that it is the

UHI, more important at this time of the year, that is more likely to favour precipitation in the surroundings of cities. The UHI has already proven to have increased during the 1988–2017 period, and to be the highest in summer, matching precipitation amount and frequency trends.

So, the UHI, precipitation amount and frequency seem to be correlated in Montreal. The UHI is likely to reduce precipitation by re-evaporation of water drops as they fall to the ground. Moreover, the UHI favours convection, which has a direct impact on the formation of precipitation (Oke *et al.*, 2017). But whether this convective phenomenon is likely to increase precipitation amount and frequency inside or outside the city is still poorly understood and needs to be studied further. However, one should keep in mind that the minimum temperature UHI seen here is representative of what happens at night, a time when convection is also more likely to be inhibited. These results seem to indicate that the secondary evaporation linked to the UHI is the main process impacting the decrease of precipitation amount and frequency in town.

1.5.4 Managing the impact of urban practices on our health

In rural areas where precipitation can infiltrate the soil, the evaporation of this moisture can act as a natural air cooler, reducing the temperature by using energy in the form of latent heat. With less precipitation and less infiltration in urban areas, this cooling effect is inhibited, thus enhancing temperatures in the town compared to its surroundings. This effect could be seen in the city of Montreal between 2015 and 2017. The cross-correlation between the daily minimum temperature UHI and precipitation (Figure 1.12 a) showed that the correlation coefficient was negative and more important the day following the precipitation event (Figure 1.12 b). This means that precipitation contributes to reduce the urban-rural difference in daily minimum temperature, for a period of 1 day following the precipitation event. Moreover, the UHI is generally lower for higher precipitation amounts (Figure 1.12 c). Further investigation is needed to better understand the complex retroactions between all phenomena mentioned here, particularly the relationship between precipitation and UHI.

Figure 1.12: 365 days moving average of Montreal's daily precipitation and urban-rural difference in daily minimum temperature (a), cross-correlation coefficients between daily precipitation and urban-rural difference in daily minimum temperature for different days shifts of precipitation (b), scatter plot of urban-rural difference in daily minimum temperature and daily precipitation shifted a day before (c) over the period 2015–2017

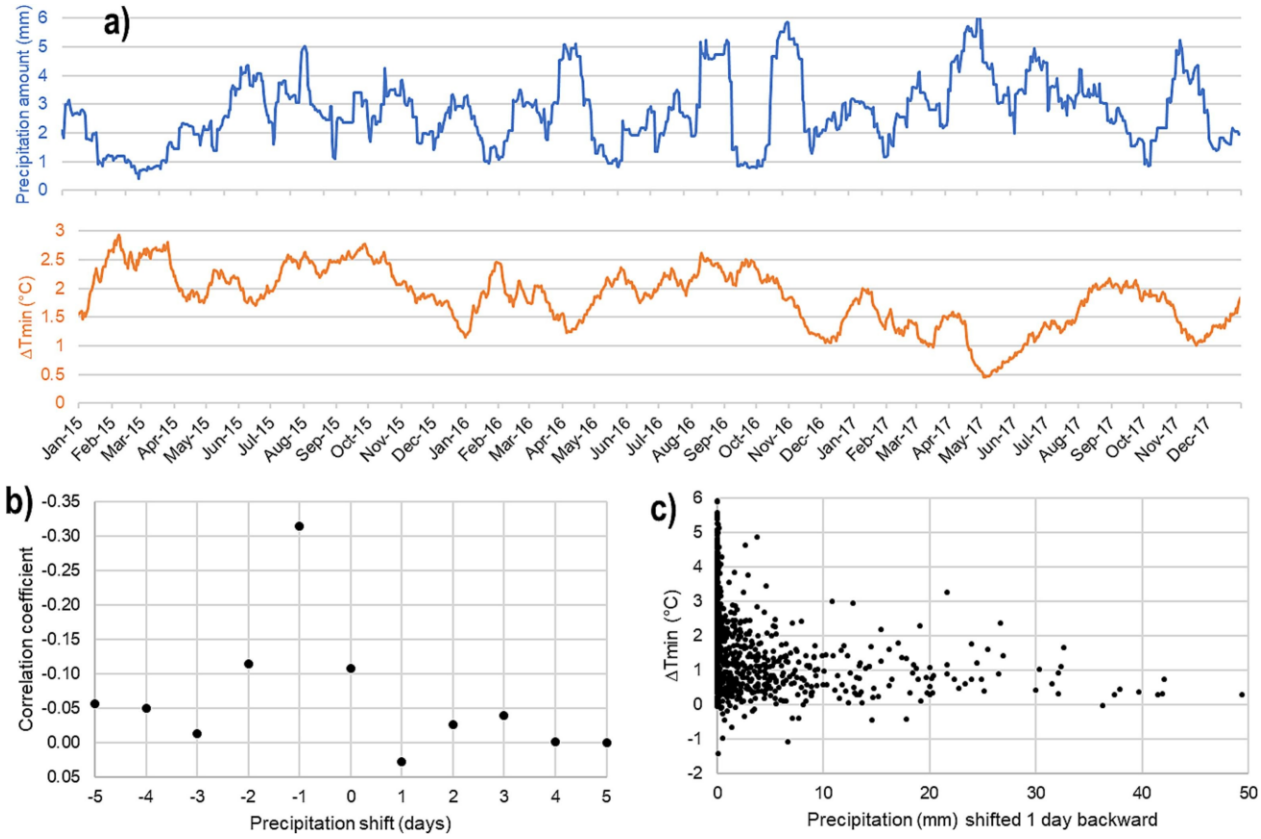

UHIs in summer are particularly harmful to human health, as they amplify the magnitude of heat waves experienced in cities (Ahrens et Henson, 2019). Water management practices aiming to store rainfall so that it can be used to compensate for the cooling effect of soil evaporation during dry days may be a way to mitigate the impacts of UHIs. Instead of routing rainfall directly away from urban areas, stormwater storage and reuse may be an approach to reduce the UHI effects. In summer, rainfall frequency is on average 1 day out of 3, and adapting water management practices to maintain sufficient soil water contents to sustain the cooling effect during dry days may help reduce the UHI effect during summer months.

Similar patterns are observed for both cities of Montreal and Quebec (Figure 1.13 a), and at the seasonal scale, by separating Montreal's data into warmer months (May–October) and colder months (November–April) (Figure 1.13 b). This highlights the fact that not only rain but also snow have a decreasing impact on the UHI, validating the idea that the albedo strongly impacts the UHI. The day after snowfall, the difference in albedo between urban and rural areas is decreased. Snow removal and de-icing of roads by urban practices are not immediate.

Figure 1.13: Correlation coefficient comparison between daily precipitation and daily minimum temperature UHI for Montreal and Quebec City (a) and for rain and snow in Montreal (b) over the period 2015–2017

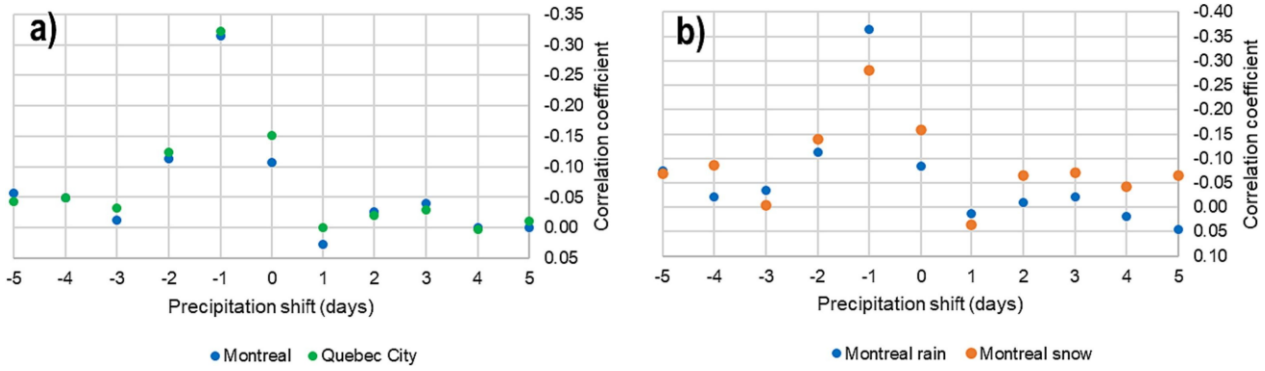

In winter, and especially in extremely cold climates such as those of Eastern Canada, there might be opportunities to take advantage of the UHI to improve living conditions, by reducing the energy needed for home heating for example. Better planning the use of construction materials to account for the albedo effect on the local climate could be of great value for future cities. However, the interactions with the environment can be numerous, and cities should adjust their practices to take them all into account. For example, the use of salt on roads for de-icing can improve winter driving conditions, but salt particles act as condensation nuclei and favour the formation of precipitation (Ahrens et Henson, 2019) and can impact surface and groundwater quality (Tiwari et Rachlin, 2018). The use of salt can have societal benefits but may also have environmental costs that need to be considered.

Similar to the relationship between precipitation and urban-rural difference in minimum temperatures, the cross-correlation between Montreal's daily precipitation and PM2.5 atmospheric concentrations between 2015 and 2017 (Figure 1.14 a) showed that the correlation coefficient was negative and the most important the day following the precipitation event (Figure 1.14 b). This means that precipitation contributes to reduce PM2.5 atmospheric concentrations, and this effect is the most visible the day following the precipitation event. However, in this case, the impact seems to be more diffuse, and a gradual increase in PM2.5 concentrations can be observed in the next few days. The same pattern was observed for the cities of Ottawa, Montreal and Quebec City (Figure 1.15 a), and for rain-driven months (May–October) and snow-driven months (November–April) (Figure 1.15 b). This highlights the fact that snow scavenges particulate matter from the atmosphere in the same manner as rain does. Moreover, PM2.5 concentrations are generally lower for higher precipitation amounts (Figure 1.14 c).

Figure 1.14: 365 days moving average of Montreal's daily precipitation and PM2.5 concentrations (a), cross-correlation coefficients between daily precipitation and PM2.5 concentrations for different days shifts of precipitation (b), scatter plot of daily PM2.5 concentrations and daily precipitation shifted a day before (c) over the period 2015–2017

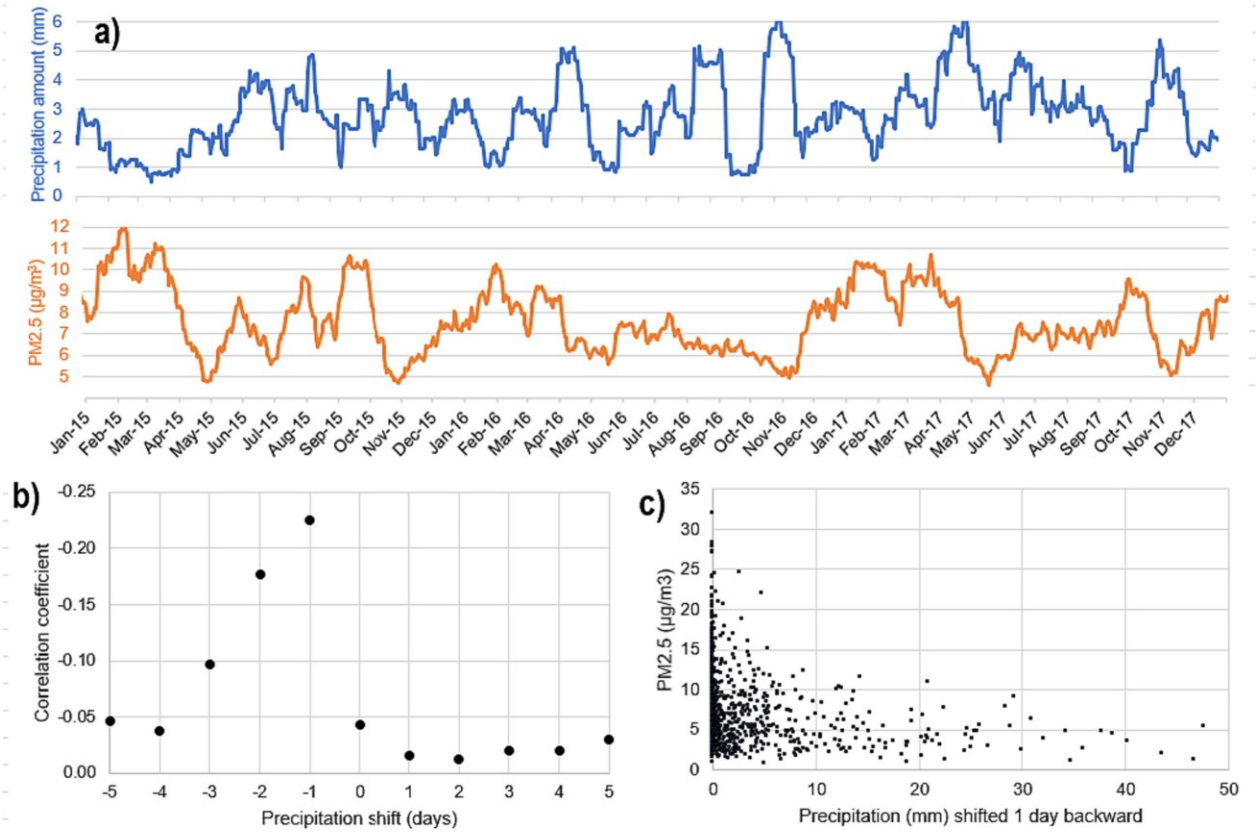

Figure 1.15: Correlation coefficient comparison between daily precipitation and daily PM2.5 for Ottawa, Montreal and Quebec City (a) and for rain and snow in Montreal (b) over the period 2015–2017

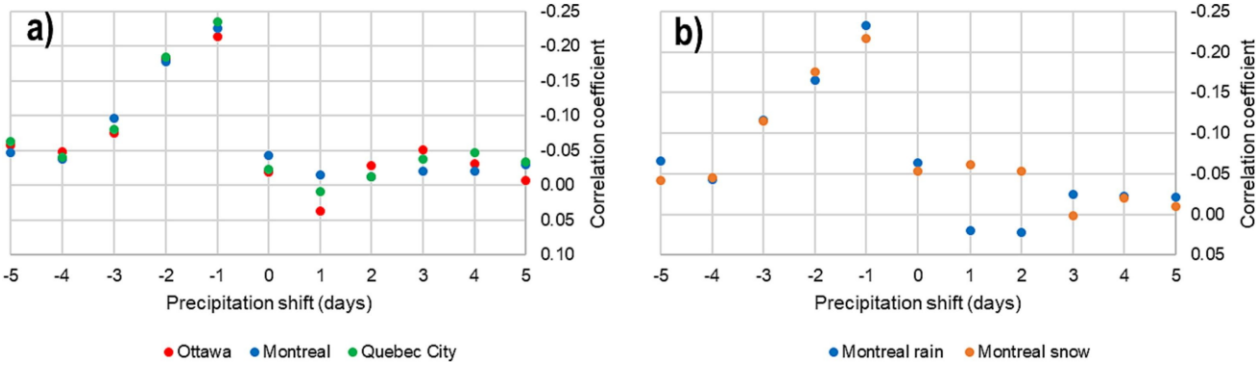

As particulate matter is significantly harmful to human health and is responsible for 4000 deaths per year in the province of Quebec (Health Canada, 2021), it is truly important to understand and limit the anthropogenic impact on urban precipitation to protect the most vulnerable citizens.

1.6 Conclusion

Cities' climates are influenced by a wide variety of urban processes interacting with each other at different temporal and spatial scales. To define the impact of urbanization on urban precipitation, one of the difficulties encountered is to understand and consider the different interactions and retroactions that each of these processes have upon each other.

It is also difficult to obtain long-term, high spatial resolution measurements, representative enough of the heterogeneity of urban microclimates, or high spatial resolution simulations representative of the impact of urbanization on cities' climates on a climatological scale. The use of daily gridded climate data over the 1988–2017 period has given a new insight into how temperature and precipitation have been modified over time in the Eastern Canadian cities of Toronto, Ottawa, Montreal, and Quebec City, compared to their surrounding rural areas. Factors behind these changes and interactions between these variables in a mid-latitude, North American context, have been discussed and compared between cities. In the context of climate change, the alteration of urban temperature and precipitation is of major interest for the strategic management of water resources, but also for health and safety aspects, as has been shown in the study. To the best of our knowledge, no such study had been conducted in the region.

However, the understanding of the mechanisms behind this alteration still needs improvement. In particular, the physical processes modifying urban precipitation are subject to large and rapid variations and do not affect in the same way all types (convective or frontal), phases (solid or liquid), and intensities of precipitation. Both spatial and temporal resolutions of the monitoring locations used to produce the data studied here might not be fine enough to fully capture the variability of the processes involved. This is particularly the case in the regions of Toronto and Ottawa where the weather stations used are very scarce compared to Montreal and Quebec City. This is why the impact of urbanization on these cities is not as visible, in the same manner as many other studies conducted since the 1960s to understand the variability of precipitation in cities. Until now, finding a consensus on the exact location and intensity of these changes has remained a challenge, making urban precipitation such a controversial topic.

Moreover, a spatially distributed monitoring is essential to accurately describe the spatial variability of a precipitation event. In particular, in this study, nodes belonging to rural areas are averaged as a whole. However, a storm arriving over a city can undergo several phenomena: intensification, split, initiation, or dissipation in or around the urban area (Lorenz *et al.*, 2019 ; Niyogi *et al.*, 2011). This is why improved, high spatial and temporal resolution and long-term monitoring of meteorological events are needed, both to achieve a better comprehension of the processes involved and ultimately generalize the representation of

urban environments in atmospheric models. Predicting the future consequences of the current accelerating urbanization on urban climates is necessary for cities to attenuate this impact on citizens' health, by supporting the adaptation (adjustments of practices and developments) of the urban hydrological cycle.

1.7 Contribution de l'article A

Dans cette analyse réalisée sur les quatre plus grandes villes de l'Est canadien, Montréal est la ville de l'Est canadien qui a été la plus impactée par l'urbanisation sur la période 1988-2017. Outre l'îlot de chaleur urbain nocturne qui est devenu de plus en plus important, jusqu'à atteindre 2°C en moyenne sur l'année, les précipitations sont devenues de moins en moins fréquentes en ville qu'aux alentours, deux phénomènes qui semblent d'ailleurs corrélés.

Il est à noter que ces différences entre climats urbain et rural ont pu être biaisées dans une certaine mesure par différents phénomènes qui n'ont pas été pris en compte dans cette étude, tels que la topographie et les erreurs instrumentales. De plus, la base de données québécoise utilisée n'était pas la plus adéquate pour étudier les climats urbains de Toronto et Ottawa. L'utilisation de réanalyses devrait être priorisée dans de futures études.

Néanmoins, le climat de Montréal a montré des interactions complexes notables entre précipitations, chaleur urbaine et pollution. Cette ville représente ainsi un site idéal pour étudier le signal isotopique des précipitations urbaines. En particulier, nous montrons que la qualité de l'air et les températures ressenties sont notablement améliorées par les précipitations jusqu'à plusieurs jours suivant l'événement. Comprendre comment les précipitations sont modifiées est ainsi d'une importance majeure pour la ville.

En parallèle, nous mettons en évidence que pour atténuer l'impact des ICU, il serait pertinent de considérer l'utilisation de moyens et/ou matériaux permettant de stocker l'eau des précipitations afin de maintenir l'humidité du sol et ainsi rafraîchir l'atmosphère par évaporation du sol durant les journées les plus sèches. À l'heure actuelle, les surfaces hautement imperméables utilisées pour la construction de la ville favorisent le ruissellement et limitent ainsi cet aspect bénéfique des précipitations.

CHAPITRE 2 :
ÉCHANTILLONNAGE DES PRÉCIPITATIONS URBAINES À HAUTE RÉSOLUTION SPATIALE ET TEMPORELLE - PARTIE I

2.1 Mise en contexte de l'article B

Mettre au point une méthodologie efficace pour atteindre une haute résolution spatiale d'échantillonnage avec un personnel et un budget limités a nécessité tout un travail de réflexion. En effet, l'étude isotopique des précipitations nécessite que la composition isotopique des échantillons reste stable, et les collecteurs de précipitations couramment utilisés dans les études isotopiques représentent un coût non négligeable. Pour augmenter le nombre de points de collecte, nous nous sommes appuyés sur la littérature afin de développer des collecteurs de pluie à bas coût permettant de limiter l'évaporation après échantillonnage. Nous avons ensuite testé ces collecteurs en laboratoire afin de déterminer s'ils permettent de conserver la composition isotopique des échantillons pour une période de 3 jours, équivalente à la durée maximale pendant laquelle nous échantillonnerons nos événements. En plus des collecteurs événementiels, des collecteurs mensuels sont également construits, afin que cette méthodologie puisse être appliquée aux besoins de différents projets.

Affordable event and monthly rain samplers: Improving isotopic datasets to understand meteorological processes (Article B)

Published in Rapid Communications in Mass Spectrometry (February 2024)

Cécile Carton [a], Florent Barbecot [a], Jean-François Hélie [a],
Viorel Horoi [b], Jean Birks [c], Antoine Picard [a], Jorge Mona [a]

[a] Department of Earth and Atmospheric Sciences, Geotop—Université du Québec à Montréal, Montreal, Canada
[b] Department of Earth and Atmospheric Sciences, Université du Québec à Montréal, Montreal, Canada
[c] Department of Earth, Energy, and Environment, University of Calgary, Calgary, Canada

2.2 Abstract

Rationale: Water-stable isotopes in rainfall are powerful tracers of atmospheric processes at different spatial and temporal scales. However, commercially available rain samplers for isotopic analysis are prohibitively

expensive, especially for high spatial resolution networks and studies conducted in developing countries. A low-cost, simple, and robust sampler was designed for event and monthly rainfall samplings.

Methods: Rainfall collectors were built based on existing designs provided in the literature and using easily accessible materials. Event samplers were filled with different volumes of reference water and left for 72 h in laboratory conditions to determine the minimum amount of rainfall to be collected to minimize isotopic fractionation, from both postsampling evaporation and equilibration. Samples were analyzed using dual-inlet isotope ratio mass spectrometry and cavity ring-down spectroscopy.

Results: For samples larger than 4% of the bottle's capacity, the evaporative enrichment due to Rayleigh distillation is negligible compared to the overall analytical uncertainty. Using a tube connecting the funnel to the water sample has proved to reduce postsampling evaporation by at least five times. To limit water self-diffusion, we recommend collecting the largest rainfall amount possible. Under these conditions, these collectors are suitable for rainfall sampling for isotopic analysis.

Conclusions: This low-cost methodology will enable isotopic sampling of precipitation at high spatial resolutions and democratize the use of isotopes for hydrological studies in developing countries. All instructions for building and using these samplers are made openly accessible to the scientific community so they can be repeated and adapted to the needs of each project.

2.3 Introduction

Over the past decades, stable isotopes of the water molecule have emerged as powerful tracers that have transformed our understanding of the hydrological cycle across spatial and temporal scales (Clark et Fritz, 1997 ; Leibundgut *et al.*, 2009a). Their distribution in precipitation is an exceptional source of information on the conditions and trajectories of meteorological events (Aggarwal *et al.*, 2016 ; Cortecci *et al.*, 2008 ; Dansgaard, 1964). They have great potential to trace the partitioning of rainfall along different flow paths and to identify surface water sources (Kuhlemann *et al.*, 2020). Water-stable isotopes have the power to give us an unparalleled understanding of the dynamics of precipitation at different spatial and temporal scales. But for that understanding, adequate sampling resolutions are required.

Sampling techniques also need to consider and avoid postsampling evaporation and related fractionation, and satisfying this criterion has driven the design of precipitation samplers described in the literature (Gröning *et al.*, 2012) that are currently available. However, the high cost of commercialized isotopic rain samplers makes it difficult to collect precipitation samples at the spatial resolution needed to study the

dynamics of a meteorological event. Moreover, many developing countries cannot afford these types of samplers.

Therefore, we have designed two versions of a low-cost, simple, and robust rain sampler capable of sampling precipitation for isotopic analysis on the event and monthly scales, based on existing designs provided in the literature (Gröning *et al.*, 2012). We have tested event samplers to determine the amount of rainfall they can sample to minimize isotopic fractionation, from both postsampling evaporation and equilibration. In this paper, we share our simplified method for building these samplers so that it can be repeated based on each project's needs.

2.4 Methods

2.4.1 Instrument development and costs

An existing precipitation collector design that was proven to successfully prevent postsampling evaporation without the use of a sealing oil surface (Gröning *et al.*, 2012) was modified and built using the least expensive materials possible.

To make the sampler resistant to the influence of weather conditions (in particular, ultraviolet radiation from sunlight), both the outer and inner cylinders making the structure of the collector are made of easily available and low-cost polyvinyl chloride (PVC) hard plastic caps and pipes used for plumbing installations. The design of our collector relies on a three-dimensional (3D) printed piece connecting a plastic funnel to an inner polypropylene tube that is screwed to an inner and an outer PVC cap (Figure 2.1). The inner and outer PVC pipes are then connected to the corresponding PVC pipe caps. A high-density polyethylene (HDPE) bottle cap is screwed to the inner PVC pipe cap. When in use, a HDPE bottle can easily be screwed and unscrewed from the bottom of the system.

Figure 2.1: (A), A rain collector mounted on a rebar post (credit: Nathalie St-Pierre, UQAM); (B), 125-mL high-density polyethylene (HDPE) bottle inserted and screwed to the sampler; (C), graphical cross-section of the rain sampler

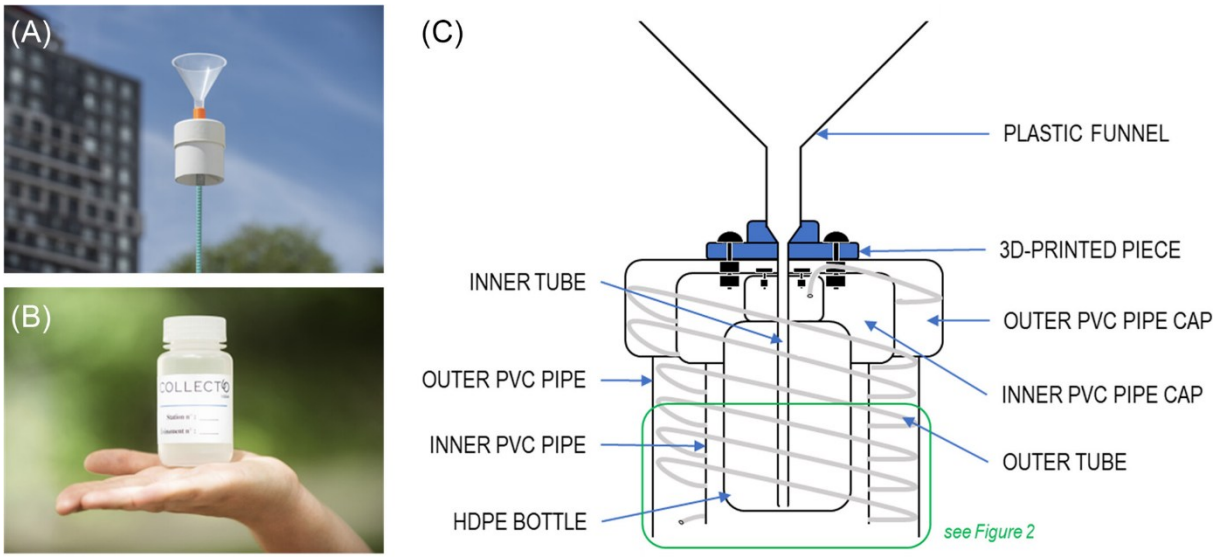

The rain enters the funnel and flows through the inner tube that reaches the bottom of the bottle, progressively filling the bottle. The small inside diameter of the inner tube reduces the surface of evaporation, thus limiting (a) the evaporation flux that can take place through the funnel and (b) the exchange between the small fraction of the water that can evaporate and the water stored in the bottle. This means that even if evaporation occurs, it always takes place in the same small volume of water (shaded red in Figure 2.2), and the evaporation flux is thus continuously fed as the water level is drawn down. Even if the isotopic composition is highly modified in this small fraction of water, the overall isotopic composition of the sample will be very slightly or even negligibly modified. With the diameters of the bottles and the inner tube described here, the overall surface and thus evaporative flux of the water in the inner tube (flux 1, Figure 2.2) are equal to 0.9% of those of the rest of the water sample (flux 2, Figure 2.2) for event-based samplers and 0.3% for monthly samplers (due to the larger bottle size).

Figure 2.2: Schematic of the evaporation fluxes taking place for the water sample inside the bottle (purple) and for the fraction of water contained in the inner tube (red)

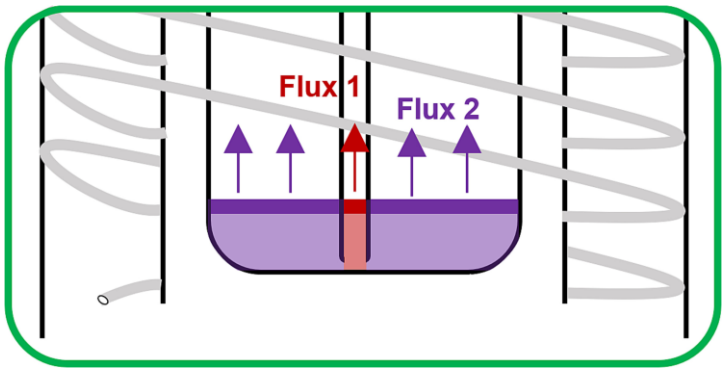

As the bottle is gradually filled with precipitation, the original air present in the bottle needs to escape to equilibrate the pressure. This equilibration is also needed to compensate for variations in atmospheric pressure so that water does not rise from the collector through the plastic tube, back up into the funnel, and get in contact with the open air during low-pressure phases. Therefore, an outer tube is connected to the cap of the bottle, playing the role of a buffer tank. The volume of the tube must be large enough so it can accommodate changes in volume caused by pressure and temperature variations during the monitoring period. This volume was calculated using the ideal gas law (Equation 2.1), with V, P, and T, respectively, the volume, pressure, and temperature of the bottle:

Equation 2.1

$$dV = V\left(\frac{-dP}{P} + \frac{dT}{T}\right)$$

In our study region (Quebec, Canada), variations in temperature and pressure dT and dP are typically ~20 K and ~50 hPa, respectively, with initial values of ~290 K and ~1013 hPa. This leads to a variation in volume dV of ~15 mL maximum for the event sampler, over 125 mL for the empty bottle, and ~118 mL for the monthly sampler, over 1000 mL for the empty bottle.

Finally, we divide dV by the internal surface of the tube to obtain the tube's length needed to contain the predicted dV, which is ~0.5 m for event samplers and ~4 m for monthly samplers. To have a safety margin, we use 5 m of tube length for both samplers.

This plastic tube is coiled up around the inner PVC pipe surrounding the bottle and is protected from sunlight by the outer PVC pipe, which is finally mounted on a rebar with eyebolts screwed into the outer PVC pipe. The bottle can be installed and removed from the bottom of these cylinders. Between sampling events, the

operator only needs to grip the lowest part of the bottle from below, unscrew it from the sampler, and close it with a cap. Then, another empty bottle can be screwed into the sampling device.

Unlike most commercially available rain samplers, no metallic parts were used in this design, making it suitable for collecting samples for most geochemical analyses, in addition to water isotopes. Samplers with metallic surfaces have the potential to contaminate the precipitation sample due to the leaching of metallic ions, limiting their suitability for metal analyses. Contamination from metallic bird deterrents installed on the top of some commercially available samplers has been anecdotally identified as a potential concern for sample quality, so avoiding metallic surfaces was a priority in the design. Because the event sampler is expected to be out only for a few days, a bird deterrent was not included. We would recommend nonmetallic nets to reduce contamination in the monthly sampler model.

PVC parts in the sampler will eventually degrade due to long-term exposure to sunlight and photooxidative degradation of plastic materials. This deterioration is accompanied by changes in appearance, including color changes (progressing from white to yellow, brown, and finally black), cracking, brittling, or softening of the material, and/or formation of a deposit on the surface (Yousif et Hasan, 2015). However, the time period over which this degradation occurs is unpredictable. Users should visually control the appearance of their sampler so that PVC parts can be replaced as soon as the degradation appears. After 2 years of using these collectors, none of the coauthors has observed an aging of these PVC parts.

These rain samplers were not designed to be used in frost-prone conditions. Rainwater falling on the collector would be prone to freezing in the funnel or tube. Before melting and entering the collector, this frozen water could undergo evaporation and/or sublimation, which would alter the isotopic composition of the sample before reaching the inside of the bottle. Users should remove these samplers from the field before such conditions are experienced.

Between all parts, the cost of materials was calculated to be ~34 CAD for the event-based sampler and ~90 CAD for the monthly sampler, which is less expensive than what can be found on the market (~300 CAD for the smaller size and ~900 CAD for the bigger size, without freight charges). All materials and costs of an event-based and a monthly rain sampler are presented in Annexe A.

A video explaining the different steps of the construction of a rain sampler is available at https://youtu.be/oM72V1WqUiM. One main advantage of these samplers compared to what can be found on the market is that different sizes of funnels and bottles can be chosen, and different types of 3D-printed

pieces can be designed, depending on the needs of each project and especially the amount of rainfall to be collected. Equation 2.2 can be used for the specific evaluation of the user's needs in terms of dimensions. The SketchUp design of the 3D-printed piece is available at https://app.sketchup.com/share/tc/northAmerica/byNNPxDKcUE?stoken=HzT4j3jYB80txqZyQkgXyozUdZ96T5zmA7XhXe4ZTiyOh_5RR4dBqBzKeqX5Ccu_&source=web. How to modify and export the piece for 3D printing is explained in Video S1 *(this additional supporting information can be found online in the Supporting Information section at the end of this article)*.

The maximum amount of rainfall that can be collected per event, R_{max} (mm), can be calculated as follows:

Equation 2.2

$$R_{\max} = \frac{V}{\pi R^2}$$

where V is the volume of the bottle (L) and R is the radius of the funnel's top opening (m). The dimensions we use enable us to collect up to 11 mm of rainfall for event-based samplers and 157 mm for monthly samplers.

2.4.2 Evaporation tests

A series of evaporation tests were conducted to evaluate whether the modified design used for the event-based samplers was able to minimize postsampling evaporation (and thus fractionation) and to determine the minimum amount of rainfall that could be collected by the samplers so that its isotopic composition would not be modified by postsampling evaporation. Reference water of known isotopic composition was poured into different 125-mL bottles. The total volume of reference water added to each bottle varied from 5 mL (equal to 0.5 mm of rain) to 125 mL (equal to 11 mm of rain) (Figure 2.3). Each bottle was then screwed back into a dry collector and left in the laboratory for 72 h to reflect field conditions, because we plan to collect the bottles 24–48 h after each event. The reference water was sampled before and after being added to all bottles, and each of these reference samples was analyzed four times. The same series of volumes were added to 125-mL bottles that were sealed with caps so that the results from the bottles stored in the collectors could be compared to those in a completely closed system.

Figure 2.3: Design of the evaporation tests performed on the event rain samplers

If the precipitation amount exceeds the maximum bottle capacity, water may overflow and pool outside the bottle through the outer tube. To test the evaporation and equilibration taking place between the water inside the outer tube and the atmosphere, 200 mL of the reference water was poured through the funnel into a bottle already screwed to the collector.

2.4.3 Analysis

Isotopic analyses were performed in the light-stable isotope geochemistry laboratory of the Geotop research center at the Université du Québec à Montréal. Because very small variations in isotopic compositions are expected, we aimed for the lowest uncertainty possible. In our facility, we achieve lower uncertainties using a cavity ring-down spectrometer for δ^2H, and a dual-inlet isotope ratio mass spectrometer using the equilibration method for δ^{18}O measurement, following the procedures described hereafter.

2.4.3.1 Isotope ratio mass spectrometry

Exactly 200 µL of sample water was pipetted into a 3-mL vial; the vial was closed with a septum cap and then transferred to a 40°C heated rack. After 1 h, the air in the vials was replaced with CO_2 using the AquaPrep system. Samples were left to equilibrate for 7 h. The equilibrated samples were analyzed with an Isoprime 100 IRMS coupled to an AquaPrep system in dual-inlet mode.

Three internal reference waters ($\delta^{18}O = 0.11‰ \pm 0.07‰$, $-13.80‰ \pm 0.06‰$, and $-20.37‰ \pm 0.03‰$) were used to normalize the results. A fourth reference water ($\delta^{18}O = -4.37‰ \pm 0.06‰$) was analyzed as a control to assess the exactness of the normalization. Results are given in delta units (δ) in ‰ versus Vienna Standard

Mean Ocean Water (VSMOW) on the VSMOW-SLAP scale assigning 0‰ to the VSMOW materiel and −55.5‰ to the SLAP material.

The overall analytical uncertainty (1σ) is better than ±0.1‰ for $\delta^{18}O$ based on the propagation of uncertainties of the normalization of the internal reference materials and the samples.

2.4.3.2 Cavity ring-down spectroscopy

One milliliter of water was pipetted into a 2-mL vial that was closed with a septum cap. The samples were analyzed using a Picarro model L2130-i CRDS. Each sample was injected and measured 10 times in express mode, and 1.8 µL was injected into the vaporizer. In the express mode, the first six injections were wet flushed, and the four last injections were measured. The first measured injection was rejected to limit memory effects.

Three internal reference waters ($\delta^2H = 1.22‰ \pm 0.29‰$, $-99.45‰ \pm 0.56‰$, and $-155.92‰ \pm 0.33‰$) were used to normalize the results. A fourth standard water ($\delta^2H = -50.84 \pm 0.72‰$) was analyzed as an unknown to assess the exactness of the normalization. The overall analytical uncertainty (1σ) is better than ±1.0‰ for δ^2H and is based on the long-term measurement of the fourth reference water. Results are given in delta units (δ) in ‰ versus VSMOW on the VSMOW-SLAP scale assigning 0‰ to the VSMOW materiel and −428‰ to the SLAP material.

2.5 Results and discussion

2.5.1 Modeling the extent of evaporation

In a closed system, the isotopic composition of the sample inside the bottle can be approached considering both the equilibration between the liquid and vapor phases of the sample inside the bottle (Equation 2.3) and the mass conservation (Equation 2.4). Overall, the final isotopic composition of the sample can be estimated using the combination of these two equations (Equation 2.5):

Equation 2.3

$$\delta_{V_f} = \delta_{W_f} - \varepsilon_{W/V}$$

Equation 2.4

$$\delta_{W_i} \times V_{W_i} = \delta_{W_f} \times V_{W_f} + \delta_{V_f} \times V_{V_f}$$

Equation 2.5

$$\delta_{W_f} = \frac{\delta_{W_i} \times V_{W_i} + \varepsilon_{w/v} \times V_{V_f}}{V_{V_f} + V_{W_f}}$$

where δ_W and δ_V are the isotopic compositions (either $\delta^{18}O$ or $\delta^{2}H$) of the bottle's liquid water and vapor, respectively, at initial i and final f stages; V_W and V_V are the volumes of the bottle's water and vapor at initial i and final f stages; and $\varepsilon_{w/v}$ is the separation factor of water over vapor.

To ensure that we understand the results of the evaporation experiment, we model the maximum evaporation that would take place to saturate the entire volume of the sampler in a closed system, and what would be the isotopic composition of the water sample having lost the related amount of water, without further contact between the bottle and the surrounding environment.

The temperature inside the laboratory being 20°C, we use a separation factor of 9.7‰ for $\delta^{18}O$ and 82‰ for $\delta^{2}H$ (Majoube, Michel, 1971). We modeled an initial relative humidity of 0% to determine the highest change in isotopic compositions possible.

By using Equation 2.5, the resulting isotopic compositions remain statistically unchanged for all volumes. This means that for a closed system, the evaporation taking place inside the bottle itself should theoretically be negligible compared to the overall analytical uncertainty. By extension, we calculate that the evaporative enrichment should remain negligible for all volumes greater than 0.1 mL of water; however, it was not verified experimentally, mainly because of the minimum volume requirements for isotopic analysis.

In contrast, in an open system such as the inner tube, evaporation will take place if the contact between the sampler's content and the surrounding atmosphere is significant, but the resulting vapor phase will be immediately removed due to the humidity gradient with the atmosphere, and there will be no mass conservation inside the bottle. Postsampling evaporation in an open system will undergo kinetic fractionation following a Rayleigh distillation model, with f the fraction of the remaining liquid water (Equation 2.6). For a constant temperature, this will lead to higher fractionation of the sample than in the closed system:

Equation 2.6

$$\delta_{W_f} = \delta_{W_i} - \varepsilon_{w/v} \ln(f)$$

Using Equation 2.6, we determine that the number of hours (t) before which evaporative enrichment can be detected (i.e., when the change in the isotopic composition is greater than the overall analytical uncertainty) inside the sampler through the inner tube can be determined using Equation 2.7:

Equation 2.7

$$t = \frac{V}{g}\left(1 - \exp\left(-\frac{OAU}{\varepsilon_{\mathrm{w/v}}}\right)\right)$$

Equation 2.8

$$g_{(\mathrm{L/h})} = q\ A\ (x_{\mathrm{s}} - x)$$

Equation 2.9

$$q = 25 + 19v$$

where V is the sample's volume (L), g is the evaporation rate (L/h), OAU is the overall analytical uncertainty (‰), θ is the evaporation coefficient (kg/m^{2}h), A is the water surface area (m^2), x_s is the maximum humidity ratio of saturated air at the same temperature as the water surface (kg/kg), x is the humidity ratio of air (kg/kg), and v is the velocity of air above the water surface (m/s).

We were able to represent how many days will be needed for the sample's evaporation to be seen in the event rain sampler, for different volumes of water, diameters of the inner tube, and overall analytical uncertainties (Figure 2.4).

Figure 2.4: Time after which the fractionation due to the sample's evaporation through the inner tube exceeds the overall analytical uncertainty in $\delta^{18}O$, for water sample volumes ranging from 1 to 120 mL. Evaporation rates observed experimentally (green) and calculated using inner tube inside diameters (ID) of 1/8 in. (blue) and 3/16 in. (orange), and overall analytical uncertainties of 0.1‰ (plain line) and 0.2‰ (dashed line) in $\delta^{18}O$, are investigated

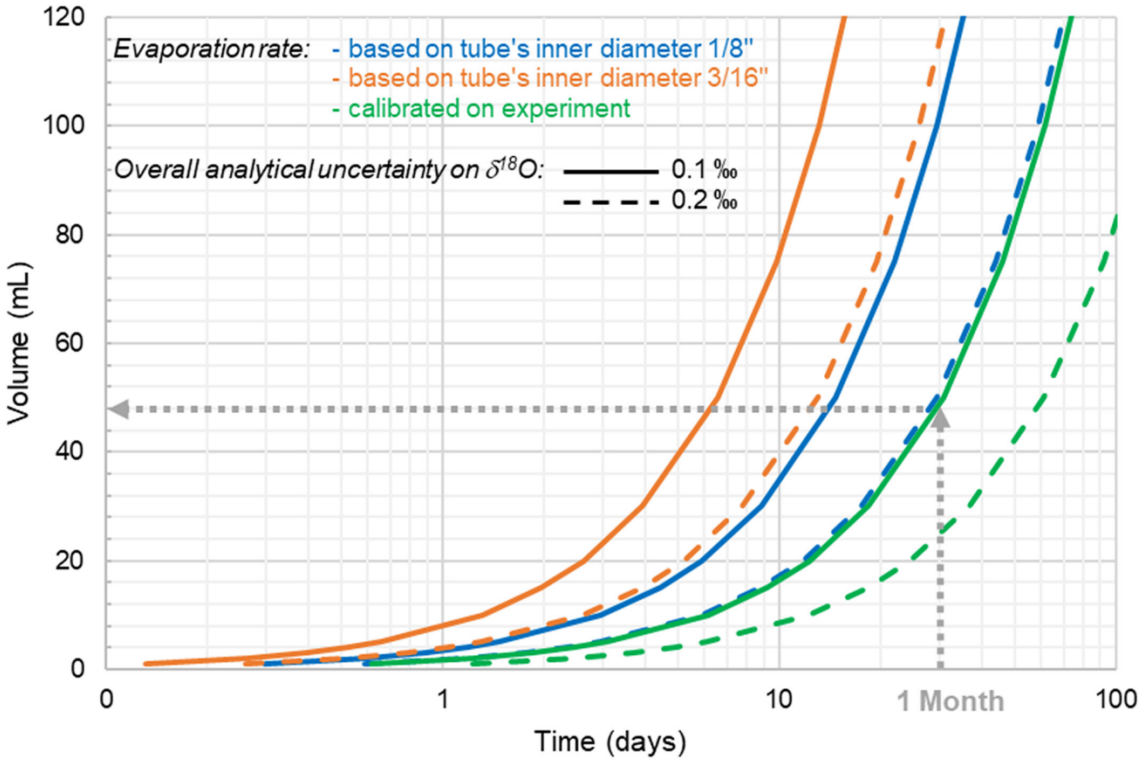

However, one should consider that the sampler is designed so that the inner tube goes to the bottom of the bottle. If the evaporation inside the tube takes place rapidly enough, there will be no fractionation of the sample because the self-diffusion of water inside the tube will not be fast enough to equilibrate the volume of evaporated water inside the tube. This is why we need to compare the evaporation rate (Equation 2.10) to the self-diffusion of water inside the tube (Equation 2.11):

Equation 2.10

$$g_{(\mathrm{m/h})} = q\ (x_s - x)\ 10^{-3}$$

Equation 2.11

$$l_{(\mathrm{m})} = \sqrt{2 \times D \times t}$$

where g is the evaporation rate (m/h), l is the diffusion length (m), D is the self-diffusion coefficient of water (m^2/s), and t is the time of diffusion (s).

The experimental water self-diffusion coefficient (D) being 2.025×10^{-9} m^2/s at 20°C (Holz *et al.*, 2000), in laboratory conditions ($T = 20$°C, $v = 0$ m/s, and a relative humidity [RH] = $(x / x_s) \times 100\%$ of 50%) this leads to evaporation and self-diffusion rates of, respectively, 2×10^{-4} and 2×10^{-3} m/h. Self-diffusion of water is thus an order of magnitude faster than the evaporation rate. However, if the water level is high enough, not only will the evaporation rate be higher due to stronger humidity gradients between the surface and the atmosphere, but self-diffusion of water from the bottom of the tube to the water's surface will take longer.

2.5.2 Results of the experiment

The average isotopic composition of the reference water used for the experiment was −7.2‰ for δ^{18}O and −54.0‰ for δ^{2}H, with an overall analytical uncertainty of 0.1‰ and 1.0‰, respectively.

For all volumes tested here (5–125 mL), the evaporation effects on the isotopic composition of the water in the collector were less than the overall analytical uncertainty for both δ^{18}O and δ^{2}H (Figure 2.5). The smallest sample used in the evaporation tests was 5 mL, or 4% of the collector's capacity.

Figure 2.5: (A) $\delta^{18}O$ and (B) $\delta^{2}H$ isotopic compositions obtained with different sample volumes from 5 to 125 mL, left for 72 h in a bottle screwed to a rain collector (blue) and in a bottle closed with a cap (red). The dashed black line represents the average reference water isotopic compositions, and the gray area is the overall analytical uncertainty surrounding the average reference water isotopic composition

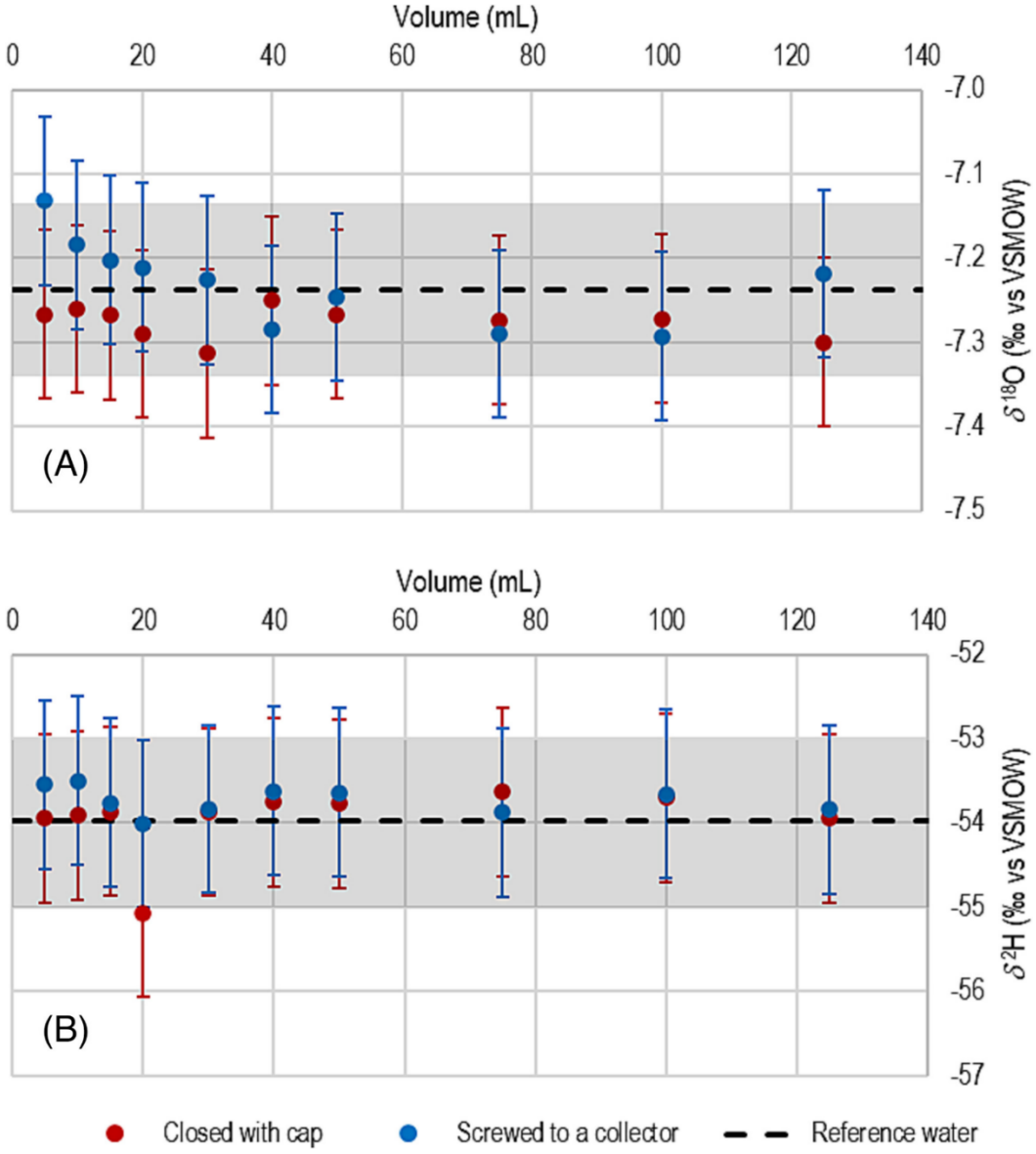

The experimental results are consistent with the model, meaning that the system's design is efficient enough so that for volumes larger than 4% of the bottle's capacity, the fractionation related to Rayleigh distillation can be considered negligible.

Moreover, by overflowing the system (200 mL added to the system), isotopic compositions remain equal to that of the reference water ($\delta^{18}O = -7.3‰$, $\delta^{2}H = -53.5‰$), meaning that isotopic changes caused by the equilibration between the water filling the equilibration tube and the atmosphere are negligible compared to

the overall analytical uncertainty. The reduced inner diameter and important length of the tube contribute to limit the self-diffusion of water inside the tube.

An evaporation effect can be observed on smallest volumes (up to 40 mL), in adequation with our model: smaller volumes mean smaller heights of water inside the inner tube, leading to quicker water self-diffusion from the bottom of the tube to the water's surface. Moreover, for larger volumes, the humidity gradient between the water's surface and the atmosphere is stronger, which leads to higher evaporation rates. This hypothesis was verified with a last experiment that is provided in Annexe B. With a reduced evaporation rate, the isotopic composition of smaller volumes is more affected by the self-diffusion of water. This is why we recommend designing collectors so that they can sample the largest amounts of water, ideally without overflowing the system. As the mass difference between molecules $^{1}H^{1}H^{16}O$ and $^{1}H^{1}H^{18}O$ is greater than that between molecules $^{1}H^{1}H^{16}O$ and $^{1}H^{2}H^{16}O$, the evaporation effect is more pronounced for $\delta^{18}O$ than $\delta^{2}H$.

Moreover, a theoretical evaporation rate of 0.003 mL/h ($RH = 50\%$, $v = 0$ m/s) was calculated using Equation 2.8, which would lead to a cumulated water loss of 0.2 mL after 72 h of the experiment. For all volumes tested, our experimental results show from 0.017 to 0.043 mL of cumulated loss, which means at least five times less evaporation. As the inner tube's length was not a parameter considered in Equation 2.8, this result shows the ability of the inner tube to reduce postsampling evaporation by decreasing the humidity gradient between the water sample's surface and the surrounding atmosphere. Reducing the tube's inner diameter would further limit postsampling evaporation (Figure 2.4); however, this parameter was not tested experimentally.

Experimental results show that the water loss due to evaporation was <0.05 mL in 3 days, giving an evaporation rate of <0.0007 mL/h. Figure 2.4 was adapted to show the theoretical time after which the fractionation due to the sample's evaporation through the inner tube exceeds the overall analytical uncertainty in $\delta^{18}O$, calculated using not only previous theoretical free surface evaporation rates (Equation 2.8) but also this experimental evaporation rate.

Monthly samplers were not tested experimentally; however, Figure 2.4 shows that the event samplers tested in this article are valuable for monthly sampling for a minimum cumulated volume of 48 mL. It should be noted that the length of the inner tube in the event sampler is shorter than that of the monthly sampler. The self-diffusion of water in the tube will be less important in the monthly sampler. The minimum volume to be considered for the monthly sampler is then even lower than 48 mL, or 8 mm of rainfall with the funnel

size used in the monthly sampler design (9 cm diameter). This amount is generally largely exceeded in mid-latitude, nonarid climates.

2.6 Conclusion

We designed event-based and monthly rain samplers so that they could be made at a much lower cost than samplers currently available on the market. Even with sample volumes that are only 4% of the bottle's capacity, and after 72 h of storage, the isotopic composition of the sample collected in event-based rain samplers does not show any indication of evaporative enrichment. The use of a tube connecting the funnel to the water sample has proved to reduce postsampling evaporation by at least five times. We were able to predict the time required for evaporative enrichment effects to be seen for different volumes of water, diameters of the inner tube, and overall analytical uncertainties. Under these conditions, postsampling evaporation due to Rayleigh distillation can be considered negligible, and these collectors are adapted for the sampling of rainfall for stable water isotope analyses. The self-diffusion of water has more potential to affect the sample's isotopic composition for smaller volumes of water. Both for this reason and to limit evaporation inside the bottle itself, we would recommend using sizes of funnels and bottles allowing to collect an amount of rain that is the closest to the maximum amount of rain that can be collected, while making sure it does not exceed it.

These new rain samplers will enable the sampling of precipitation for water isotope measurements at spatial resolutions that were not previously available. All the instructions for constructing and using them are made openly accessible to the scientific community. The materials chosen are easily found in any hardware store. This open-access and low-cost methodology will also help democratize the use of stable water isotopes for hydrological studies in developing countries.

2.7 Contribution de l’article B

Dans cet article, nous nous sommes ainsi appuyés sur la littérature afin de construire des collecteurs événementiels et mensuels de pluie en utilisant des matériaux à bas coût, facilement trouvables sur le marché. Pour la suite de ce projet, nous avons ainsi construit une cinquantaine de collecteurs événementiels, nous permettant de collecter jusqu’à 12 mm de pluie. Nous avons montré que pour les échantillons dont le volume est supérieur à 4% de la capacité de la bouteille, soit 0.5 mm dans le cas des échantillonneurs événementiels, le fractionnement lié à l’évaporation post-échantillonnage reste négligeable. Nous recommandons de collecter les échantillons les plus volumineux possible, sans toutefois dépasser la capacité de la bouteille.

En partageant en détail la méthodologie à moindre coût utilisée, adaptable aux besoins de chaque projet, nous espérons ainsi faciliter l'échantillonnage de pluie pour étude isotopique, que ce soit pour augmenter les résolutions spatiales d'échantillonnage, tel que pour ce projet, mais également pour démocratiser l'utilisation des isotopes dans les pays en développement.

CHAPITRE 3 :
ÉCHANTILLONNAGE DES PRÉCIPITATIONS URBAINES À HAUTE RÉSOLUTION SPATIALE ET TEMPORELLE - PARTIE II

3.1 Mise en contexte de l'article C

La difficulté de l'échantillonnage de pluie à l'échelle intra-événementielle réside principalement dans l'investissement en temps requis pour l'opérateur. Pour remédier à ce problème, l'utilisation d'échantillonneurs automatiques de pluie est une solution efficace, qui permet de collecter des échantillons à un pas de temps ou un volume programmés avant l'événement. Cependant, construire de tels échantillonneurs demande un budget et des ressources qui dépassaient largement ceux de ce projet.

Comme dans de nombreux laboratoires d'hydrologie, nous avions accès à des échantillonneurs automatiques d'eau de surface, et c'est ainsi que nous avons eu l'idée de les adapter pour échantillonner la pluie tout en conservant la signature isotopique des échantillons après collecte. Comme pour les collecteurs événementiels de pluie, nous avons effectué des tests d'évaporation en laboratoire sur une période de 3 jours, qui nous ont permis d'évaluer l'efficacité de différents designs pour limiter l'évaporation post-échantillonnage, et ainsi choisir le plus adapté.

Adapting automatic water samplers for the isotopic study of rainfall at high temporal resolution (Article C)

Published in Rapid Communications in Mass Spectrometry (March 2025)

Cécile Carton [a], Florent Barbecot [a], Jean-François Hélie [a], Viorel Horoi [b], Jean Birks [c]

[a] Department of Earth and Atmospheric Sciences, Geotop–Université du Québec à Montréal, Montréal, Québec, Canada

[b] Department of Earth and Atmospheric Sciences, Université du Québec à Montréal, Montréal, Québec, Canada

[c] Department of Earth, Energy, and Environment, University of Calgary, Calgary, Alberta, Canada

3.2 Abstract

Rationale: Stable water isotopes in precipitation are powerful tracers of atmospheric processes. Automatic rain samplers are valuable for high temporal resolution isotopic studies but building them from scratch

requires significant financial and material resources. A commercial water autosampler has been modified to prevent post-sampling evaporation and to allow for intra-event precipitation sampling.

Methods: New sampling bottles were created by reducing the original volume and opening area. Evaporation tests were carried out on different volumes of water for 72 h under laboratory conditions. These were used to determine the minimum amount of rain to collect to minimize the impact of isotopic fractionation by evaporation. The impact of the autosampler's air moisture saturation was also tested. Samples were analyzed by dual-inlet isotope ratio mass spectrometry and cavity ring-down spectroscopy.

Results: For samples larger than 10 mL, evaporative heavy isotope enrichment due to Rayleigh distillation remains negligible compared with the overall analytical uncertainty. Intentional saturation of the autosampler's atmosphere significantly reduces post-sampling evaporation but leads to equilibration of the samples with the added water. We have investigated the maximum time that samples must be left for this fractionation to remain negligible. Under these conditions, this autosampler is suitable for intra-event rainfall sampling for isotopic analysis.

Conclusions: It is now possible to perform low-cost high-resolution precipitation sampling for isotopic analysis. The intentional air saturation of the sampler, which effectively prevents post-sampling evaporation, had never been proposed before. All instructions for modifying this sampler are now available in open access so the scientific community can easily repeat them.

3.3 Introduction

Rainfall isotopic analyses are very relevant for the tracing of the conditions, surface water sources, and trajectories of meteorological events. In particular, intra-event rainfall sampling gives valuable information on the atmospheric dynamics behind the formation of precipitation (Aggarwal *et al.*, 2016 ; Cortecci *et al.*, 2008 ; Dansgaard, 1964). However, the time and resources needed for operators to sample rainfall at this high temporal resolution make it difficult to achieve. In any location without on-site personnel, it may not be possible to obtain intra-event data. Moreover, sampling techniques must consider and avoid post-sampling evaporation and related fractionation.

Previous studies have investigated the design of automatic rain samplers to satisfy these criteria (Michelsen *et al.*, 2019). However, building them from scratch requires financial and material resources that many laboratories cannot afford.

However, it is quite common for hydrological laboratories to possess surface water automatic samplers. Although most of them do not have an efficient evaporation reduction mechanism, more complex samplers are commercially available but usually expensive (several thousand euros). Finding a low-cost way to modify and use simple surface water samplers to collect rainwater and prevent post-sampling evaporation would be very useful. Previous work has already shown the possibility of modifying the opening of an autosampler to collect both surface water and rainfall (von Freyberg *et al.*, 2020), but the 1-L bottles would be too large to prevent evaporative fractionation if used to collect small intra-event volumes expected in midlatitude areas.

Intra-event sampling can provide important information on local atmospheric processes. First, the heavy isotope depletion of precipitation associated with Rayleigh distillation can be tracked over the course of an event. This can be particularly important for characterizing the precipitation formation temperature and the remaining fraction of water vapor in the cloud. In addition, an increase in d-excess can give indications of water vapor inputs into the cloud or allow us to identify secondary evaporation of precipitation as it falls to the ground (Tang *et al.*, 2023).

Hence, we have modified an automatic surface water sampler to collect intra-event rainwater samples in situations where it is possible to retrieve the sampler a few days later. We have tested different designs to prevent post-sampling evaporation and determined the minimum amount of rainfall each sample should contain so the isotopic fractionation remains negligible. In this paper, we share our simplified method for modifying this sampler so that it can easily be reproduced.

3.4 Methods

3.4.1 Instrument development and costs

We use PST8 automatic samplers from Manning Environmental, initially built to collect surface water samples. A programmable electronic panel device allows one to choose a sampling timestep from minutes to hours. At each timestep, the rotating spout moves to 1 of the 24 bottles designed for the sampler, and a peristaltic pump collects surface water flowing through the rotating spout into this bottle.

To adapt these automatic samplers, the peristaltic pump was disconnected. A 30-cm diameter funnel collecting the rainfall directly feeds the rotative spout (Figure 3.1). The funnel is connected to the spout using a 3D-printed piece assemblage (Figure 3.1), whose design can be found on the following links:

- Funnel support (https://app.sketchup.com/share/tc/northAmerica/467_TY4vkxI?stoken=BrkUx5l3BEHEnT4l68aRhn-48VTkcX5ffdE6oEkoLf5UU1Su6QViQ9xKTCbjftx2&source=web);

- Inner piece 1 (https://app.sketchup.com/share/tc/northAmerica/O_PW10__-PU?stoken=2HTmnwM4wiMWif5fAL09W2MJo_Be90HNvaqL87GYimgLMfUvTF-9G74FMZlqnMg0&source=web);

- Inner piece 2 (https://app.sketchup.com/share/tc/northAmerica/aIgedp5PVIc?stoken=4cyFkNkXeu5fu19Gs63L3SfEAEUhYf53kd87QgjMycJnhSliPtz6e1rxBPFQj5O7&source=web).

Figure 3.1: Graphical cross-sections and pictures of each panel of the modified autosampler (modified from https://manningenvironmental.com/).

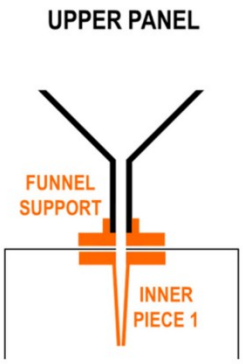

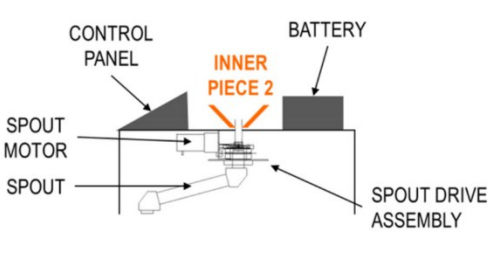

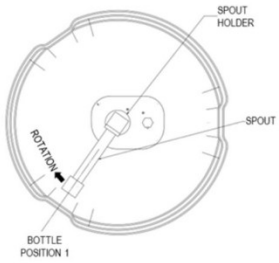

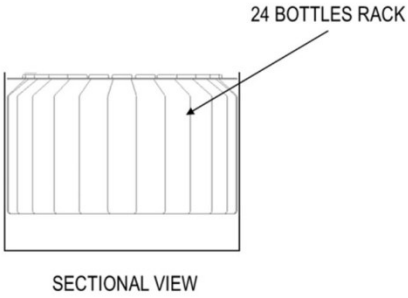

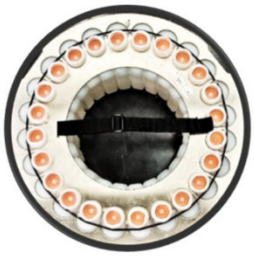

The rain flows down the funnel and then the spout without any electronic intervention, finally reaching the programmed bottle position. The sampling timestep, meaning the period during which each bottle will be filled, can be chosen according to forecasts. Please note that it is also possible to trigger the sampling in combination with a rain gauge.

The 24 bottles originally designed for use with the sampler are 500 mL, thus too large for intra-event rainfall sampling in midlatitude areas without evaporation taking place inside the bottle itself.

The maximum amount of rainfall that can be collected per bottle, R_{max} typically expressed in mm, can be calculated as the following:

Equation 3.1

$$R_{\max} = \frac{V}{\pi R^2}$$

with V the volume of the bottle (L) and R the radius of the funnel's top opening (m).

We modified the sampling bottles by placing an insert in each of them. The insert is made from a 50-mL centrifuge tube, more adapted to this temporal resolution. Along with the 30-cm funnel, 50 mL allows us to get an average of 0.5 mm of rain per sample, which is more realistic at a sub-event scale.

To furthermore prevent post-sampling evaporation, we reduced the surface of evaporation, by placing small funnels on top of each centrifuge tube, connected to an inner tube going to the bottom of the centrifuge tube (Figure 3.2 A-C), as recommended in several studies (Carton *et al.*, 2024b ; Gröning *et al.*, 2012 ; Michelsen *et al.*, 2019 ; von Freyberg *et al.*, 2020). With the diameters of the centrifuge tube and the inner tube described here, the overall surface and thus evaporative flux of the water comprised in the inner tube (Flux 1, Figure 3.2D) are equal to 12% of those of the rest of the water sample (Flux 2, Figure 3.2D).

Figure 3.2: (A) The funnel, 3D-printed piece, and inner tube used to prevent evaporation from the centrifuge tube; (B) three adapted centrifuge tubes, with a plastic ball inside each funnel; (C) upper view of the modified bottle; (D) cross-section of the design used to prevent post-sampling evaporation.

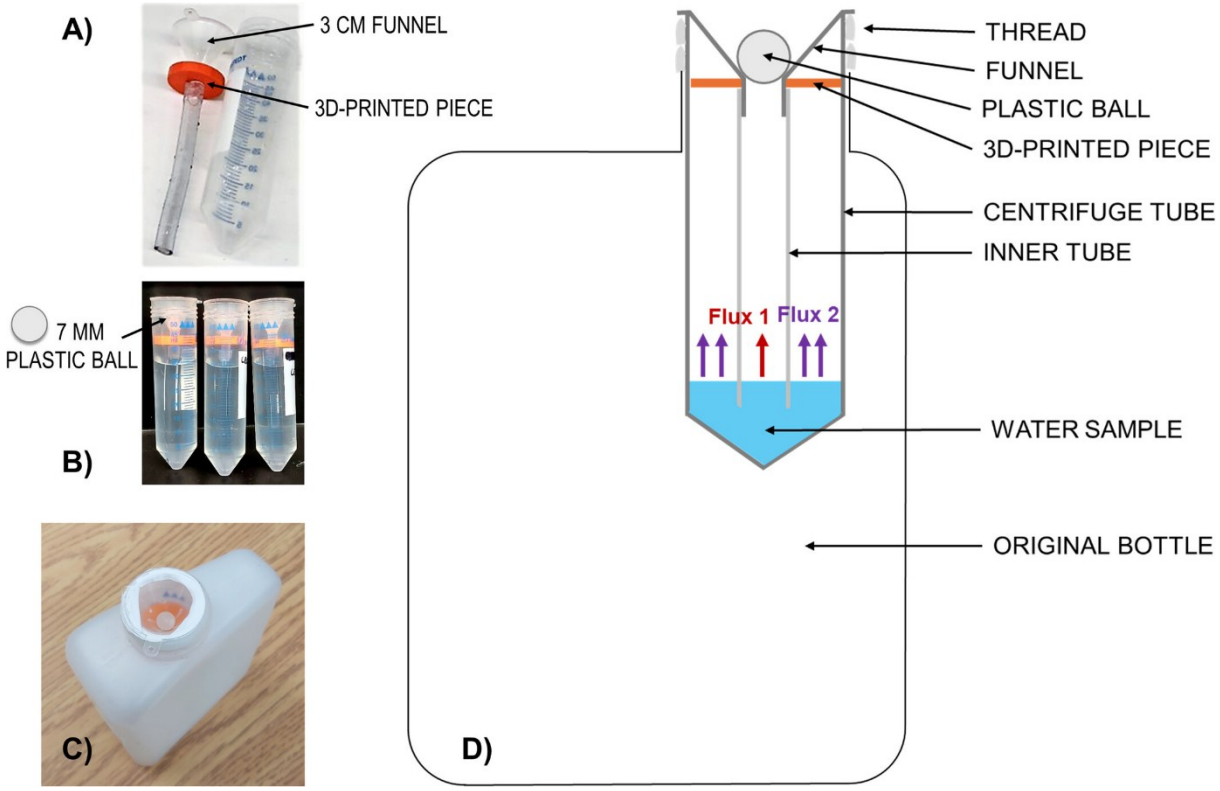

A 3D-printed plastic piece stabilizes the small funnel and helps for isolation between the sample and the atmosphere (orange ring on Figure 3.2). Its design can be found on the link (https://app.sketchup.com/share/tc/northAmerica/9cj2HL_FgUs?stoken=tBhxp7p_8DGZOkhS1rKtsTVZUZOqw3ToehBp5t7h__p3HI3vJac0wyROa2pCNcVk&source=web).

It is worth noting that the 3D-printed part is deliberately not sealed inside the centrifuge tube, making it easy to remove the sample evaporation prevention system, close the centrifuge tube with its original cap, and store the water sample before isotopic analysis. This means that the system is not air-tight and allows pressure equilibration with the atmosphere without the use of an external tube (von Freyberg *et al.*, 2020).

Because the 3D-printed pieces do not completely seal the funnel-tube assembly, we have taped the edges of the funnel with the tube using Teflon tape before each sampled event. For further limitation of the samples' evaporation, a polypropylene ball is placed inside each funnel, so that the rain can flow inside, but once collected the sample's water vapor cannot escape from it (Prechsl *et al.*, 2014) (Figure 3.2 B,C). As the

funnel's plastic is smooth, we have noticed that it is difficult for water to flow under the ball. This is why we made shallow vertical cuts in the funnel's plastic to allow water flow.

Finally, we tested the possibility of saturating the autosampler by pouring water into the bottom of the autosampler before the rainfall sampling. The surface of the sampler's bottom being ~10 times bigger than the surface of the centrifuge tube's opening, the evaporation will preferentially take place from the bottom of the autosampler and prevent evaporation of the samples.

The initial cost of a surface water peristaltic automatic sampler is high, the one used in this study being around 3000 CAD. However, adapting it to automatically sample rainfall is very easy and low-cost, with a total price of ~160 CAD (Table 3.1). The time needed to do this modification is not included in the cost. It should be noted that modifying the automatic sampler does not damage it, and it can still be used for its initial function.

Table 3.1: Materials and costs of the modification of the automatic rain sampler.

Piece (quantity)	Total price
30 cm funnel (1)	20 CAD
3D printed connectors (1)	14 CAD
Centrifuge tubes (100)	48 CAD
3 cm funnels (24)	48 CAD
3D printed discs (24)	12 CAD
7 cm pieces of Tygon (24)	6 CAD
Plastic balls (100)	15 CAD

Please note that these parts were designed for PST8 automatic samplers from Manning Environmental. They may have to be adjusted for different models. This can easily be made using the SketchUp designs shared in this article.

3.4.2 Evaporation tests

A series of evaporation tests were conducted to determine the best way to limit evaporation when collecting intra-event precipitation samples for situations when the sampler can be visited and emptied within a few days of the event.

First, we wanted to limit evaporation through the opening of the centrifuge tube itself. In particular, our aim was to assess if the funnel is efficient enough to prevent evaporation from the centrifuge tube; if using the plastic ball makes a significant difference in preventing evaporation through the funnel itself; and what is the minimum volume to sample to consider the isotopic change negligible compared with the overall analytical uncertainty.

For that, reference water of known isotopic composition was poured into each 50-mL centrifuge tube of the 24-bottle rack. The isotopic composition of the reference water used for the experiment was −7.3‰ for $\delta^{18}O$ and −54‰ for $\delta^{2}H$.

The total volume of reference water added to each bottle was 2, 5, 10, and 20 mL (respectively equivalent to 0.02, 0.05, 0.1, and 0.2 mm of rain). For each quantity, three centrifuge tube closing systems were tested: one with a funnel, one with a funnel + plastic ball, and one completely open (Table 3.2, Annexe C). For a better representativity of the results, each test was replicated two times.

Table 3.2: Evaporation tests experimented on each sample's volume.

	Open tube	Funnel	Funnel + Ball	Closed by a cap
Free atmosphere	aa bb cc dd	aa bb cc dd	aa bb cc dd	aa bb cc dd
Dry sampler	aa bb cc dd	aa bb cc dd	aa bb cc dd	
Saturated sampler	aa bb cc dd	aa bb cc dd	aa bb cc dd	

Note: a, 2 mL; b, 5 mL; c, 10 mL; d, 20 mL.

For each volume, a test was also realized for centrifuge tubes closed by their caps. For the rest of this study, they will be used as a reference to show the maximum evaporation that can take place for different volumes inside the centrifuge tube itself.

Moreover, the tests were also designed to determine how the automatic sampler prevents evaporation compared with samples left in the laboratory air and if moisture saturating the sampler's air by filling the bottom of the sampler with water is helpful to prevent evaporation from the samples.

This is why one rack of the 24 centrifuge tubes described before was placed in three different systems: in a free laboratory atmosphere, in a dry automatic sampler, and in a sampler filled with water of isotopic composition very different from the tap water filling the samples (Table 3.2, Annexe C).

The experiment was performed in laboratory conditions for 72 h because samples are planned to be collected 24 to 48 h after each meteorological event is sampled. Each of these centrifuge tubes was weighed before and after the experiment to calculate the evaporation losses. The reference tap water was sampled before and after each filling of the different systems, as well as the water in the bottom of the saturated sampler. That makes a total of 86 samples (Table 3.2).

For intra-event sampling and at the site we modified these samplers for, we were not expecting large temperature variations and did not plan to test or reduce this phenomenon on our autosamplers. If the user expects large temperature changes during sampling, we recommend adding cooling devices to reduce dilatation and compression of the air in the system and/or testing the impact these variations have on the system's water vapor isotopic composition.

3.4.3 Analysis

Isotopic analyses were performed in the light-stable isotope geochemistry laboratory of the Geotop Research Center at the *Université du Québec à Montréal*. Because very small variations in isotopic compositions are expected, we aimed for the lowest uncertainty possible. In our laboratory, we achieve lower uncertainties using a cavity ring-down spectrometer for δ^2H, and a dual-inlet isotope ratio mass spectrometer using the equilibration method for δ^{18}O measurement, following the procedures described hereafter.

3.4.3.1 Isotope ratio mass spectrometry

Exactly 200 µL of sample water was pipetted into a 3-mL vial, sealed with a septum cap, and then transferred to a 40°C heated rack. After 1 h, the air in the vials was replaced with CO_2 using the AquaPrep system. Samples were left to equilibrate for 7 h. The equilibrated samples were analyzed with an Isoprime 100 IRMS coupled to an AquaPrep system in dual-inlet mode.

Three internal reference waters ($\delta^{18}O = 0.11‰ \pm 0.07‰$, $-13.80‰ \pm 0.06‰$, and $-20.37‰ \pm 0.03‰$) were used to normalize the results. A fourth reference water ($\delta^{18}O = -4.37‰ \pm 0.06‰$) was analyzed as a control. Each set of standards was measured at each sequence's beginning, middle, and end. The overall analytical uncertainty (1σ) is better than ± 0.1‰ for δ^{18}O based on the propagation of uncertainties of the normalization of the internal reference materials and the samples. Results are given in delta units (δ) in ‰ versus Vienna Standard Mean Ocean Water (VSMOW) on the VSMOW-SLAP scale assigning 0‰ to the VSMOW material and −55.5‰ to the SLAP material.

3.4.3.2 Cavity ring-down spectroscopy

One milliliter of water was pipetted into a 2-mL vial that was closed with a septum cap. The samples were analyzed using a Picarro model L2130-i CRDS. Each sample was injected and measured 10 times in express mode, and 1.8 µL was injected into the vaporizer. In the express mode, the first six injections were wet flushed, and the four last injections were measured. The first measured injection was rejected to limit memory effects. Thus, each value represents three injections.

Three internal reference waters (δ^2H = 1.2‰ ± 0.3‰, −99.5‰ ± 0.6‰, and −155.9‰ ± 0.3‰) were used to normalize the results. A fourth standard water (δ^2H = −50.8 ± 0.7‰) was analyzed as a control. Each set of standards was measured at each sequence's beginning, middle, and end. The overall analytical uncertainty (1σ) is better than ± 1.0‰ for δ^2H and is based on the long-term measurement of the control. Results are given in delta units (δ) in ‰ versus VSMOW on the VSMOW-SLAP scale assigning 0‰ to the VSMOW material and −428‰ to the SLAP material.

3.5 Results & discussion

3.5.1 The centrifuge tube sensitivity to evaporation

It is expected that vials left outside the sampler will show the highest evaporation and therefore higher fractionation. To determine the efficiency of the funnel and the funnel + plastic ball in preventing post-sampling evaporation, we compared the samples left outside the autosampler with three different openings: completely open samples, samples closed by a funnel, and samples closed by a funnel + plastic ball (Figure 3.3 A,B).

Figure 3.3: Relative loss of each sample's volume for the test on the centrifuge tube sensitivity to evaporation (A) and the test on the automatic sampler's internal conditions (C); isotopic composition differences ($\Delta\delta^{18}O$) between the samples and the reference water for the test on the centrifuge tube sensitivity to evaporation (B) and the test on the automatic sampler's internal conditions (D).

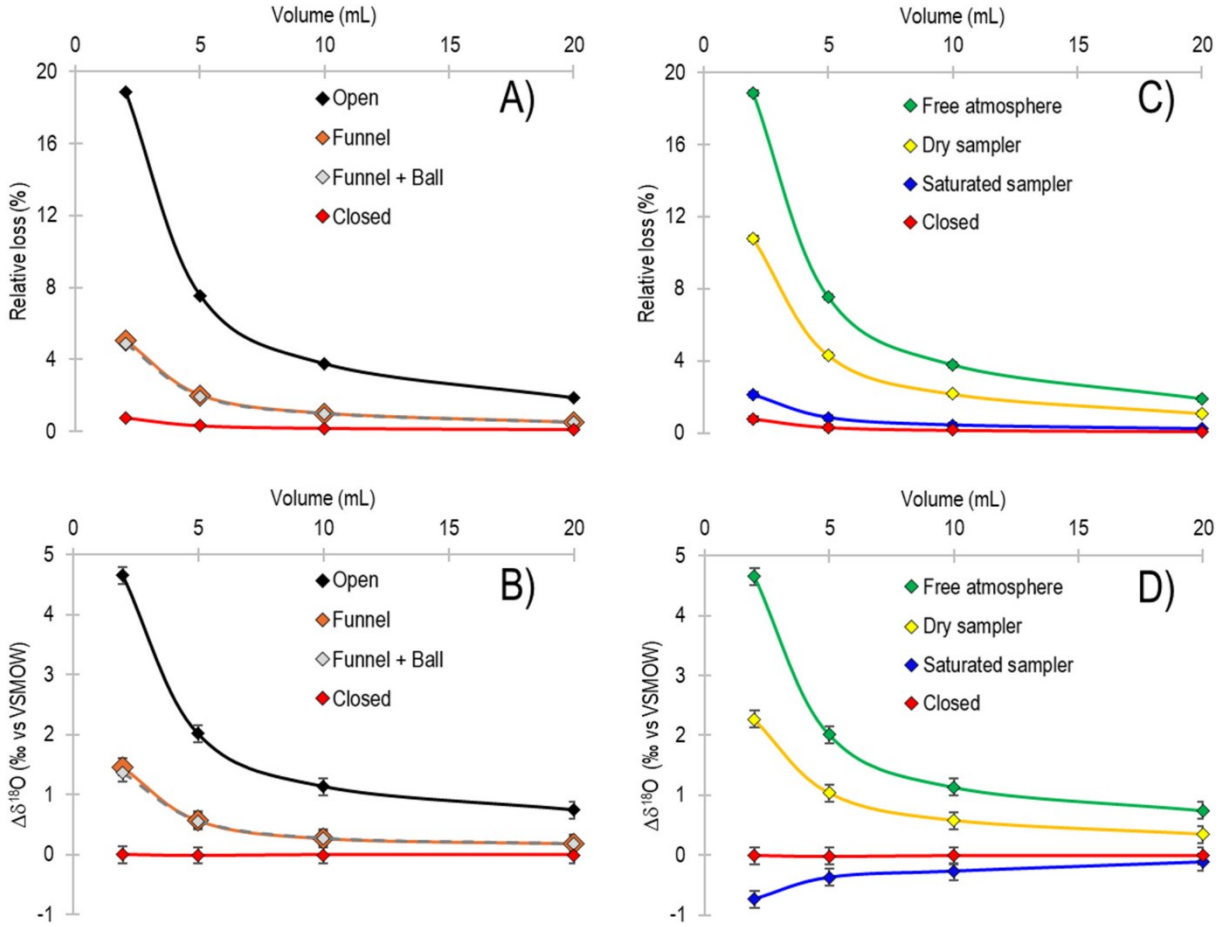

Evaporation tests carried out on centrifuge tubes closed with a cap are used as a reference to discuss the effectiveness of different closure systems (funnel or funnel + plastic ball) in limiting post-sampling evaporation.

We have modeled the maximum evaporation that would occur in centrifuge tubes closed by a cap to saturate the entire interior volume with air. This evaporation can slightly modify the isotopic composition of water samples without any further exchange between the tube and the surrounding environment.

In a closed system, the isotopic composition of the sample can be approached considering both the equilibration between the liquid and vapor phases of the water sample inside the centrifuge tube (Equation 3.2) and the mass conservation of the sample (Equation 3.3). Overall, the final isotopic composition of the sample can be estimated with the combination of these two equations (Equation 3.4).

Equation 3.2

$$\delta_{V_f} = \delta_{W_f} - \varepsilon_{W/V}$$

Equation 3.3

$$\delta_{W_i} \times V_{W_i} = \delta_{W_f} \times V_{W_f} + \delta_{V_f} \times V_{V_f}$$

Equation 3.4

$$\delta_{W_f} = \frac{\delta_{W_i} \times V_{W_i} + \varepsilon_{w/v} \times V_{V_f}}{V_{V_f} + V_{W_f}}$$

with δ_W and δ_V, respectively, the isotopic compositions (either $\delta^{18}O$ or δ^2H) of the tube's liquid water and vapor at initial i and final f stages; V_W and V_V are the volumes of the bottle's water and vapor at initial i and final f stages; and $\varepsilon_{w/v}$ the separation factor of water over vapor.

For the calculation of the final isotopic composition of the sample in Equation 3.4 and as the temperature inside the laboratory is 20°C, we use a separation factor $\varepsilon_{w/v}$ of 9.7‰ for $\delta^{18}O$ and 82‰ for δ^2H (Majoube, Michel, 1971); δ_{Wi} and V_{Wi} are measured, as they refer to the original reference water; and V_{Wf} and V_{Vf} are calculated based on the maximum water content the air inside the centrifuge tube can contain. We considered an initial relative humidity of 0% to determine the highest change of isotopic compositions.

By extension of Equation 3.4, we calculated that the resulting isotopic composition change remains negligible for all volumes greater than 0.05 mL. This result was verified experimentally for volumes of 2, 5, 10, and 20 mL. For all these volumes tested in the centrifuge tubes closed with caps, not only the relative mass loss is small even for 2-mL samples (Figure 3.3A) but changes in isotopic compositions of the water were less than the overall analytical uncertainty for both $\delta^{18}O$ and δ^2H (Figure 3.3B). This means that the isotopic effect of the evaporation that takes place inside the centrifuge tube itself (closed system) is negligible for the tested water volumes. Any isotopic change will be directly linked to exchange with the surrounding atmosphere. We could not verify experimentally that it is the case for all water volumes greater than 0.05 mL below 2 mL, mainly because of the minimum volume requirements for isotopic analysis.

In a non-fully closed system such as a completely open centrifuge tube, or a centrifuge tube modified with a funnel or a funnel + plastic ball, evaporation can have a greater impact. Post-sampling evaporation in such an open system will undergo a Rayleigh distillation model (Equation 3.5). This will lead to higher isotopic signature change of the water sample than in the closed system.

Equation 3.5

$$\delta_{W_f} = \delta_{W_i} - \varepsilon_{w/v} \ln(f)$$

with f the fraction of the remaining liquid water.

Considering identical evaporation conditions, the relative water loss is expected to be higher for smaller volumes than for larger volumes. Then smaller samples are expected to be the most enriched in heavy isotopes compared with the reference water isotopic composition. This can be observed for all modifications of the centrifuge tube opening left outside the sampler (Figure 3.3 A,B and Tables Table 3.3 and Table 3.4).

Table 3.3: Evaporative losses averaged between samples of all volumes and their uncertainty at 1σ.

	Open	Funnel	Funnel + Ball
Free atmosphere	**0.38** ± 0.06 g	**0.10** ± 0.01 g	**0.10** ± 0.02 g
Dry sampler	**0.22** ± 0.04 g	**0.06** ± 0.01 g	**0.06** ± 0.01 g
Saturated sampler	**0.04** ± 0.01 g	**0.01** ± 0.01 g	**0.02** ± 0.01 g

Table 3.4: Measured $\delta^{18}O$ differences ($\Delta\delta^{18}O$) between the average of the two duplicates of the 2-mL samples and the reference water.

	Open	Funnel	Funnel + Tube
Free atmosphere	**4.7** ± 0.1 ‰	**1.5** ± 0.0 ‰	**1.4** ± 0.0 ‰
Dry sampler	**2.3** ± 0.0 ‰	**0.8** ± 0.0 ‰	**0.7** ± 0.0 ‰
Saturated sampler	**-0.7** ± 0.1 ‰	**-0.3** ± 0.0 ‰	**-0.2** ± 0.0 ‰

In addition, the evaporation fluxes will be controlled by the exchange surface between the centrifuge tube's inner part and the surrounding atmosphere. According to the mass loss results, the evaporation is significantly reduced using a funnel, compared with the case where the centrifuge tube is left open (Figure 3.3A). For 2-mL samples, the evaporation loss is divided by 4 (Table 3.3). The same behavior can be observed for isotopic compositions. For each volume and particularly smaller ones, the use of a funnel significantly reduces the change in isotopic compositions (Figure 3.3B). For 2-mL samples, the change in isotopic compositions is divided by 3 (Table 3.4).

The evaporation and the related enrichment of isotopic compositions are nonetheless significantly different than the reference water for 2- and 5-mL samples (Figure 3.3B, Table 3.4). As expected, the isotopic compositions of the samples closed by a funnel are more enriched than the samples closed by a cap (Table 3.4). At first glance, it seems that there is evaporation taking place in the inner tube through the hole of the funnel. However, for each volume, both the changes in isotopic compositions and mass losses due to using a plastic ball on top of the funnel compared with using a bare funnel are equivalent (Figure 3.3 A,B, Table 3.3 and Table 3.4). It seems that using a plastic ball does not significantly prevent evaporation.

This means that even if the hole of the funnel is reduced, diffusion can still happen in the space between the funnel and the centrifuge tube and that the use of the 3D-printed piece and Teflon tape, although reducing these fluxes, does not allow for suppressing them entirely. It should be noted that using a scanning electron microscope (SEM), we could see no porosity of the 3D-printing material itself (Annexe D).

Overall, the funnel system has proved to be efficient in preventing evaporation of the samples. We recommend checking the weather forecasts before the event, to program the autosampler so that the collected samples are the largest possible and can be contained in the centrifuge tube.

3.5.2 Automatic sampler's internal conditions

To determine if both the autosampler's confinement and the saturation of the autosampler's atmosphere are efficient in preventing post-sampling evaporation, we compared the open centrifuge tubes left in three different systems: the free atmosphere (outside any autosampler), a dry autosampler, and a saturated autosampler (Figure 3.3 C,D).

Regarding relative weight losses, we can observe that using the dry sampler reduces the loss compared with letting the system in the free atmosphere (Figure 3.3C, Table 3.3). For 2-mL samples, the water loss was divided by 1.7 (Table 3.3). Furthermore, filling the bottom of the autosampler with water significantly reduces the loss compared with a dry autosampler. In this case, the water loss was divided by 4.5 for 2-mL samples (Table 3.3).

By comparing the isotopic compositions, the same evaporative trends can be observed for the systems left in a free atmosphere and in a dry sampler (Figure 3.3D). However, as the saturated sampler's isotopic compositions are slightly depleted in heavy isotopes compared with the reference water, it is not relevant to consider evaporation as the dominant process in the isotopic composition change. When water is added to the bottom of the autosampler chamber, it evaporates until it reaches air saturation. We can expect that this

would limit the samples' evaporation, expressed as a flux from the samples to the air of the autosampler chamber. We specifically used water of isotopic composition (−14.2‰ in $\delta^{18}O$; −101‰ in $\delta^{2}H$) very depleted in heavy isotopes compared with the tap water used as a reference water for our samples. The sample isotopic signatures show that a partial equilibration occurs with the water at the bottom of the sampler chamber (Figure 3.3D, Table 3.4). The $\delta^{18}O$ is depleted up to 0.7‰ for 2-mL samples.

With this equilibration, we can expect the measured isotopic composition δ_{meas} (either $\delta^{18}O$ or $\delta^{2}H$) to result from the mixing between the sample's water that has undergone a Rayleigh distillation due to evaporation, of isotopic composition δ_{evap}, and the water in the bottom of the autosampler, of isotopic composition δ_{bottom}:

Equation 3.6

$$\delta_{meas} = \frac{1}{V_f}\left[\delta_{evap} \times (V_f - V_{exch}) + \delta_{bottom} \times V_{exch}\right]$$

with V_f the sample's volume after evaporation and V_{exch} the equivalent volume of water that has been exchanged between the sample and the autosampler's atmosphere.

We can calculate δ_{evap}, the isotopic composition of the evaporated sample, using a simple Rayleigh distillation adjusted on the weighed water losses:

Equation 3.7

$$\delta_{evap} = \delta_{initial} - \varepsilon_{w/v} \times \ln(f)$$

with $\delta_{initial}$ the isotopic composition of the initial water, represented by the reference water, $\varepsilon_{w/v}$ the separation factor of water over vapor, and f the fraction of the remaining liquid water, as the relative difference between the sample's volume (5, 10, 15, or 20 mL), and the averaged evaporative loss of the system (Table 3.3).

Still considering open samples, the measured values of the three environments lay on three apparent fractionation lines if considered as Rayleigh distillation processes (Annexe E). However, their measured $\delta^{18}O$ separation factors $\varepsilon_{w/v}$, represented as the slopes of the lines, are not equal to what is expected at equilibrium for a laboratory temperature of ~20°C ($\varepsilon_{w/v}$ = 9.7‰ for $\delta^{18}O$) (Annexe E).

Outside the sampler, the evaporation of the samples will in no case be enough to saturate the surrounding atmosphere, and the difference between the expected separation factor and the calculated separation factor

is likely due to kinetic fractionation specific to laboratory conditions because the centrifuge tube is an open system and the laboratory air is relatively dry.

As the separation factors calculated in the dry sampler and the saturated sampler are different from the one found outside the sampler, we hypothesize that this difference is due to the equilibration of water samples with the air contained in the autosampler's chamber. To a lesser extent than the saturated sampler, the samples of the dry autosampler probably equilibrated with the water vapor contained in the autosampler's chamber, partly coming from the evaporation of all samples themselves. If the experiment had been led long enough, all samples' isotopic compositions probably would have tended to the same value. For a 3-day experiment, this process slightly lowered the separation factor compared with the system in the free atmosphere (Annexe E).

As for each system, the samples still lay on distinct fractionation lines; this means that for each volume, there is as much evaporative fractionation in the samples as there is re-equilibration with the air contained in the autosampler's chamber. As smaller samples' isotopic compositions are more affected by both the kinetic fractionation and the equilibration than larger samples, this keeps samples of all volumes on the same fractionation lines. However, the slope of these lines shifts according to the volume of water exchanged and the isotopic composition of the water with which the sample equilibrates.

Due to the very low isotopic composition of the water that we specifically used in the saturated sampler, the change in separation factors due to this equilibration is greater in the saturated sampler than in the dry sampler. As for considering the evaporation process only, the separation factor of all environments is thus set to be the one of the free atmosphere ($\varepsilon_{w/v} = 23‰$ for $\delta^{18}O$ and $\varepsilon_{w/v} = 48‰$ for $\delta^{2}H$). Based on Equation 3.6 we are then able to calculate the exchanged volume V_{exch} that took place in the autosampler filled with water of known isotopic composition:

Equation 3.8

$$V_{exch} = \frac{\delta_{meas} - \delta_{evap}}{\delta_{bottom} - \delta_{evap}} \times V_f$$

By dividing V_{exch} by the number of hours of the experiment and averaging values calculated with $\delta^{18}O$ and $\delta^{2}H$, we obtain an average exchange rate τ_{exch} of 0.006 ± 0.001 mL/h for the open centrifuge tube and 0.002 ± 0.001 mL/h for the centrifuge tube modified with the funnel system. This shows that the isolation

offered by the funnel system not only helps prevent the sample's evaporation but also helps limit the equilibration of the sample with the surrounding atmosphere.

Following these results, we were finally able to represent the order of the magnitude of the maximum time that the samples should be left in the autosampler before the equilibration causes isotopic changes that will be non-negligible compared with the overall analytical uncertainty:

Equation 3.9

$$t = \frac{OAU \times V_{sample}}{\tau_{exch} \times |\Delta\delta_{bottom-rain}|}$$

with OAU the overall analytical uncertainty and $|\Delta\delta_{\text{bottom-rain}}|$ the absolute difference in isotopic compositions between the rainfall and the water inserted in the bottom of the autosampler. The results can be found in the Annexe F. Please note that the presented values are theoretical and will vary notably according to the equilibration rate between the water sample and the surrounding atmosphere.

Overall, we would recommend using centrifuge tubes that have been modified with a funnel to prevent both evaporation and equilibration. The choice of using a dry autosampler or pouring water in the bottom of the autosampler should be left to the user. However, one should consider that in this experiment, we purposefully used water of isotopic composition significantly different than the samples. Even with this bias, we have shown that manually saturating the autosampler gives significant results in keeping the samples' isotopic compositions the closest possible to their initial value. Considering the same volumes, even if the samples slightly equilibrate, the related change in isotopic compositions is significantly lower than the change in isotopic compositions due to the evaporation with a higher relative water loss in the dry autosampler (Figure 3.4, Table 3.4). As in the dry autosampler, 2 and 5 mL should be considered with precaution, in the saturated autosampler the isotopic compositions of the samples of the same volumes remain equal to their initial isotopic compositions, considering analytical uncertainties. Ideally, the water poured in the bottom of the sampler should have an isotopic composition the closest possible to the expected rainfall isotopic composition. The sampling protocol can be found in Annexe G.

Figure 3.4: Comparison of the measured $\delta^{18}O$ differences ($\Delta\delta^{18}O$) and the relative water losses between the centrifuge tubes closed by a funnel let in the dry autosampler (yellow) and in the saturated autosampler (blue). The gray area represents the uncertainty at 1σ surrounding a $\Delta\delta^{18}O$ of 0‰.

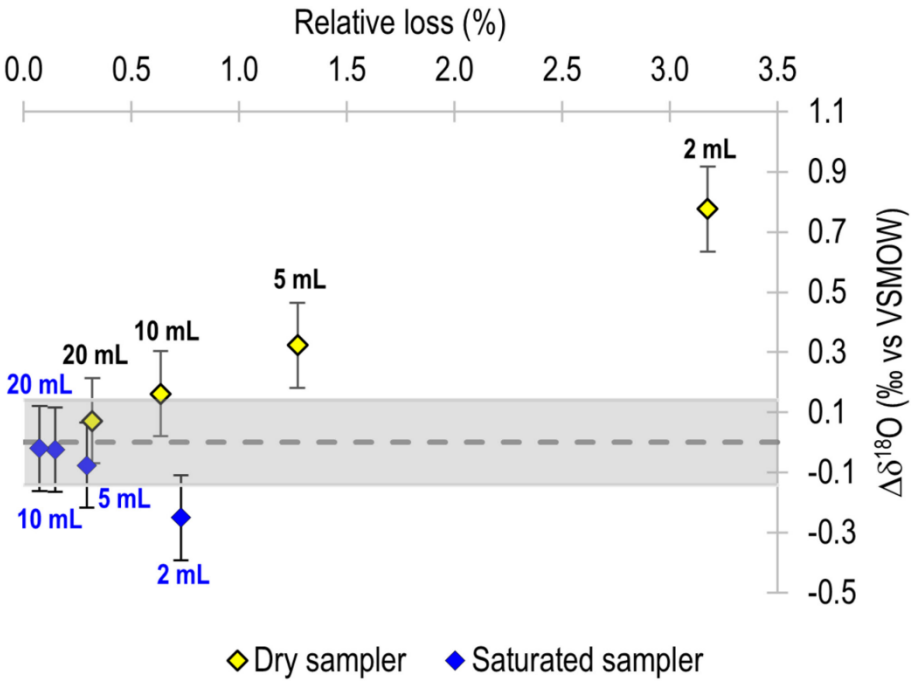

3.6 Conclusions

A simple modification has allowed the successful design of a sampler capable of collecting intra-event rain samples for isotopic analysis, for time intervals from minutes to hours, suitable for programs where samples can be retrieved within a few days of the precipitation event. The ability to collect high-quality precipitation samples for isotopic analysis throughout individual storm events provides powerful information that can be used to understand moisture sources and processes impacting rainfall. A 72-h laboratory experiment has shown that the reduction in the surface of the sample's opening limits fractionation due to post-sampling evaporation. The minimum amount of rainfall to be collected to keep this fractionation negligible could be investigated.

Intentionally filling the autosampler's bottom with water creates saturated atmospheric conditions and further prevents post-sampling evaporation of the samples, allowing to collect samples of smaller volumes than in a dry autosampler. However, as the humidity builds up the samples are also more prone to equilibration with the surrounding air moisture. In this experiment, we purposefully used a water of isotopic composition significantly different than the samples. Filling the sampler with water of isotopic composition closer to what is expected for the samples helps preserve the samples' initial isotopic compositions.

The maximum duration the samples should remain in the automatic sampler so that the relative isotopic shift remains negligible compared with the overall analytical uncertainty was investigated. This duration is highly dependent on the sample's volume and the isotopic composition of the water used. Ideally, the water poured in the bottom of the sampler should have an isotopic composition the closest possible to the expected rainfall isotopic composition.

To our knowledge, the intentional saturation of the sampler's air to prevent post-sampling evaporation has never been reported before. This low-cost methodology is shared with the scientific community with the overall goal of helping democratize high temporal resolutions of precipitation sampling for isotopic analysis.

3.7 Contribution de l'article C

Dans cet article, nous avons développé et testé une méthodologie à moindre coût permettant d'adapter des échantillonneurs automatiques d'eau de surface pour l'échantillonnage isotopique des précipitations à l'échelle intra-événementielle. Sur une période de 3 jours, l'évaporation post-échantillonnage reste négligeable pour les échantillons de plus de 0.1 mm. Chaque échantillon peut contenir jusqu'à 0.5 mm de pluie.

Cette méthodologie est facilement reproductible dans tout laboratoire possédant un échantillonneur automatique d'eau de surface, ce qui est souvent le cas dans les laboratoires d'hydrologie. Il est important de noter que ces échantillonneurs sont toujours utilisables pour leur fonction initiale. En particulier, nous avons proposé la saturation intentionnelle de l'air contenu dans l'échantillonneur afin de limiter l'évaporation post-échantillonnage, ce qui à notre connaissance n'avait jamais été fait avant.

CHAPITRE 4 :
ÉCHANTILLONNAGE DES PRÉCIPITATIONS URBAINES À HAUTE RÉSOLUTION SPATIALE ET TEMPORELLE - PARTIE III

Collect'O, premier réseau participatif d'échantillonnage dédié à l'étude isotopique des précipitations urbaines

4.1 Introduction

Dans notre étude, il est important d'utiliser des emplacements suffisamment représentatifs de chacune des zones urbaines et rurales afin de pouvoir les comparer entre elles. L'article A avait montré que l'ICU de Montréal représente un rayon d'environ 30 km (Carton *et al.*, 2024a). Nous avons donc cherché à obtenir des stations d'échantillonnage dans un rayon de 50 km autour du centre-ville, correspondant plus ou moins à la superficie du Grand Montréal. Comme il est difficile de répondre par nous-mêmes aux contraintes posées par un échantillonnage à haute résolution spatiale implémenté à une telle échelle, nous avons choisi de nous appuyer sur la volonté des citoyen·ne·s du Grand Montréal pour nous aider. Pour cela, nous avons créé et piloté le réseau de collecte participative Collect'O, et présentons ici les différentes étapes suivies pour ce faire.

4.2 Création et déploiement du réseau

Afin de rejoindre des volontaires, nous avons eu recours à l'équipe de communication de l'UQAM, qui nous a mis en contact avec de nombreux médias. Nous avons ainsi pu accorder plusieurs entrevues afin de diffuser notre projet, que ce soit à la radio dans l'émission Les Années Lumière de Radio Canada, dans des reportages télévisés pour la chaîne MétéoMédia (reportages 1, 2 et 3), ou encore dans les médias électroniques comme Le Devoir et Actualités UQAM. Le site hydro-sciences.uqam.ca/collecto/ a été créé comme plateforme pour le public, où il a pu en apprendre davantage sur le projet et se porter volontaire pour y participer.

Pour capturer la variabilité du signal isotopique des précipitations urbaines, nous avons souhaité atteindre une meilleure résolution spatiale à l'intérieur de la ville qu'à l'extérieur, car c'est là que la plus grande hétérogénéité spatiale dans la modification des précipitations est attendue. Nous avons ainsi pu installer des collecteurs de précipitations dans une cinquantaine de propriétés, dont une majorité au centre-ville de Montréal (Figure 4.1). L'emplacement de chaque collecteur a été choisi lors d'une visite chez chaque participant·e, en se plaçant le plus loin possible des obstacles environnants, pour éviter que les précipitations soient interceptées lors de leur chute. Les participant·e·s ont ainsi utilisé ces collecteurs pour échantillonner

simultanément des échantillons de précipitations lors de différents événements répartis tout au long de l'année.

Pour chaque événement pluvieux, nous avons également souhaité étudier l'évolution temporelle des compositions isotopiques des précipitations entre le centre-ville et les zones moins urbanisées. Pour cela, nous avons placé un échantillonneur automatique de pluie au cœur du centre-ville de Montréal, sur le toit de l'UQAM, tandis que deux autres étaient installés en périphérie, l'un à Longueuil et l'autre à Laval (Figure 4.1). Tous trois étaient opérés par notre équipe.

Figure 4.1: Distribution spatiale des collecteurs événementiels (bleu) et intra-événementiels (jaune)

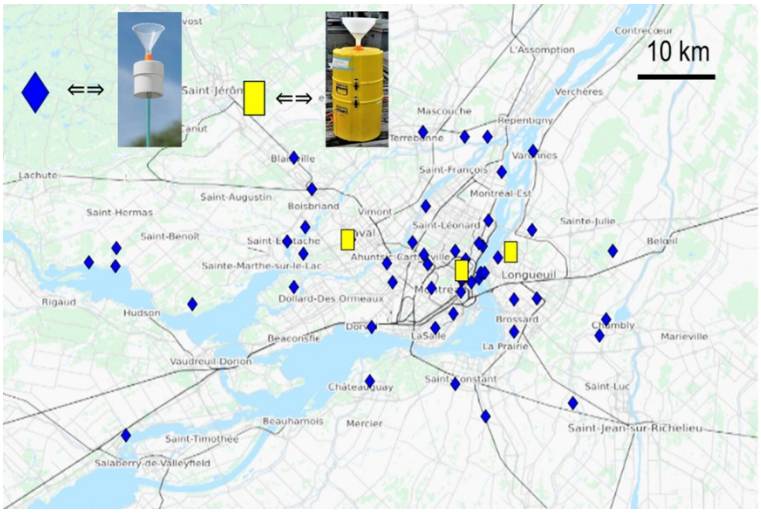

4.3 Choix des événements et taux de participation

Tout au long de l'année, nous avons sélectionné des événements météorologiques en nous référant aux bulletins météorologiques de la région. Les événements étaient choisis dépendamment de la quantité de précipitations maximale attendue afin qu'elle ne dépasse pas la capacité des collecteurs ; mais également en fonction des horaires de chaque événement. En effet, pour que les échantillons soient comparables entre eux, les participant·e·s du réseau devaient installer et récupérer leur collecteur sur des plages horaires similaires où il ne pleuvait/neigeait pas, ce qui imposait une contrainte supplémentaire à notre méthode. 19 événements ont ainsi pu être échantillonnés entre septembre 2021 et octobre 2022, dont 14 événements pluvieux et 5 événements neigeux (présentés plus tard dans le chapitre 5). Il est important de noter que, s'agissant d'un réseau participatif, toutes les stations n'étaient pas opérationnelles lors de chaque événement. Après le déploiement du réseau, nous avons observé qu'en moyenne, moins de la moitié des participant·e·s prenaient part à chaque événement (Figure 4.2).

Figure 4.2: Taux de participation des membres Collect'O aux échantillonnages

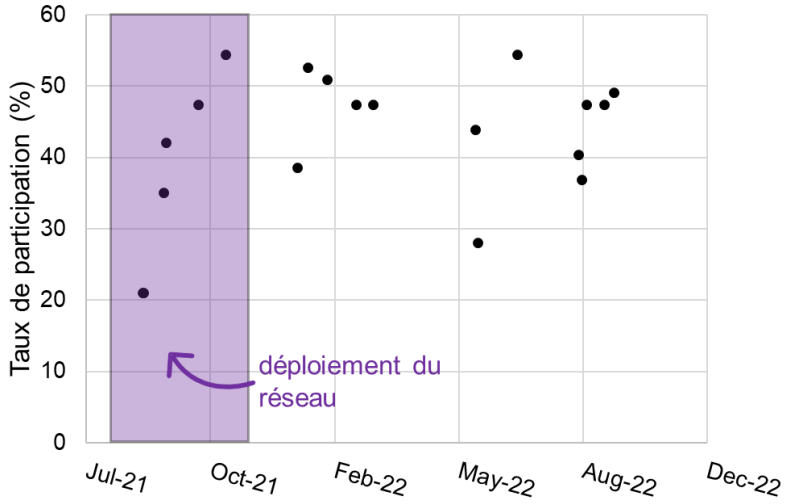

4.4 Le cas de la neige

Les entonnoirs placés sur nos collecteurs de pluie ne sont pas adaptés à la collecte de la neige. En effet, lors de sa chute la neige resterait bloquée dans l'entonnoir jusqu'à ce qu'elle fonde et finisse par couler dans le collecteur. Cela pourrait provoquer de l'évaporation post-échantillonnage, et ainsi la représentativité de l'échantillon ne serait pas assurée. Il nous a donc fallu concevoir d'autres collecteurs adaptés à l'échantillonnage de neige.

Depuis les débuts de l'analyse des isotopes stables dans les précipitations, deux techniques principales ont été utilisées pour collecter la neige (Rey *et al.*, 2018) :

1) Récupérer chaque épisode de neige dans un nivomètre ou un seau, puis le laisser fondre pendant 12 heures avant de le mettre en bouteille.
2) Creuser une tranchée de 5 à 6 mètres perpendiculairement au vent dominant. Cinq à six carottes de neige sont prélevées sur toute la profondeur du couvert forestier à la fin de l'hiver (fin mars) pour obtenir un composite de la neige avant qu'elle ne fonde.

D'un point de vue pratique, et parce que nous visons un échantillonnage événementiel et non pas mensuel, s'inspirer de la première méthode nous a semblé plus approprié à notre étude.

C'est pourquoi nous avons conçu des collecteurs de neige constitués d'un tuyau en PVC de 8 cm de diamètre, coupé à une longueur de 37 cm. Un capuchon femelle de 8 cm est collé au bas du tuyau et des attaches sont

installées sur le tuyau, permettant de l'installer sur la même barre époxy que les collecteurs de pluie (Figure 4.3a). Ces collecteurs permettent ainsi de collecter jusqu'à 30 mm de neige. Une fois l'échantillonnage terminé, un second capuchon peut être placé sur le haut du collecteur en attendant que la neige fonde, pour éviter les échanges avec l'atmosphère environnante (Figure 4.3b).

Figure 4.3: a) Collecteur de neige ouvert, prêt à collecter, b) collecteur de neige fermé lors de la fonte de la neige

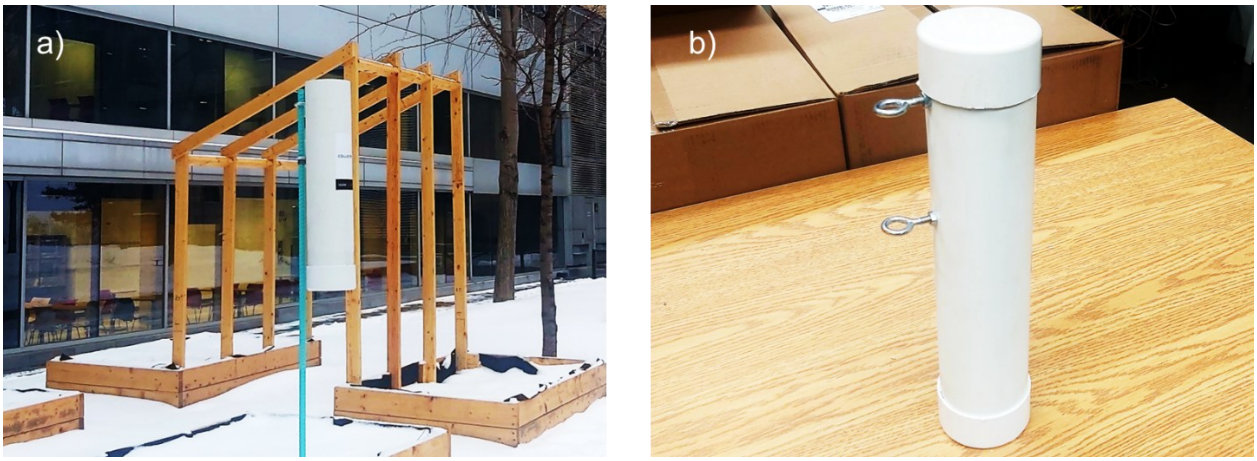

Aucun échantillonnage intra-événementiel de neige n'a été entrepris pour les 5 événements présentés dans ces travaux. Cependant, une méthodologie fut testée quelques mois plus tard, et sera présentée dans le chapitre 5.

4.5 Protocole d'échantillonnage

Les participant·e·s stockaient leurs collecteurs de pluie et de neige chez eux. Avant chacun des événements sélectionnés, nous leur envoyions un courriel et un message texte (Figure 4.4) pour les rediriger sur une page de notre site internet dédiée à l'événement (exemple en Annexe H). Iels pouvaient y retrouver des détails tels que les plages horaires de début et de fin de l'échantillonnage, généralement définies comme quelques heures avant et après l'événement, tôt le matin ou le soir. Sur cette page, iels pouvaient également trouver un formulaire à remplir précisant l'heure exacte de début et de fin de leur collecte, ou pour faire un commentaire sur leur prélèvement. Nous leur demandions de suivre les protocoles présentés en Table 4.1.

Figure 4.4: Exemple de message texte envoyé avant un événement

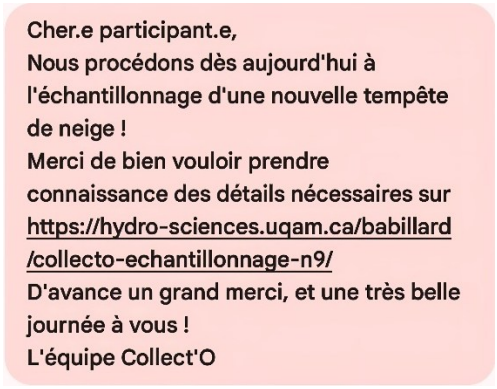

Table 4.1: Protocoles suivis par les participant·e·s pour l'échantillonnage de pluie et de neige

Échantillonnage de pluie	Échantillonnage de neige
1. Durant la plage horaire d'installation, vissez d'abord l'une des petites bouteilles Collect'O sur votre collecteur, puis installez votre collecteur sur son piquet. 2. Durant la plage horaire de récupération du collecteur, dévissez d'abord la bouteille du collecteur et refermez-la de son bouchon. Veillez à **visser de toutes vos forces le bouchon de votre bouteille** *(très important pour éviter l'évaporation !)*. 3. Retirez votre collecteur de son piquet. Stockez votre collecteur et vos échantillons à l'ombre, à température ambiante *(ex : dans un placard)*. 4. Déposez vos échantillons dans l'un de nos deux points de collecte, dès que vous le pouvez.	1. Durant la plage horaire d'installation du collecteur, retirez le capuchon de votre collecteur et installez-le sur son piquet. 2. Durant la plage horaire de récupération du collecteur, revissez bien le capuchon sur votre collecteur, puis rentrez-le à l'intérieur. 3. Placez votre collecteur sur une surface plane, éloignée de toute source de chaleur, pendant quelques heures. 4. Durant la plage horaire d'embouteillage de la neige fondue, retirez le capuchon, puis versez la neige fondue dans la bouteille Collect'O grâce à l'entonnoir qui vous a été fourni. 5. Veillez à **visser de toutes vos forces le bouchon de votre bouteille** *(très important pour éviter l'évaporation !)*, puis stockez-la à l'ombre, à température ambiante. 6. Rincez votre collecteur et votre entonnoir, puis laissez-les sécher pour la prochaine collecte.

Durant la plage horaire d'installation, il suffisait aux participant·e·s d'aller accrocher leurs collecteurs sur leurs supports. Une fois la collecte terminée, iels refermaient les bouteilles, puis indiquaient leur numéro de station et les heures d'installation et de récupération du collecteur sur une étiquette dédiée, spécifiquement collée sur chaque bouteille vide avant l'échantillonnage (Figure 4.5). Iels plaçaient ensuite leurs échantillons à température ambiante, à l'ombre. Un local était spécialement aménagé au département des sciences de la Terre et de l'atmosphère de l'UQAM afin que chaque participant·e puisse apporter son échantillon et le remplacer par une nouvelle bouteille.

Figure 4.5: Étiquette collée sur chaque bouteille servant à l'échantillonnage

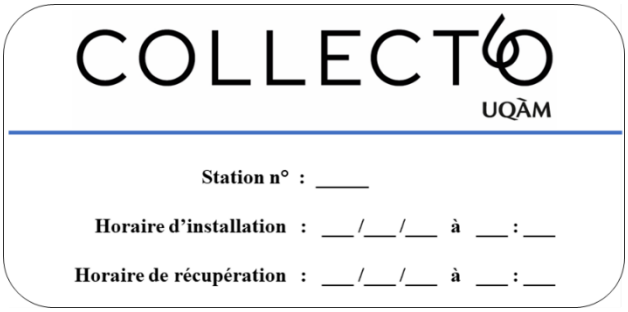

Pour la neige, une fois le prélèvement terminé, iels plaçaient un capuchon sur le dessus du collecteur, rentraient le collecteur à température ambiante afin de faire fondre leur échantillon pendant 12 heures. Ils versaient ensuite l'eau liquide obtenue dans une bouteille dédiée, dont la taille était choisie avant l'événement en fonction des quantités de neige prévues (Annexe H). En choisissant des bouteilles plus petites pour les plus faibles quantités de neige fondue, nous limitions ainsi l'évaporation de l'échantillon au sein même de la bouteille.

Pendant que les participant·e·s collectaient des échantillons cumulatifs de pluie, les échantillonneurs automatiques étaient programmés à un même pas de temps compris entre 1 min et plusieurs heures, défini sur la capacité des échantillonneurs (0.5 mm de pluie) et les prévisions émises pour l'événement à venir. Il est à noter que pour des raisons pratiques (problèmes de configuration, manque de disponibilité), nous n'avons pas pu obtenir des échantillonnages intra-événementiels à chacune des trois stations pour chacun des 14 événements de pluie collectés par le réseau Collect'O. C'est avec la pratique que nous sommes arrivés au protocole d'échantillonnage proposé dans l'article C (Annexe G).

4.6 Suivi des participant·e·s

Les échantillonnages se sont étalés sur une longue période, et il était attendu que la motivation des participant·e·s à continuer les échantillonnages finisse par décliner. Pour éviter cela, nous avons cherché à fréquemment interagir avec elleux, à leur faire comprendre l'importance du projet, et à valoriser leur participation en leur montrant ce que leurs échantillonnages permettaient d'observer.

En plus des courriels échangés, nous avons également commencé à produire des capsules vidéo (https://hydro-sciences.uqam.ca/collecto/avancees/) dès la création du réseau, la première d'entre elles montrant l'avancement de l'installation des collecteurs chez les participant·e·s. Quelques mois après les premiers échantillonnages, nous avons ensuite cherché à mieux vulgariser certains concepts, tels que les isotopes, l'importance d'étudier les climats urbains, l'intérêt d'une étude isotopique à haute résolution d'échantillonnage, mais aussi le type d'analyses et d'interprétations effectuées sur les échantillons collectés. La dernière vidéo publiée sur cette page web montre la présentation de Collect'O effectuée lors du 16e colloque sur les risques naturels au Québec, à l'occasion du 89e congrès de l'Acfas en mai 2022.

Collect'O fut également présenté à l'international, lors de l'International Symposium on Isotopic Hydrology (ISIH) organisé par l'Agence Internationale de l'Énergie Atomique (AIEA) en juillet 2023. Nous en avons informé les participant·e·s, et en avons profité pour organiser une réunion d'information en septembre 2023 afin de leur communiquer les résultats partagés lors de ce congrès. Ce fut également l'occasion pour les volontaires de visiter le laboratoire de géochimie des isotopes stables légers du Geotop, et ainsi comprendre où et comment leurs échantillons étaient analysés depuis le début du projet.

Au fil des mois qui ont suivi, nous avons communiqué aux participant·e·s quelques informations sur l'avancement du projet, telles que la parution des articles liés à cette thèse et leur présentation lors du congrès de la Goldschmidt en août 2024. Enfin, en juillet 2025, lorsque nous avons proposé aux participant·e·s de participer au dernier chapitre de cette thèse, nous leur avons également partagé une vidéo montrant l'état actuel des résultats et retombées du projet. Nous leur avons indiqué qu'iels seraient également invité·e·s à la soutenance de thèse, ce qui leur permettra notamment de voir les résultats du dernier chapitre auquel iels ont contribué.

Les dernières communications se sont beaucoup espacées au cours des mois qui ont suivi la fin des échantillonnages. Nous nous sommes questionnés quant à la perception qu'ont eue les participant·e·s de cette baisse de fréquence. Ce point sera discuté dans l'enquête présentée au chapitre 6.

4.7 Conclusion

Dans le cadre de cette thèse nous avons créé le premier réseau participatif d'échantillonnage au monde dédié à l'étude isotopique des précipitations urbaines. Nous avons ainsi atteint une résolution d'échantillonnage inespérée, avec 57 points de collecte répartis dans le Grand Montréal. Nous avons développé un protocole simple, permettant de comparer les échantillons des différentes stations lors d'un même événement, et qui de notre perspective a été facilement suivi par les participant·e·s.

Il est à noter que la nature bénévole de ce réseau a rendu le taux de participation variable pour chaque échantillonnage. De ce fait, il n'était pas toujours aisé de comparer le comportement isotopique d'une même zone lors de différentes collectes. Pour garder la motivation des participant·e·s tout au long du projet, nous avons eu recours à différents moyens de communication, que ce soit par courriel, capsules vidéo, ou présentations orales et visite de laboratoire. Toutefois, il serait recommandable de garder la durée du projet relativement courte, afin que les participant·e·s s'investissent pleinement sur une courte période. De plus, nous avons noté que la mise en place d'un deuxième point de collecte a permis de rejoindre des citoyen·ne·s plus éloigné·e·s de l'université, qui n'auraient probablement pas participé n'eût été la possibilité de rapporter les échantillons dans un point plus proche de chez eux. Augmenter le nombre de points de collecte aurait pu permettre d'augmenter encore le nombre de participant·e·s et donc la couverture du réseau.

Quoi qu'il en soit, la méthodologie que nous avons mise en place s'est révélée prometteuse et montre la valeur ajoutée des réseaux participatifs dans l'acquisition de données à haute résolution. Nous espérons que le partage de cette méthode pourra ainsi bénéficier aux projets environnementaux futurs cherchant à étudier le signal isotopique des précipitations urbaines.

CHAPITRE 5 :
ANALYSE À HAUTE RÉSOLUTION SPATIALE ET TEMPORELLE DU SIGNAL ISOTOPIQUE DES PRÉCIPITATIONS URBAINES

5.1 Mise en contexte de l'article D

Nous devons prendre en considération que l'effet des processus à l'origine de la modification des précipitations urbaines risque d'évoluer selon le type de précipitations considéré (pluie/neige, convectif/stratiforme). En effet, les signatures isotopiques reflètent les proportions du type de pluies convectives par rapport aux pluies stratiformes, et peuvent donc être utilisées pour surveiller les changements dans le caractère des précipitations (Aggarwal *et al.*, 2016). C'est pourquoi nous avons choisi de sélectionner des événements météorologiques de différents types répartis tout au long d'une année hydrologique. Compte tenu du coût important représenté par les analyses des échantillons, nous avons choisi de nous en tenir à 20 événements.

Dans ce chapitre, nous présentons les résultats associés à l'échantillonnage à haute résolution de 19 événements entre septembre 2021 et octobre 2022. Le volume d'informations à traiter étant particulièrement important, nous choisissons de recourir à une étude de corrélation des signatures isotopiques des précipitations avec différentes variables météorologiques, avant d'explorer plus finement la distribution isotopique de quelques événements ressortant de l'analyse.

Cet article soumis à *Urban Climate* vise notamment à montrer à la communauté scientifique, en particulier non familière aux isotopes stables de la molécule d'eau, le potentiel de ces traceurs pour mieux appréhender la modification des précipitations urbaines, dans l'espoir de permettre la démocratisation de leur utilisation dans ce domaine de recherche.

Tracing the impact of cities on urban precipitation, a water-stable isotopic study at high spatial and temporal resolution (Article D)

Submitted to Urban Climate (August 2025)

Cécile Carton [a], Florent Barbecot [a], Jean-François Hélie [a], Jean Birks [b]

[a] Department of Earth and Atmospheric Sciences, Geotop–Université du Québec à Montréal, Montréal, Québec, Canada

[b] Department of Earth, Energy, and Environment, University of Calgary, Calgary, Alberta, Canada

5.2 Abstract

Purpose: This study assesses the added value of monitoring stable isotopes of the water molecule at high spatial and temporal resolution to trace the processes driving the modification of urban precipitation.

Methods: Low-cost rain and snow collectors were developed to preserve samples' isotopic composition at both event and intra-event scales. A participatory sampling network was created over Montreal, Canada, a city whose climate is strongly influenced by urban conditions. Between September 2021 and October 2022, 19 precipitation events were simultaneously sampled across stations.

Results: Isotopic signatures revealed important spatial variability between stations, a heterogeneity not previously documented at this urban scale. Correlation analyses and sequential event comparisons indicated that sub-cloud evaporation was not the primary driver of this variability. Instead, events' isotopic variability was correlated with the time elapsed since the last precipitation, suggesting precipitation recycling through evaporation and re-precipitation, likely enhanced by the urban heat island. The residence time of rainwater within the city was estimated at ~50 hours. Combustion-derived water vapour contributed up to 5 % of precipitation.

Significance: To our knowledge, this is the first study to demonstrate the potential of high-resolution stable isotope monitoring in detecting subtle dynamic processes impacting urban precipitation. We share the low-cost methodology used so it can be applied in other cities, enabling comparison with different urban environments.

5.3 Introduction

The 21st century has seen unprecedented urbanization: by 2025, more than 2 people out of 3 are expected to live in cities (United Nations, Department of Economic and Social Affairs, Population Division, 2019). To support this growing population, cities' structures are undergoing significant modifications, becoming higher, larger, and denser. Made of highly solar-absorbing materials, such as tar, bitumen, asphalt, cities' albedo and structure lead to important Urban Heat Islands (UHI), with temperatures several degrees higher in cities compared to their rural environment, especially at night (Carton *et al.*, 2024a ; Roberge and Sushama, 2018).

Increased temperatures in urban areas have been the most extensively studied aspect of urban climate research; however, alterations in precipitation patterns have also been documented, e.g., in Berlin as early as 1892 (Oke *et al.*, 2017). Subsequent studies have demonstrated that localized changes in cloud formation and precipitation can arise from a range of physical processes associated with urban environments, including the influence of the UHI, enhanced surface roughness, and anthropogenic emissions of heat, water vapor, and aerosols (Oke *et al.*, 2017).

However, the biases encountered by traditional measurement tools, such as the strong local turbulence and airflow distortion, have made it difficult to accurately describe the spatial variability of precipitation (Maier *et al.*, 2020), and, thus, reach consensus on how precipitation is impacted in a city. In densely urbanized areas, identifying representative locations for rain gauges is challenging due to interference from buildings and other obstructions, which can compromise the accuracy of precipitation measurements. Moreover, radar-derived rainfall estimates are affected by errors in reflectivity measurements, conversions of reflectivity into rainfall rate, and geometry of the radar measurement field (Villarini *et al.*, 2014). Correcting or adjusting precipitation data collected in urban environments, with these known limitations, is also challenging and depends on the temporal and spatial rainfall coverage of the rain gauge network (Matrosov *et al.*, 2005).

Nonetheless, understanding how precipitation forms and behaves within urban areas is necessary for planning and adaptation, particularly in the context of global warming. Environmental tracers such as stable water isotopes ($\delta^{18}O$ and $\delta^{2}H$) provide valuable complementary information for improving our understanding of water sources and processes influencing precipitation in urban environments. Several isotopic studies around the world have already shown that urban precipitation is altered by local thermodynamic processes such as:

- Evaporation beneath the cloud, exacerbated by the UHI effect, leading to increases in $\delta^{18}O$ and a decrease in d-excess (Cortecci *et al.*, 2008 ; Zhu *et al.*, 2024).
- Enhanced convection associated with the UHI effect, generating intense rainfall events with isotopically distinct signatures (Uchiyama *et al.*, 2017).
- Higher evapotranspiration fluxes in rural areas, resulting in a higher d-excess compared to urban areas (Zhao *et al.*, 2023).

Thus, stable water isotope data have been shown as useful tools for tracing the processes that modify urban precipitation. Despite this potential, isotopic studies of urban precipitation remain underdeveloped, with

most being limited by very small spatial or temporal datasets, or monthly composite data. Unlike natural environments, urban environments are highly heterogeneous in both space and time, so monitoring scales need to reflect that variability if all of the processes and net impacts are to be evaluated. To our knowledge, no study has investigated the isotopic labelling of urban precipitation at high spatial and temporal resolutions. This study addresses this gap using high resolution monitoring of the isotopic labelling of precipitation at the scales necessary to capture the dynamic processes in urban environments.

For short-duration precipitation events, large-scale atmospheric conditions can reasonably be assumed to be homogeneous across a city. Thus, variations in the isotopic signal of precipitation over the city could provide valuable information to investigate the mechanisms affecting precipitation in an urban area. In addition, intra-event sampling could help identify the dynamics responsible for this heterogeneity, such as changes in atmospheric processes controlling precipitation formation and transformation, changes in air masses, or re-evaporation under clouds.

Stable water isotopes also have great potential for tracing atmospheric pollution at the city scale. For example, a study conducted in Salt Lake City demonstrated that isotopes could be used to trace water vapor emitted from the combustion of gas for domestic heating, and gasoline for transportation (Gorski *et al.*, 2015). That study showed that combustion water vapor has a distinct isotopic signature characterized by very high $\delta^{18}O$ and very low $\delta^{2}H$, which cannot be obtained from natural sources of water vapor (Gorski *et al.*, 2015), and determined that combustion-derived water vapor accounted for up to 13 % of local atmospheric water vapor. To our knowledge, no similar study has been conducted on precipitation within a city. Quantifying the contribution of combustion water in urban precipitation using stable water isotopes will also be incorporated into the current study.

The study is based in Montreal, Eastern Canada, a city showing an increasing UHI, with daily minimum temperatures 2°C higher on average than its surroundings (Carton *et al.*, 2024a). Between the 1988-1997 period and the 2013-2017 period, precipitation in the most urbanized area has become less frequent and less abundant than in its surroundings (Carton *et al.*, 2024a). Both the UHI and PM2.5 concentrations were found to be lower on the days following precipitation events (Carton *et al.*, 2024a).

Because the precipitation isotopic signal can be greatly affected by post-sampling processes, we had to come up with an appropriate sampling technique to preserve the isotopic signal of precipitation while enhancing the spatial resolution of sampling and maintaining a low budget. For that, we designed appropriate

precipitation samplers and created the first participatory network dedicated to the isotopic study of urban precipitation.

A brief overview of stable isotope principles is provided in Annexe I as background on stable water isotopes ($\delta^{18}O$ and $\delta^{2}H$).

5.4 Methods

5.4.1 Implementation of a participatory network

As it is difficult to aim for a high spatial and temporal resolution in precipitation sampling by ourselves, we chose to rely on the willingness of the citizens of Greater Montreal and created Collect'O, the first participatory network dedicated to the isotopic study of urban precipitation. Our goal was to set up between 50 and 100 stations in a radius of 50 km from Montreal's city center, to allow for a rigorous comparison of isotopic labeling of precipitation within and outside the UHI (Carton *et al.*, 2024a). The participatory network would allow for the simultaneous collection of a spatially dense set of precipitation samples from homes located within Montreal's city center and the surrounding areas during different events distributed throughout the year.

Volunteers were found through outreach activities that included interviews in newspapers, on television, and in electronic media. The website hydro-sciences.uqam.ca/collecto/ was created as a platform for the project, where the public could volunteer to participate. Potential volunteers were contacted and visited to identify the best collection sites, so that the collector was situated as far as possible from potential obstacles such as trees or buildings. This also provided an opportunity to inform the participants in more detail about sampling protocols, to allow for comparison between all stations.

5.4.2 Sampling method

To assess the isotopic signal of urban precipitation, it was important to use samplers that would limit post-sampling fractionation. However, the samplers usually available on the market are expensive, and it was unreasonable to expect to reach a high spatial and temporal resolution while using them. We had to aim for a low-cost methodology, and this is why we have used the literature to design affordable cumulative rain samplers adapted to event-based rain sampling for isotopic analysis (Carton *et al.*, 2024b). Based on Montreal's rainfall over the previous years, the samplers were designed to collect up to 12 mm of rain.

To capture the dynamics of rainfall events, we also adapted three automatic surface water samplers to automatically collect 24 rainfall samples for isotopic study at the intra-event scale, from minutes to hours (Carton *et al.*, 2025). One of these samplers was located on the rooftop of the Faculty of Science of the *Université du Québec à Montréal* (UQAM), while the other two were located in the cities of Longueuil and Laval, in the suburbs of the city of Montreal (Figure 5.1a). As the wind generally comes from the southwest, these locations would serve as references to compare the signal obtained in the city center. Each one of these automatic samplers was operated by a member of our team.

As for snow events, it was impossible to use rain samplers. The snow would stagnate in the funnel, melt, and evaporate before entering the collector, which can change the isotopic composition of the signal and bias the results. This is why we used simple 30 cm high cylinders, closed with caps, left for several hours at room temperature so the snow would melt. All samples were then poured and stored in high-density polyethylene bottles before their analysis.

We relied on the forecasts issued by The Weather Network (https://www.theweathernetwork.com/en), based on several global and regional numerical weather prediction models, to choose our events. We selected the events depending on the expected precipitation amount, in order not to overflow the bottle capacity, and we avoided sampling two consecutive events in the same bottle. Before each selected event, the participants received an email and a text message to redirect them to a page of the website. There, they could find details about the event, such as the starting and ending time windows of the sampling, usually defined as a few hours before and after the event, in the early morning or evening. They could also fill out a form to detail the exact time they started and ended their collection, or to make any comments on their sampling.

Once the collection was over, they could fill in their bottle labels with their station number, place them at ambient temperature (avoiding direct sunlight), and return them in the following days. A location was especially set up for that effect at the Department of Earth and Atmospheric Sciences of UQAM. There, each participant could also pick up a new bottle to take back home. A diagram showing the different steps of this protocol can be found in Annexe J.

In the end, 57 samplers were distributed over the city (Figure 5.1a). 19 rain and snow events were sampled between September 2021 and October 2022 (Figure 5.1). It is important to note that, as this is a participatory network, not all stations were operating during all events. After the network was deployed, we observed that, on average, less than half of the participants were participating in each event (Figure 5.1b).

Figure 5.1: a) Location of the samplers and b) percentage of operating stations during each event distributed along the year.

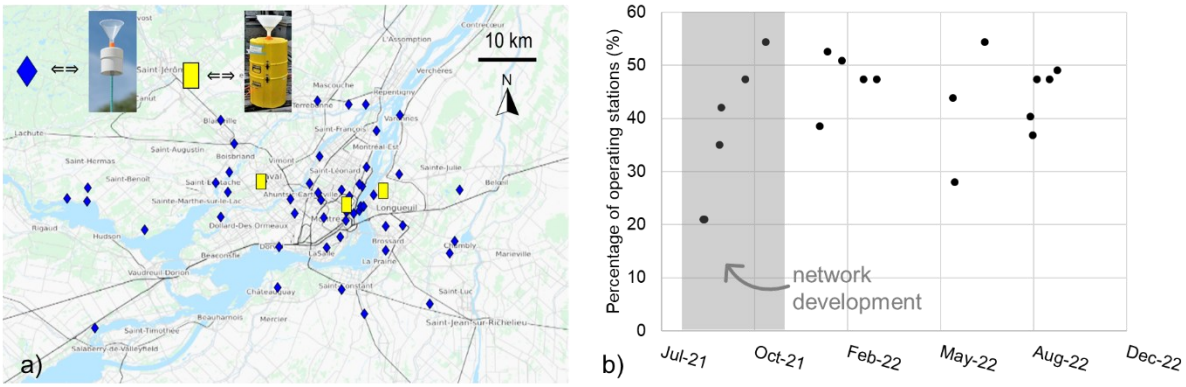

5.4.3 Stable isotope analysis

Isotopic analyses were performed in the light-stable isotope geochemistry laboratory of the Geotop Research Center at the Université du Québec à Montréal. Because very small variations in isotopic compositions are expected, we aimed for the lowest uncertainty possible. We used a cavity ring-down spectrometer for δ^2H (either LGR or Picarro) and δ^{18}O (Picarro) measurement, and/or a dual-inlet isotope ratio mass spectrometer using the equilibration method for δ^{18}O measurement, following the procedures described hereafter. A table summarizing the time coverage of all events sampled and the instrument used for their analysis can be found in Annexe K.

5.4.3.1 Isotope ratio mass spectrometry

Exactly 200 µL of sample water was pipetted into a 3-mL vial, sealed with a septum cap, and then transferred to a 40°C heated rack. After 1 h, the air in the vials was replaced with CO_2 using the AquaPrep system. Samples were left to equilibrate for 7 h. The equilibrated samples were analyzed with an Isoprime 100 IRMS coupled to an AquaPrep system in dual-inlet mode.

Three internal standard waters ($\delta^{18}O = 0.11‰ \pm 0.07‰$, $-13.80‰ \pm 0.06‰$, and $-20.37‰ \pm 0.03‰$) were used to normalize the results. A fourth reference water ($\delta^{18}O = -4.37‰ \pm 0.06‰$) was analyzed as a control. Each set of standards was measured at each sequence's beginning, middle, and end. The overall analytical uncertainty (1σ) is better than ±0.1‰ for δ^{18}O based on the propagation of uncertainties of the normalization of the internal reference materials and the samples. Results are given in delta units (δ) in ‰ on the VSMOW-SLAP scale (Camin *et al.*, 2025), assigning 0‰ to the VSMOW2 material and −55.5‰ to the SLAP2 material.

5.4.3.2 Cavity ring-down spectroscopy using the LGR

One milliliter of water was pipetted into a 2 ml vial and closed with a septum cap. The samples were analyzed using an LGR (Los Gatos Research) model T-LWIA-45-EP Off-Axis Integrated Cavity Output Spectroscopy (OA-ICOS). Each sample was injected (1 µL) and measured 10 times. The first 2 injections of each sample were rejected to limit memory effects.

3 internal standard waters (δ^2H=1.2±0.3 ‰, -99.5±0.6 ‰ & -155.9±0.3 ‰) were used to normalize the results on the VSMOW-SLAP scale. A fourth standard water (δ^2H=-25.8±0.4‰) was analyzed as a control. Each set of standards was measured at each sequence's beginning, middle, and end.

The overall analytical uncertainty (1σ) is better than ±1.0‰ for δ^2H and is based on the long-term measurement of the control. Results are given in delta units (δ) in ‰ on the VSMOW-SLAP scale (Camin *et al.*, 2025), assigning 0‰ to the VSMOW2 material and −428‰ to the SLAP2 material.

5.4.3.3 Cavity ring-down spectroscopy using the Picarro

One milliliter of water was pipetted into a 2-mL vial that was closed with a septum cap. The samples were analyzed using a Picarro model L2130-i CRDS. Each sample was injected and measured 10 times in express mode, and 1.8 µL was injected into the vaporizer. In the express mode, the first six injections were wet flushed, and the four last injections were measured. The first measured injection was rejected to limit memory effects. Thus, each value represents 3 injections.

Three internal standard waters (δ^{18}O=0.11±0.07 ‰, -13.80±0.06 ‰ & -20.37±0.03 ‰; δ^2H = 1.2‰ ± 0.3‰, −99.5‰ ± 0.6‰, and −155.9‰ ± 0.3‰) were used to normalize the results. A fourth standard water (δ^{18}O = −4.37‰ ± 0.06‰; δ^2H=-25.8±0.4‰) was analyzed as a control. Each set of standards was measured at each sequence's beginning, middle, and end.

The overall analytical uncertainty (1σ) is better than ±0.1‰ for δ^{18}O and ±1.0‰ for δ^2H and is based on the long-term measurement of the control. Results are given in delta units (δ) in ‰ on the VSMOW-SLAP scale (Camin *et al.*, 2025), assigning 0‰ to the VSMOW2 material and −428‰ to the SLAP2 material.

5.4.4 Tools for interpretation

5.4.4.1 Weather data

To better understand the isotopic signal of each sampled event, we extracted both weather radar images and hourly meteorological data obtained at the McTavish station, available on the Environment and Climate Change Canada historical data website. The PM2.5 air quality index (AQI) was estimated by the *Réseau de surveillance de la qualité de l'air* (RSQA) of Montreal and defined as $PM2.5_{index} = 50 (PM2.5_{measurement}/AQI_{standard})$, with $AQI_{standard} = 35$ µg/m^3. AQI values are defined as good from 1 to 25, acceptable from 26 to 50, and poor above 50.

A correlation analysis was performed between the isotopic and meteorological variables, such as the temperature, relative humidity, amount, duration, maximum intensity, the average PM2.5 AQI of the event, and the evolution of the PM2.5 AQI through the event, defined as the difference between the PM2.5 AQI at the end and the beginning of the event. For each event, the average PM2.5 AQI and the evolution of the PM2.5 AQI are calculated over the timeslot during which precipitation occurred at the McTavish station.

To ensure that the events chosen were representative of the period sampled, we produced boxplots of the meteorological variables representative of the events and compared them with the mean values of these variables.

To better assess the impact of the city on different precipitation types, we also analyzed accumulated convective and total precipitation outputs from the North American Regional Reanalysis (NARR) to calculate convective/stratiform ratios and better classify the precipitation between these two types.

Air mass trajectories are particularly relevant to explain regional precipitation isotopic variations in North America (Sinclair and Marshall, 2009), which is necessary to isolate the local impact of the city on the precipitation isotopic signal. We used the Hybrid Single-Particle Lagrangian Integrated Trajectory model (HYSPLIT), developed by the National Oceanic and Atmospheric Administration (NOAA) (Stein *et al.*, 2015), to produce normal 120-hour backward trajectories of air parcels at mid-boundary level, using pressure-level data. The model used, the Global Forecast System (GFS), is commonly used for producing weather forecasts in North America. Vertical motion was computed using the model vertical velocity.

Finally, we accessed Maniwaki weather balloon atmospheric soundings, available on the weather website of the University of Wyoming, for the interpretation of Event 11.

5.4.4.2 Measuring the isotopic signature of combustion water

As already mentioned, the isotopic compositions of the combustion water resulting from reactions between gases and atmospheric oxygen are distinct, with very high $\delta^{18}O$ and very low $\delta^{2}H$ values reported in the literature (Gorski *et al.*, 2015). For this study, we sampled water issued from condensing boilers at UQAM. As expected, the isotopic composition of combustion water measured at UQAM was significantly different from precipitation isotopic signatures, which are, at a given sampling site, located on a Local Meteoric Water Line (LMWL), the regression line of all local precipitation isotopic compositions (Figure 5.2a). If there is a contribution from combustion water vapor, the sampled precipitation isotopic composition δ_{sample} should have an intermediate isotopic composition (gray triangle in Figure 5.2a), as a mixing between $\delta_{combustion}$, the isotopic composition of the combustion water vapor, and δ_{LMWL}, the expected isotopic composition of precipitation if it were on the LMWL.

Figure 5.2: a) Determination of the contribution of combustion water vapor in the formation of precipitation; b) Overview of the isotopic range of combustion water.

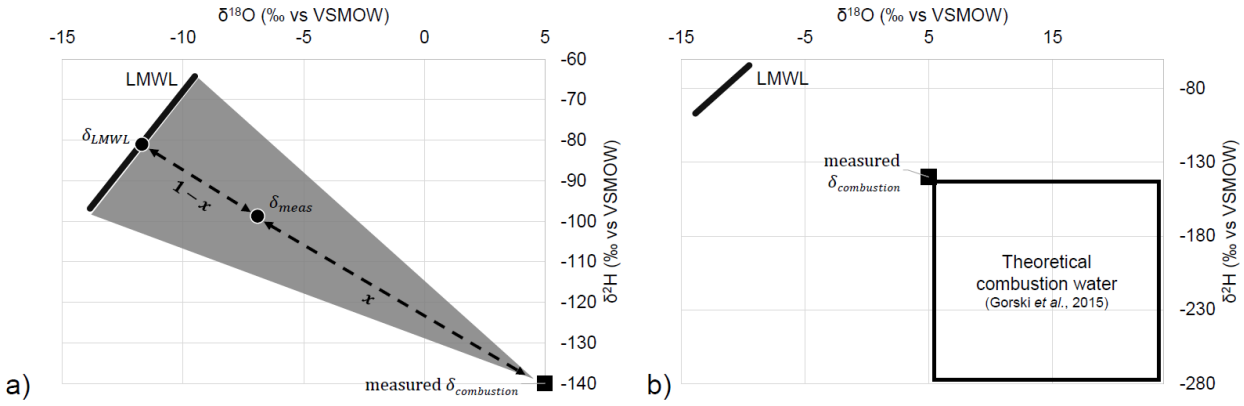

Under conservative mixing, the isotopic composition of the impacted precipitation is expected to vary in proportion to the relative contributions of background precipitation and combustion water vapor. Thus, the resulting $\delta^{18}O$ and $\delta^{2}H$ signatures can reasonably be approximated as a linear combination of the two endmembers. We can then calculate x, the proportion of combustion water that interacted with the precipitation, as follows:

Equation 5.1

$$\delta_{sample} = x \times \delta_{combustion} + (1 - x) \times \delta_{LMWL}$$

Equation 5.2

$$x = \frac{\delta_{sample} - \delta_{LMWL}}{\delta_{combustion} - \delta_{LMWL}}$$

By practicality, $\delta_{\text{combustion}}$ was defined in this study as the isotopic composition of combustion water measured at UQAM. However, it is worth noting that the theoretical isotopic composition of combustion water spans a much wider range than the single measured value used here (Figure 5.2b), potentially resulting in significantly larger ranges of x than reported later in this study.

5.4.4.3 Electrical conductivity

The air's electrical conductivity is mainly due to the mobility of small ions (Kamsali *et al.*, 2011). In a polluted atmosphere, aerosol particles attach to these small ions and form larger ions, thus depleting the small ion content. The electrical conductivity and aerosol concentration are therefore generally considered to have an inverse relationship in the atmosphere, and the electrical conductivity has been proposed as an index of air pollution (Kamsali *et al.*, 2011).

In turn, precipitation washes these ions to a degree that depends on the duration and intensity of precipitation. However, it remains unclear in the literature whether, in a polluted atmosphere, precipitation exhibits reduced electrical conductivity because of a lower amount of small atmospheric ions, or increased conductivity because of the dilution of ionic species into the liquid water. Either way, comparing the spatial distribution of our samples' electrical conductivity with isotopic indicators could provide complementary information on the contribution of pollution to urban precipitation.

We measured the electrical conductivity of our samples, using a conductometer WTW model 3320 calibrated with a solution of 1413 µs/cm (HI70031, Hanna Instruments). A standard solution of 84 µs/cm (HI7033, Hanna Instruments) was used as a control.

5.5 Results & Discussion

To ensure that the sampled events were representative of precipitation in Montreal, we compared several meteorological variables from our sampling periods with those of all recorded events during the same timeframe. The variables analyzed included total precipitation, event duration, intensity, and average temperature (Annexe L). Event 19, which exhibited an anomalously high intensity relative to the others, was excluded from subsequent correlation analyses. All remaining events fell within the expected range for these variables and were considered representative.

From there, we aimed to separate urban controls from the regional controls driving the isotopic distribution of these events. We assessed correlations between key meteorological parameters and the isotopic signatures of the sampled events (Figure 5.3) to sustain the rest of this analysis, based on the data table that can be found in Annexe M.

It should be noted that due to a limited selection of specific events (Figure 5.1b), the exclusion of extreme events, and the fact that less than half of the deployed stations were active during many events, the observed correlations are proper to this sampling series, rather than representative of annual precipitation patterns. For this reason, we retained correlations with p-values below 0.1. While not strictly statistically significant, this approach allows us to observe and discuss trends within our dataset.

Figure 5.3: Multi-variable correlation matrix for all events sampled. The color and size of the dots represent the correlation coefficient between two variables, for all p-values < 0.1. P-values < 0.05 and < 0.01 are represented by * and ** symbols, respectively. The closer to dark red, the more direct the link between two parameters. The closer to dark blue, the more the parameters vary inversely.

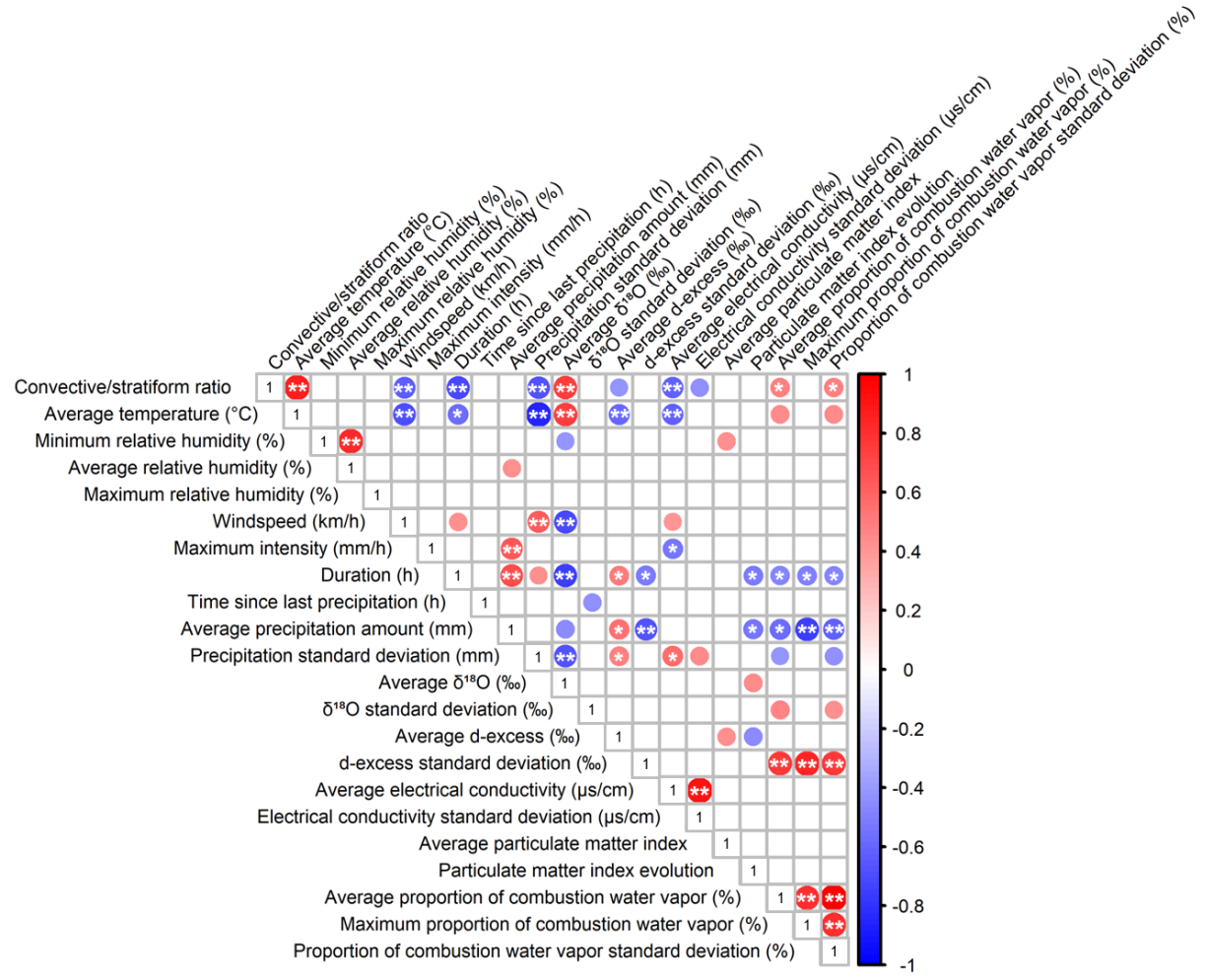

5.5.1 Climatic controls on the isotopic distribution of precipitation

To have a better overview of the isotopic distribution of our events, we plotted all precipitation samples on a $\delta^{18}O$-$\delta^{2}H$ diagram (Figure 5.4). With a global regression equation of $\delta^{2}H = 7.8\ \delta^{18}O + 11$, all events align closely with the Global Meteoric Water Line (GMWL). Except for one snow event that overlaps with rain, rain and snow events are clearly separated on the diagram, with rain exhibiting higher isotopic compositions than snow. Overall, there was a range up to 25 per mil in $\delta^{18}O$ between all events. This difference appears to be influenced by both temperature and precipitation type, as indicated by the positive correlation between temperature, convective/stratiform ratio, and average $\delta^{18}O$ values (Figure 5.3 and Figure 5.5a). This can be attributed to the fact that the isotopic fractionation factor between vapor and liquid water (or ice) decreases with increasing temperature, meaning that the residual cloud water vapor isotopic composition (and subsequent precipitation) rapidly decreases. Additionally, in the region, convection predominantly occurs during the summer months, when increased surface heating warms the near-surface air, as indicated by the positive correlation between the convective/stratiform ratio and temperature (Figure 5.3). Convective precipitation tends to be more enriched in heavy isotopes compared to stratiform precipitation (Aggarwal *et al.*, 2016). Indeed, for the case of stratiform precipitation, air masses usually go long distances from their formation location, enhancing progressive condensation and the draining of heavier isotopes on their trajectories, following the Rayleigh distillation model. On the other hand, convective precipitation is usually more local, meaning that the cloud has undergone less condensation before precipitating. The resulting precipitation remains closer to the high isotopic composition of the water vapor from which it condensed, whether the cloud originated from re-evaporated surface water or evaporated seawater. Locally, such a rainout of heavier isotopes is also favored by long and intense local precipitation events. This explains why the average $\delta^{18}O$ values were negatively correlated with the average precipitation amount and event duration (Figure 5.3).

By opposition to $\delta^{18}O$, the average temperature and the convective/stratiform ratio are both negatively correlated with average d-excess values (Figure 5.3). In other words, the events showing the highest isotopic compositions, meaning the highest average $\delta^{18}O$ values, typically rain events, tend to have lower d-excess values. Interestingly, rain and snow events appear to align along two distinct meteoric water lines on the $\delta^{18}O$-$\delta^{2}H$ diagram, with a lower slope for rain samples than for snow samples (Figure 5.4). Several mechanisms could explain this divergence: (1) kinetic processes linked to sub-cloud precipitation evaporation, (2) the non-linearity of isotopic fractionation effects, as higher temperatures lead to a weaker fractionation, which reduces the slope in a $\delta^{2}H$ vs $\delta^{18}O$ plot as oxygen fractionates less than hydrogen, (3) or the mixing of two moisture sources, which may lie in the lower-right quadrant of the diagram and would then be representative of combustion water vapor (Figure 5.4). Based on the hypothesis of fractionation

non-linearity, we have calculated the expected slopes using the events' average temperatures and have found a maximum of 9.4 for snow and a minimum of 8.5 for rain. While this might contribute to the observed lowering of the rain slope compared to the snow slope, this is not enough to explain the average slope of 7.5 that was found for rain. Another phenomenon, either sub-cloud evaporation or moisture mixing, had to occur.

On the other hand, a few events exhibited particularly high d-excess values (highlighted in green in Figure 5.4). Using HYSPLIT back-trajectory analysis, we found that for most of these events, the air masses had passed over the Great Lakes during the previous days (Annexe N), suggesting an input of evaporated surface water into the atmospheric moisture. However, it was not always the case. For instance, Event 4, sampled on 24 September 2021, displayed unusually high d-excess values despite no recent trajectory over a major water body, indicating the influence of another process, yet to be identified.

Figure 5.4: Distribution of rainfall (red) and snowfall (blue) events relative to the Global Meteoric Water Line (GMWL). 1 snow event and 3 rainfall events exhibiting notably high d-excess values are highlighted in green, and zoomed on in the gray boxed area.

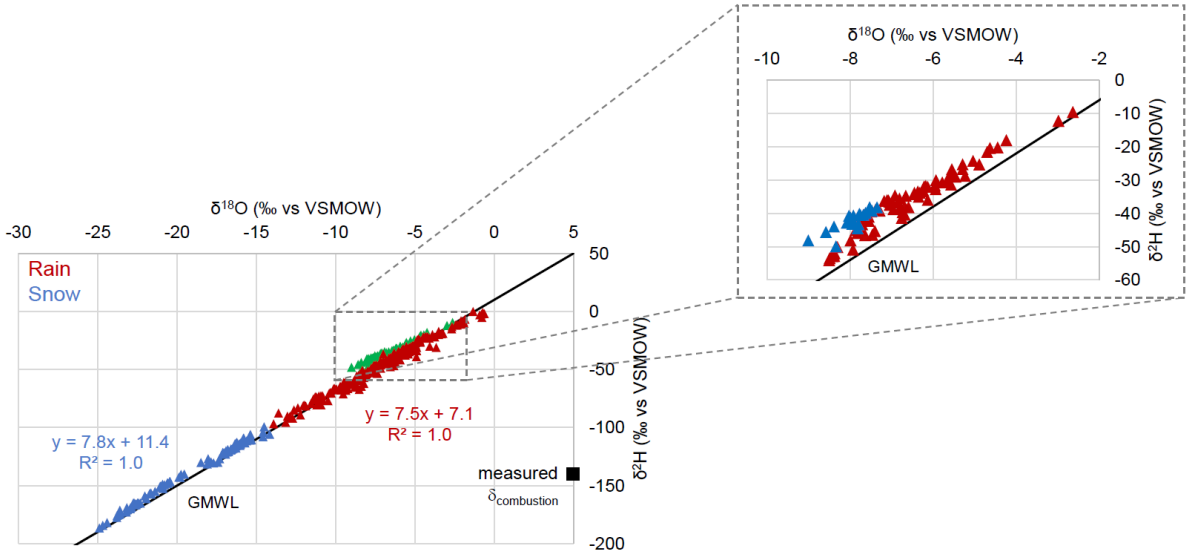

Figure 5.5: Distribution of each of the precipitation events' isotopic compositions as a function of (a) average hourly temperature and (b) convective-to-total precipitation ratio, for rainfall (red) and snowfall (blue) events.

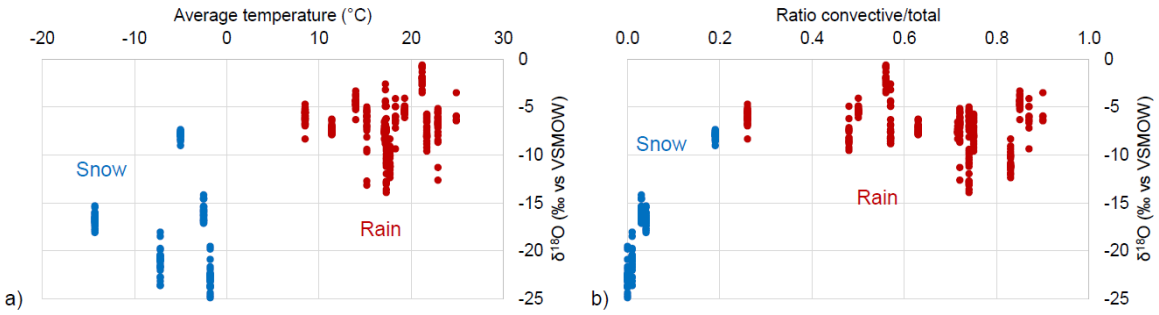

5.5.2 Local atmospheric moisture depletion and recharge

In terms of intra-event spatial variability, both rain and snow events showed considerable differences across the monitoring network, with differences reaching up to 8‰ for $\delta^{18}O$ and 65‰ for $\delta^{2}H$ between stations over a single event (Figure 5.5). To our knowledge, such an isotopic variability had never been reported before at this urban scale. One possible explanation for this increased variability could be the localized re-evaporation of lighter isotopes under the influence of the UHI for stations located in the city center. However, contrary to what we expected and upon examining spatial distributions within individual events, we did not observe a consistent enrichment in heavy isotope patterns over the urban core relative to its surroundings (as illustrated later in Figure 5.6). While it might mean that the UHI has a greater spatial influence than previously thought, and that we haven't truly captured the isotopic compositions outside of this influence, additional information needs to be investigated to understand the mechanisms driving this observed spatial heterogeneity. Plus, with few exceptions, the meteoric water lines derived from all stations do not exhibit slopes and intercepts consistent with a global evaporation signal (as illustrated later in Figure 5.6).

D-excess is an isotopic parameter that gives a lot of information on the sources of water vapor, and particularly on sub-cloud evaporation. Across the sampled events, average d-excess values show positive correlations with average precipitation amounts and event duration, while the d-excess variability is lower for higher precipitation amounts and event duration (Figure 5.3). This reflects the fact that higher rainfall amounts usually cause higher relative humidity, limiting sub-cloud evaporation. On the contrary, lighter precipitation will fully evaporate before reaching the ground, and therefore will not contribute to the final isotopic composition of the collected sample. In the case of partially evaporated precipitation, the d-excess will be reduced until atmospheric saturation is reached.

Other than these expected correlations, the only other meteorological parameter that seems to be linked to the variability of $\delta^{18}O$, and which is a key observation of our analysis, is the time spanned since the last event (Figure 5.3). This negative correlation suggests that the isotopic variability is stronger when precipitation events are close. This trend suggests that recent precipitation may increase spatial isotopic variability, likely due to the reintegration of evaporated surface water into the local atmospheric moisture.

To illustrate this result, we analyzed two rain events occurring one day apart, Event 3 (23/09/2021) and Event 4 (24/09/2021). What was very interesting to observe was that, for very similar meteorological conditions and the same number of sampling stations, the isotopic compositions of Event 4 showed greater variability than those of Event 3 (Figure 5.6a), with respectively 6‰ and 3‰ ranges in $\delta^{18}O$. We calculated the isotopic composition of water vapor in equilibrium with Event 3 rainfall, incorporating kinetic fractionation effects (gray cloud on Figure 5.6a). Between stations, some of the isotopic compositions of Event 4 precipitation seem to be heavily influenced by the isotopic composition of this water vapor (Figure 5.6a). Notably, during Event 4, the stations with the lowest isotopic compositions were located downwind (Figure 5.6b), suggesting that the stations at the exit of the city are more affected by the re-evaporation of rainfall from Event 3.

Figure 5.6: a) Modeled isotopic composition of water vapor derived from the evaporation of rainfall from Event 3, on the 23/09/2021 (gray), compared to the isotopic composition of rainfall from Event 4, on the 24/09/2021 (black). b) Spatial distribution of $\delta^{18}O$ during Event 4. c) Intra-event evolution of $\delta^{18}O$ and d-excess during Event 4, collected at UQAM. d) Spatial distribution of d-excess during Event 4.

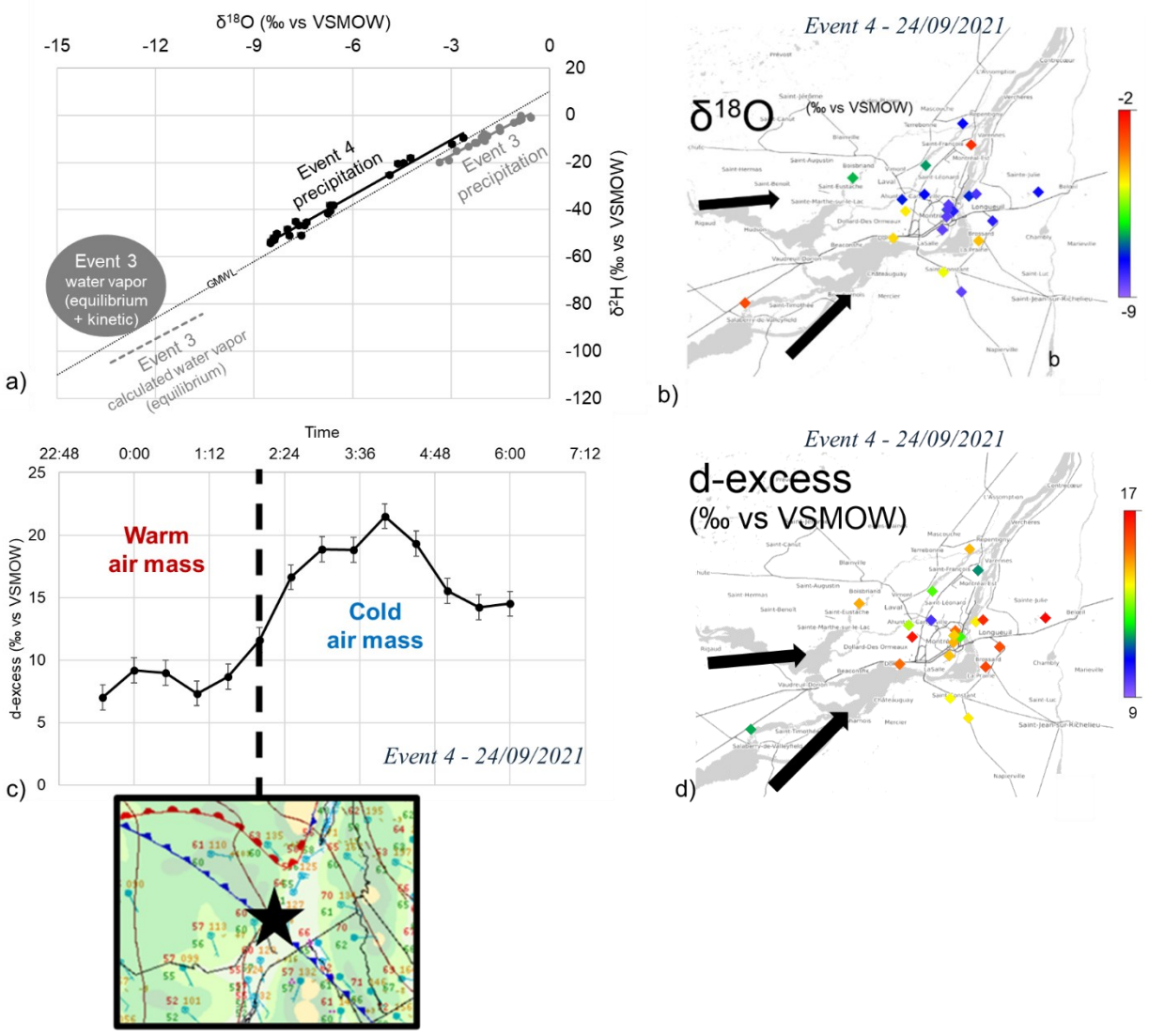

The isotopic evolution within the event itself also offers valuable insight. At the onset of event 4, d-excess values remained stable, around 8‰. However, by 2 AM, a sharp increase occurred, with d-excess rising to 22‰ within two hours (Figure 5.6c). This shift corresponds with the passage of a cold front. As the cold air mass pushed the warmer one, due to its lower density, the warm air rapidly lifted and condensed, producing precipitation. The beginning of the event likely occurred under the influence of the warm sector, transitioning into the cold sector at 2 AM.

Cumulative samples across the study area revealed a wide spatial range (up to 8‰) in d-excess values, with a notable downwind increase during this event (Figure 5.6d). This suggests that the city itself influenced d-excess values through an input of local water vapor. As the cumulative samples did not fall below the Global Meteoric Water Line, this eliminates combustion water vapor as a potential primary water vapor source. This validates the hypothesis of an injection of UHI-induced surface water vapor recycling into the precipitation system, contributing to the high spatial isotopic range observed during Event 4 (Figure 5.7).

Figure 5.7: Conceptual diagram: In-cloud injection of urban water vapor (either from reevaporated precipitation or combustion processes) progressively alters the isotopic composition of precipitation along its trajectory over the city.

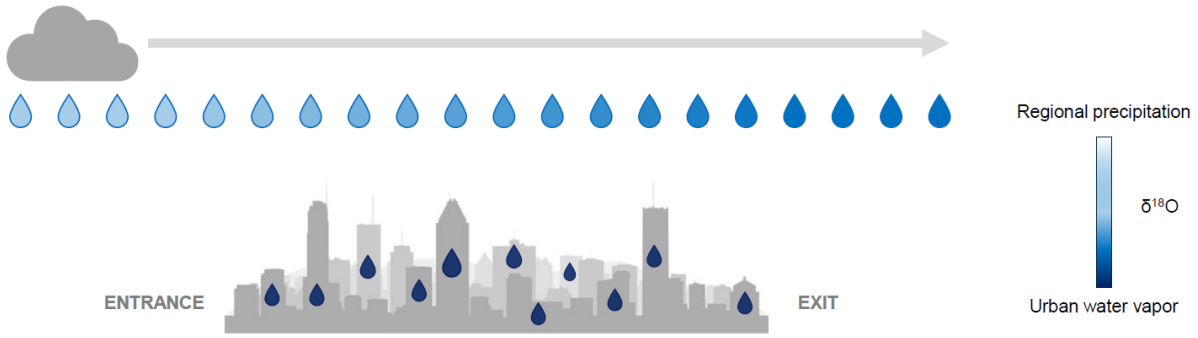

Overall, the range of isotopic compositions was higher for events with the most recent precipitation (Figure 5.8), which further validates this re-evaporation hypothesis. Here, we visually estimated that the residence time of rainwater in the city was around two days, a threshold after which the isotopic range significantly decreases from up to 9‰ to less than 3‰ (Figure 5.8). It is worth noting that Montreal is a particularly green city, and this may favour the recycling of precipitation through the evapotranspiration of vegetated areas. Whether similar processes occur as readily in less vegetated cities is yet to be determined.

Figure 5.8: Difference between the maximum and minimum $\delta^{18}O$ values ($\Delta\delta^{18}O_{max\text{-}min}$) observed across all stations for each sampled event, plotted against the time spanned since the previous precipitation event.

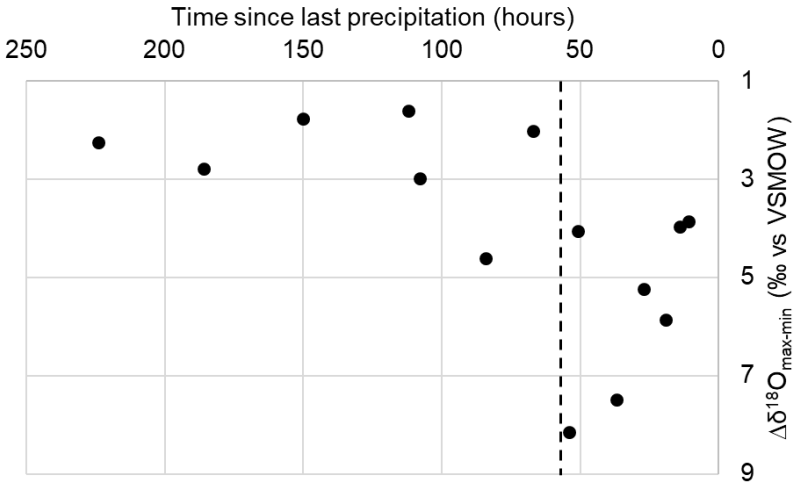

5.5.3 Pollution

5.5.3.1 Local pollution indicators

Counterintuitively, average electrical conductivity (EC) does not appear to correlate with air quality, represented as the average PM2.5 AQI, nor with its evolution across events (Figure 5.3). More importantly, no significant correlation was observed between electrical conductivity and isotopic variables (Figure 5.3). As this complementary indicator does not prove to be significant in improving our understanding of urban precipitation, it will not be investigated further in this study.

As for the PM2.5 AQI, its observed positive correlation with average d-excess (Figure 5.3) likely reflects enhanced atmospheric stability over winter, which can lead to accumulation of pollutants near the surface, where PM is typically measured. Conversely, summer conditions are typically more convective, promoting vertical mixing and reducing surface-level PM. Additional winter contributions from residential heating and road salting can further increase atmospheric PM2.5 concentrations.

The PM2.5 AQI evolution is positively correlated to average $\delta^{18}O$, while it is negatively correlated to average d-excess (Figure 5.3). Again, more than showing a real impact of particulate matter on isotopic signatures, these correlations may simply be reflecting seasonal effects (i.e., lower $\delta^{18}O$, higher d-excess in winter) and suggest that PM2.5 is more effectively washed out during colder and longer stratiform precipitation events, typical of the winter season, as suggested in our data (Annexe O).

To gain a finer understanding of these results, we developed a high-resolution snow sampling protocol (Annexe P), applied during a snow event in February 2023. The results revealed a positive correlation between $\delta^{18}O$ and PM2.5 AQI (Figure 5.9a), clearer than what was initially suggested by the correlation matrix. One possible explanation could be the co-occurrence of combustion-related water vapor and PM inputs, as suggested by the fact that in this case, the PM2.5 AQI seems to increase over the event. However, as combustion water vapor shows very low $\delta^{2}H$ and d-excess, this would likely result in a negative $\delta^{18}O$-d-excess correlation, which was not observed here (Figure 5.9b).

An alternative hypothesis involves microphysical interactions between PM2.5 and cloud water: PM could act as cloud condensation nuclei, reducing droplet size and potentially enhancing evaporation or sublimation. However, sublimation does not induce isotopic fractionation, and the positive correlation between $\delta^{18}O$ and d-excess observed during the event suggests that enhanced evaporation is not a dominant process in this case (Figure 5.9b). Moreover, neither the temperature nor the amount of precipitation was correlated with $\delta^{18}O$ nor PM2.5 AQI evolution (Figure 5.9c). In that case, an additional water vapor input seems necessary to explain the concurrent increases in PM2.5 AQI, $\delta^{18}O$, and d-excess. The potential relationship between isotopic compositions and PM concentrations remains unclear at this stage and requires further investigation.

Figure 5.9: a) Temporal evolution of the isotopic composition $\delta^{18}O$ of the snow event compared to a) the temporal evolution of PM2.5 AQI, b) the d-excess, and c) the snowfall intensity

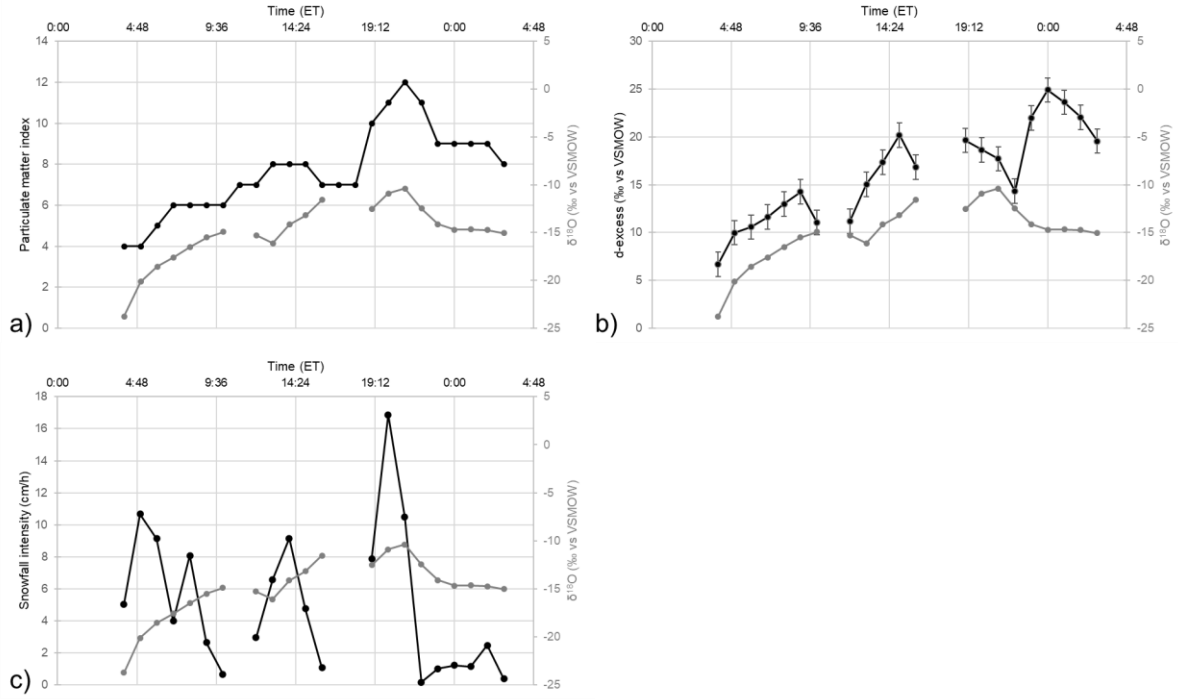

5.5.3.2 Combustion water vapor contribution

As expected, the estimated contribution of combustion water vapor was positively correlated with d-excess standard deviations. Subsequently, these variables show opposite correlations with most of the variables contained in the correlation matrix (Figure 5.3). Thus, distinguishing between the effects of sub-cloud evaporation and contributions of combustion-derived water vapor remains challenging. In both cases, the isotopic composition of samples will be shifted toward the lower-right quadrant of the diagram, either by lowering the slope of the subsequent samples due to kinetic processes, or by mixing with a pole (illustrative example in Figure 5.10c), as developed in section 5.4.4.2.

As both the d-excess and the estimated combustion water vapor contribution showed very high correlations to precipitation amounts (Figure 5.3), it appeared necessary to study in more detail the spatial distribution of d-excess and precipitation amounts to improve our understanding.

Event 11 that occurred over March 10-13, 2022, provided a particularly illustrative case, showing clear variability in snowfall intensity along its trajectory (Figure 5.10a). Snowfall was most intense at the beginning of the event, then progressively decreased as it moved downwind, toward the exit of the city. Interestingly, the snowfall associated with higher precipitation amounts tends to align with the local meteoric water line, whereas lower-amount precipitation plots below it (Figure 5.10c), suggesting that d-excess is particularly sensitive to precipitation amount (Figure 5.10 b and e).

To assess potential post-sampling evaporation effects, we calculated the maximum isotopic shift that could result from evaporation of melted snow within the collectors. These values remain within the analytical uncertainties (±0.1‰ for $\delta^{18}O$ and ±1‰ for $\delta^{2}H$). Given that sublimation does not significantly alter the isotopic composition of snow, the observed isotopic shifts cannot be attributed to sublimation of the water in the air column. Moreover, while d-excess values increased in the case of reevaporated surface water contribution (Figure 5.6e), they decreased at the exit of the city in that case (Figure 5.10b). Of course, this could be due to the subsequent melting and evaporation of snow through the air column. However, vertical atmospheric profiles from Maniwaki weather balloon soundings indicated that temperatures stayed below 0°C throughout the depth of the column during the event. Here, this situation may reflect equilibration with locally sourced combustion-derived water vapor, which would relatively have a greater impact on the isotopic compositions of precipitation of smaller amounts.

The estimated contribution of combustion water vapor reached up to 5 % (Figure 5.10d), consistent with water vapor values reported in previous studies (Gorski *et al.*, 2015 ; Xing *et al.*, 2020). One should

remember that the combustion water contribution is calculated using a single measured end-member and a linear mixing model, despite large known variability in combustion isotopic signatures (Figure 5.2b), which might impact these results.

Figure 5.10: Event 11 (a) Spatial distribution of precipitation volumes, (b) spatial distribution of d-excess values, (c) $\delta^{18}O$ vs $\delta^{2}H$ bubble chart, with bubble size proportional to snowfall amount, d) spatial distribution of the estimated proportion of precipitation equilibration with combustion water vapor, and (e) relationship between precipitation volume and d-excess values.

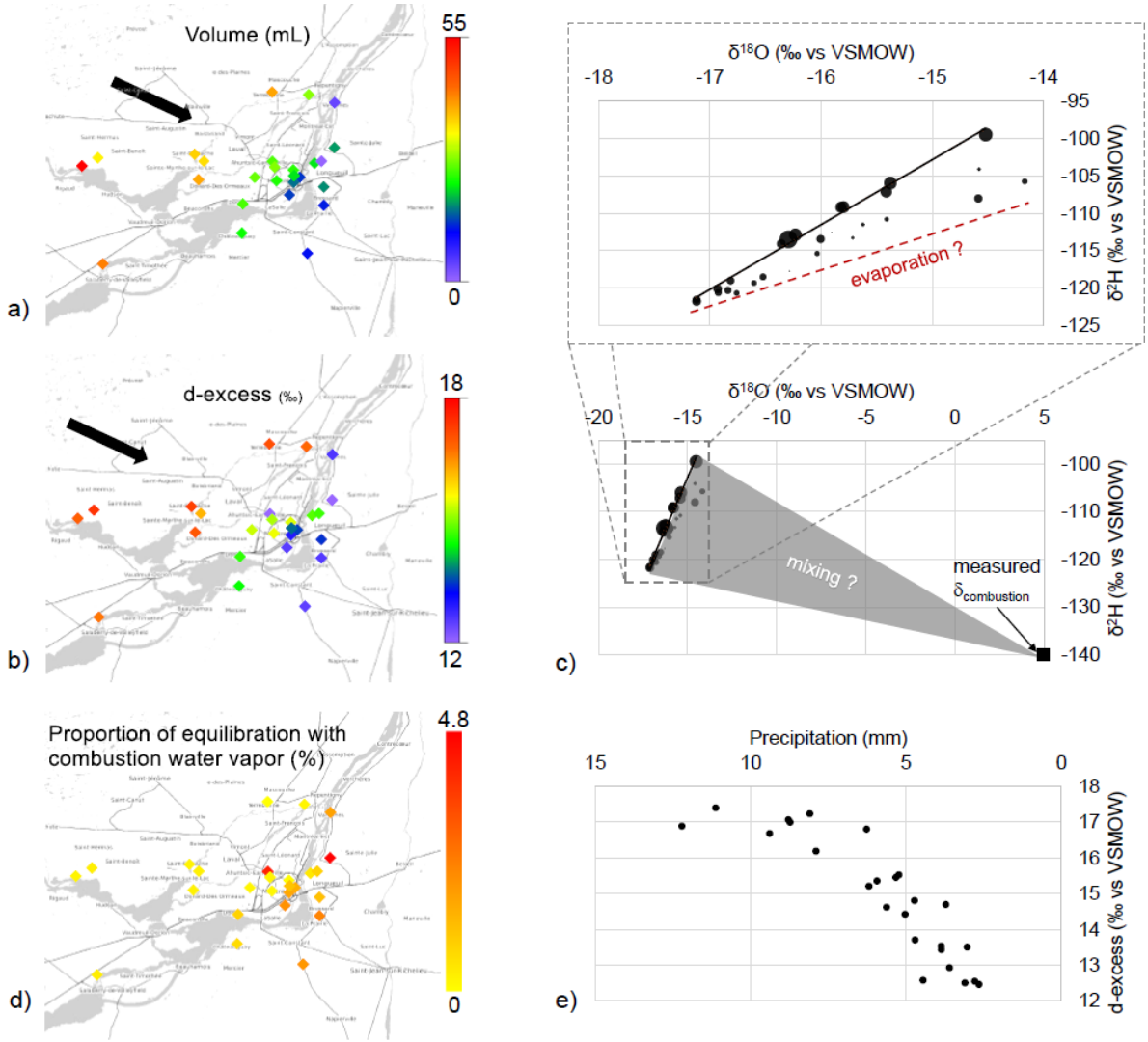

5.5.4 Recommendations for future work

While it remains challenging to systematically distinguish the impact of individual processes on urban precipitation, the methodology presented here represents an innovative approach that demonstrates the added value of stable isotope analysis at high spatial and temporal resolution in studying urban

meteorological processes, and the potential for democratizing the use of these environmental tracers. However, it is not yet clear how transferable these results are to other urban environments, and we hope this methodology will encourage the development of other larger-scale projects to provide complementary answers.

In particular, to improve our understanding of urbanization's impact on precipitation, future work should investigate multiple spatial and temporal scales. While this study focused on city-sized patterns, finer scales, such as individual streets, near industrial zones, or downwind from combustion sources, could provide valuable information. In particular, expanding to regional scales would allow the assessment of the cumulative impacts of cities on precipitation formation. Moreover, it should be noted that precipitation extremes were excluded from this study. Using our methodology to investigate precipitation extremes could bring valuable insights to our understanding.

In parallel, simultaneous monitoring of precipitation isotopic signatures and climatic variables such as temperature, relative humidity, and atmospheric CO_2 would significantly enhance interpretation. For instance, investigating whether a correlation between d-excess and atmospheric CO_2 exists in precipitation, similar to what was observed in water vapor (Gorski *et al.*, 2015), represents a promising direction for future research. It is also worth noting that the $\delta^{17}O$-$\Delta^{17}O$ relation is independent of temperature and can be used as a conservative tracer of humidity at the initial evaporation of water (Angert *et al.*, 2004 ; Kaseke *et al.*, 2018 ; Tian *et al.*, 2018), thus providing complementary information to d-excess. Incorporating these measurements into a similar study could further improve our understanding of the processes involved.

Finally, Montreal is a particularly green city, and as such, our results may not be directly transferable to more arid or industrialized urban environments. Extending this type of study to drier or more densely built environments is necessary to understand the broader applicability of our results. Additionally, coupling these observations with numerical models that incorporate urban parameterization would significantly strengthen our capacity to interpret and generalize findings.

5.6 Conclusions

Stable water isotopes $\delta^{18}O$ and $\delta^{2}H$ bring valuable information for investigating how urban environments impact the dynamics of precipitation. This study investigated the added value of the isotopic signature of urban precipitation at high spatial and temporal resolution to improve our knowledge of this phenomenon. Based on the development of a participatory citizen network over the city of Montreal, the samplings of 19

rain and snow events at this high resolution allowed to distinguish between regional and urban influences on precipitation isotopic signatures.

At the regional scale, isotopic signatures ($\delta^{18}O$, $\delta^{2}H$, and d-excess) reflected processes related to temperature and precipitation type. Convective, short-lived precipitation, often associated with higher temperatures, showed higher isotopic compositions, while longer stratiform precipitation events led to progressive depletion of heavy isotopes, as expected with Rayleigh distillation. The d-excess decreased during warmer and drier events, reflecting its sensitivity to sub-cloud precipitation evaporation.

At the urban scale, this isotopic study highlighted subtler processes. A strong spatial isotopic variability up to 8‰ for $\delta^{18}O$ and 65‰ for $\delta^{2}H$ over a single event was observed across the city, which was never reported at this urban scale. The lack of consistent enrichment over the city center eliminated the hypothesis of UHI-induced sub-cloud evaporation to explain these differences. However, our results suggest that recycled water vapor, likely enhanced by the UHI, may have a major impact on this variability. In particular, downstream increases in d-excess during events following recent precipitation suggest the injection of evaporated and recycled surface water into the atmosphere. The high range of $\delta^{18}O$ and $\delta^{2}H$ values observed between stations for most events is correlated with the time elapsed since the last precipitation. Isotopic signatures have allowed for characterising the residence time of rainwater in the city: i.e., two days.

Isotopic tracing at high spatial resolution also revealed a potential contribution from combustion-derived water vapor, reflected in reduced d-excess values, especially for smaller precipitation amounts. This water vapor may contribute to up to 5 % of precipitation.

The participatory citizen network provided a way of rapidly developing a spatially dense network at low cost in an urban area. This high-resolution data proved to be efficient in establishing the differences in isotopic compositions across Montreal city, and the potential processes contributing to these effects. A coordinated effort combining similar studies in other major cities could open exciting new avenues in urban hydrometeorology.

5.7 Contribution de l'article D

Dans cette partie, nous avons ainsi pu montrer que la signature isotopique des événements de pluie et de neige échantillonnés montre une importante variabilité entre les stations, ce qui n'avait à notre connaissance jamais été documenté à une telle résolution.

Contrairement à ce qui avait déjà été documenté dans la littérature, ce n'est pas l'évaporation des précipitations lors de leur chute vers le sol, potentiellement favorisée par l'îlot de chaleur urbain, qui semble à l'origine de cette hétérogénéité. L'échantillonnage de deux événements subséquents a permis de montrer que le temps écoulé depuis les dernières précipitations est négativement corrélé avec la variabilité des précipitations. Cela met en évidence que l'îlot de chaleur urbain favorise le recyclage des précipitations, par évaporation puis re-précipitation après ré-injection dans le nuage. En parallèle, l'estimation de la proportion d'eau de combustion dans les précipitations a montré que celle-ci pouvait atteindre un maximum de 5 %, ce qui n'avait jamais été documenté. Ainsi, cette étude met en évidence que l'échantillonnage à haute résolution spatiale et temporelle des précipitations en milieu urbain permet de retracer des processus subtils à l'origine de la modification des précipitations urbaines.

La revue scientifique *Urban Climate* s'adresse à un public dont l'intérêt est axé sur les climats urbains, et non pas spécialisé dans l'utilisation appliquée des traceurs environnementaux tels que les isotopes stables de la molécule d'eau. À travers la soumission de ces résultats dans cette revue, et le partage détaillé de la méthodologie à bas coût adoptée, nous espérons ainsi amener la démocratisation de cet outil et susciter de nouvelles idées de projets dans d'autres contextes urbains, notamment des villes moins végétalisées que Montréal. Comparer l'hétérogénéité des signatures isotopiques des précipitations urbaines dans des contextes variés permettra peut-être ainsi d'amener des résultats plus généralisables quant aux processus impactant les précipitations en ville.

CHAPITRE 6 :
ENQUÊTE SUR LA SENSIBILISATION DES MEMBRES DU RÉSEAU

6.1 Introduction

Dans la recherche scientifique, les réseaux mobilisant la contribution active de publics non issus du milieu académique suscitent un intérêt grandissant. En effet, ces réseaux participatifs présentent de nombreux avantages, notamment la possibilité d'augmenter la résolution spatiale et temporelle d'acquisition de données à un moindre coût. En ce qui concerne le domaine de l'environnement, la science citoyenne peut avoir un large éventail de retombées positives et négatives sur les participant·e·s (Walker *et al.*, 2021). Ainsi, certains projets ont notamment démontré leur capacité à sensibiliser les citoyen·ne·s aux enjeux environnementaux, voire à modifier leur comportement (United Nations Development Programme, 2023). La sensibilisation de la population est un enjeu clé dans l'action communautaire et la mise en place de mesures d'adaptation et de résilience face aux changements climatiques et environnementaux. Ainsi, l'évaluation de ces effets de sensibilisation peut constituer un outil précieux pour le développement de futurs réseaux participatifs. Cependant, ce type d'analyse reste encore peu fréquent dans les études hydrologiques.

Collect'O est le premier réseau participatif dédié à l'étude isotopique des précipitations urbaines. Il compte une cinquantaine de participant·e·s du Grand Montréal, ayant simultanément prélevé des échantillons de pluie et de neige depuis leur domicile entre 2021 et 2023. L'objectif était d'utiliser des traceurs naturellement présents dans la molécule d'eau afin de comprendre comment les précipitations sont modifiées en milieu urbain. Ce phénomène est encore peu connu et discuté du grand public, alors que les citoyen·ne·s des villes sont les premiers touchés par ce phénomène. Cela montre l'importance de sensibiliser la population à ces enjeux, particulièrement dans un contexte d'urbanisation croissant.

Le réseau Collect'O a bénéficié du soutien du volet Transfert du Geotop, centre de recherche sur la dynamique du système Terre, regroupement stratégique du Fonds de Recherche du Québec (FRQ). Ce programme vise à financer des projets susceptibles d'accroître la visibilité et les retombées de la recherche réalisée au sein du Geotop, par le biais de nouvelles activités de transfert des connaissances et de diffusion des résultats de recherche vers des publics non académiques, ou par le développement d'approches pour réaliser ce transfert.

Les participant·e·s du projet ont été recruté·e·s à travers plusieurs voies : des interviews dans différents médias (*Actualités UQAM*, *MétéoMédia*, *Le Devoir*, *Les Années Lumière*), le bouche-à-oreille, et des

courriels de diffusion, notamment via le centre de recherche Geotop, auquel plusieurs membres de l'équipe sont affilié·e·s. Il est à noter que nous avons fait en sorte de respecter la confidentialité des participant·e·s : ni leur identité ni leurs adresses n'ont jamais été partagées avec le public.

Tout au long du projet, plusieurs initiatives ont été mises en place pour garder le lien entre les chercheur·euses et les citoyen·ne·s impliqué·e·s. Des capsules vidéo ont été partagées sur la page web https://hydro-sciences.uqam.ca/collecto/avancees/, une rencontre d'information et une visite du laboratoire de géochimie des isotopes stables légers du Geotop ont été organisées fin septembre 2023, et les résultats du projet ont été partagés dans une vidéo finale. Le message principal que nous avons cherché à mettre en avant est l'impact positif que les précipitations ont sur nos vies, en particulier leur contribution au nettoyage de l'atmosphère et à la régulation des vagues de chaleur. Nous avons ainsi visé à montrer l'importance de limiter l'impact de l'Homme sur les précipitations, pour qu'elles puissent continuer à jouer ces rôles. Nous avons notamment mis en avant les risques liés à l'imperméabilisation des sols, et l'importance de verdir nos villes pour assurer le stockage de l'eau.

Au cours du projet, un questionnement a émergé, à savoir *dans quelle mesure cette démarche a-t-elle aidé à la sensibilisation des citoyen·ne·s aux enjeux des précipitations urbaines ?* Notre objectif était ainsi d'apporter des pistes à de futurs réseaux participatifs dans le domaine de l'environnement afin de mieux atteindre cet objectif de sensibilisation. Pour répondre à cette question, il nous a semblé nécessaire de permettre aux participant·e·s de ce projet de s'exprimer librement sur leur expérience dans ce réseau. C'est ainsi que nous les avons invité·e·s à participer au dernier chapitre de cette thèse.

6.2 Méthodologie

Cette enquête a fait l'objet d'une validation préalable du Comité d'éthique de la recherche pour les projets étudiants impliquant des êtres humains (CERPE) de l'UQAM. Afin de conserver l'anonymat des réponses des participant·e·s, nous avons fait le choix de recourir à un questionnaire en ligne d'environ 15-20 minutes.

Le questionnaire a été publié sur la page web https://hydro-sciences.uqam.ca/collecto/impacts-sociaux/. Sur cette page, les répondant·e·s ont d'abord eu accès à une capsule vidéo les informant quant aux résultats finaux du projet. Iels pouvaient ensuite lire un formulaire de consentement lié à la participation à cette enquête, avant de remplir le formulaire en question (Annexe Q). Aucun renseignement identificatoire direct n'a été demandé, et le consentement a été recueilli de manière implicite par le fait que le formulaire anonyme soit rendu.

L'enquête avait pour premier objectif de mieux évaluer le profil des participant·e·s, ainsi que les moyens de communication les ayant amené·e·s à prendre connaissance du projet et à s'impliquer. Elle comprenait également des questions sur les avantages et difficultés perçus lors du projet, et les connaissances initiales et l'évolution de la perception des participant·e·s quant à l'impact de l'urbanisation sur les précipitations urbaines. Enfin, nous avons cherché à déterminer si leur entourage avait également été sensibilisé indirectement par le projet.

Une lettre d'invitation générale a été envoyée à tous les membres de Collect'O le lundi 7 juillet 2025, et la date limite pour répondre à ce questionnaire était fixée au vendredi 18 juillet 2025. Des courriels de rappel généraux leur ont été envoyés le lundi 14 juillet et le jeudi 17 juillet 2025.

6.3 Résultats & Discussion

6.3.1 Profils des répondant·e·s

Un total de 20 personnes participant au réseau Collect'O ont répondu au questionnaire, ce qui représente 35 % des participant·e·s. Étant donné que nous avons envoyé ce questionnaire 4 ans après la première collecte Collect'O, nous évaluons ce taux de réponse comme positif.

Nous avons constaté qu'une grande majorité des répondant·e·s appartenait à une population relativement mature, 80 % d'entre elleux ayant plus de 40 ans (Figure 6.1a). Quelle que soit la tranche d'âge, au moins la moitié des répondant·e·s était des femmes, et nous avons comptabilisé 70 % de femmes toutes tranches d'âge comprises. La quasi-totalité des personnes ayant répondu avait une formation universitaire ou post-universitaire. Un seul répondant avait un niveau de formation secondaire. Ces résultats nous ont ainsi amenés à nous demander si le projet avait réellement eu la capacité de toucher un public extérieur au milieu académique. Si les participant·e·s restent majoritairement issu·e·s de milieux proches de la recherche, cela limite la portée de sensibilisation de la population.

En effet, parmi ces répondant·e·s, la plus grande majorité (35 %) avait entendu parler du projet à travers le média *Actualités UQAM* (Figure 6.1b), dans lequel un article avait été publié à ce sujet en 2021. Par ailleurs, 20 % avaient été contacté·e·s par l'intermédiaire d'un lien professionnel ou personnel direct avec l'un des instigateurs du projet. Cependant, 35 % des répondant·e·s avaient eu connaissance du projet par les médias télévisés, la presse écrite ou le bouche-à-oreille, sans lien direct avec le milieu universitaire. Cela représente moins de la moitié des répondant·e·s, mais nous estimons que c'est une proportion satisfaisante, étant donné que notre objectif premier n'était pas de sensibiliser la population, mais bien d'obtenir une haute résolution spatiale pour la collecte des échantillons. Nous suggérons toutefois qu'à l'avenir, des partenariats avec des

écoles ou des institutions communautaires hors milieu académique pourraient être favorisés pour diversifier le profil des participant·e·s.

Concernant les motivations ayant poussé les répondant·e·s à rejoindre le réseau, la majorité évoque la volonté de contribuer à la recherche scientifique (42 %) ou d'agir par rapport à leurs préoccupations environnementales (33 %) (Figure 6.1c). Une faible proportion a indiqué avoir rejoint le réseau par intérêt pour la météorologie (13 %). L'engagement communautaire apparaît comme une motivation très peu représentée dans ces réponses (7 %).

Quant aux avantages perçus de leur participation au projet, 35 % des répondant·e·s ont indiqué que le principal bénéfice résidait dans l'acquisition de données pour le projet de recherche. Par ailleurs, de nombreux·ses participant·e·s ont évoqué des avantages plus personnels. Ainsi, 40 % ont spontanément déclaré avoir apprécié le sentiment d'utilité et d'implication citoyenne éprouvé. Un répondant a déclaré avoir rejoint le réseau par désir d'aider, tandis qu'un autre déclarait l'avoir fait par plaisir d'être en contact avec la relève scientifique. En parallèle, 30 % ont spontanément mentionné avoir apprécié l'aspect de partage scientifique, notamment la possibilité de se tenir informé·e, de rester connecté·e aux enjeux environnementaux, et de suivre l'évolution des connaissances tout au long du projet. Cela montre l'importance d'intégrer une stratégie éducative dans les projets de science participative, tout en valorisant le travail fourni par les participant·e·s.

Figure 6.1 : Profils des répondant·e·s

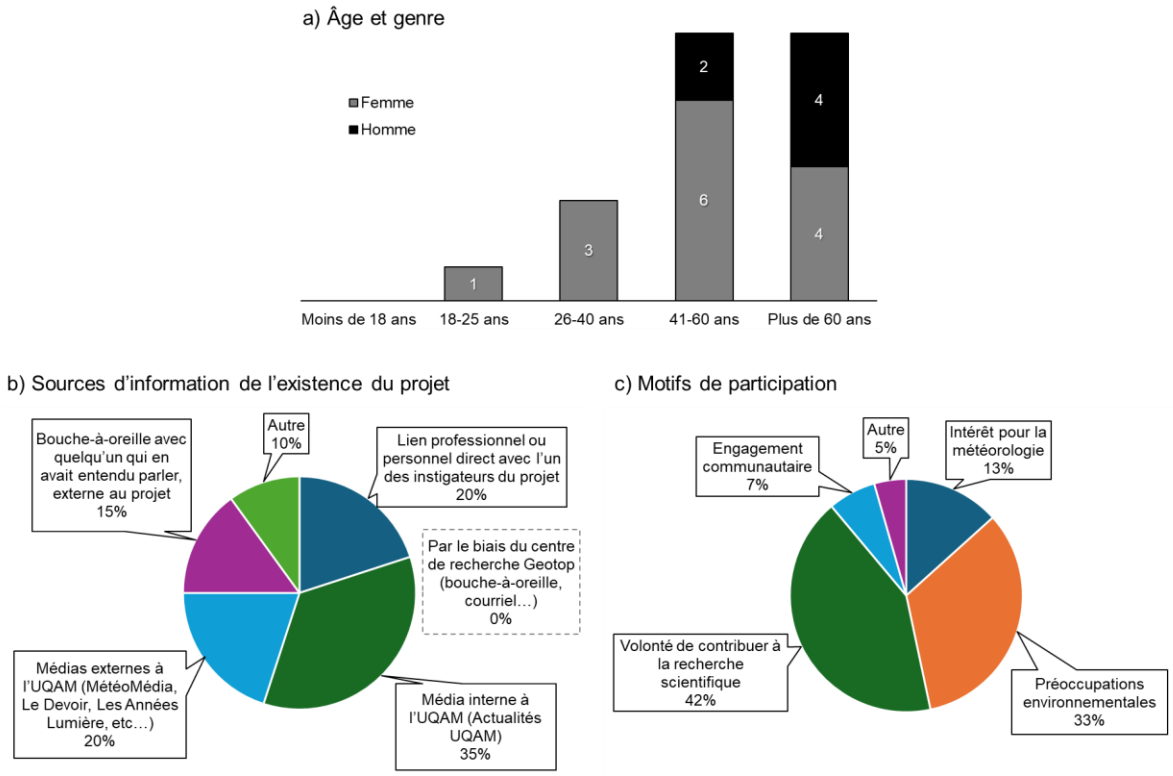

6.3.2 Accessibilité des collectes

Nous avons observé qu'une grande majorité des participant·e·s (90 %) a trouvé la collecte *facile* à *très facile* à réaliser (Figure 6.2a). 35 % des participant·e·s n'ont relevé aucune difficulté lors de leurs collectes. Les principaux inconvénients soulevés étaient relatifs au fait de devoir ramener les échantillons au point de collecte (35 %), ce qui n'était pas toujours aisé, particulièrement dans un contexte de pandémie, mais aussi parce que de nombreux participant·e·s étaient justement situé·e·s en-dehors de l'île de Montréal et n'avaient pas souvent l'occasion de se rendre à l'UQAM. Pour pallier cet aspect, nous avions instauré un deuxième point de collecte géré par le Conseil des bassins versants des Mille-Îles (COBAMIL), à Saint-Eustache. Cependant, cela n'arrangeait qu'une faible proportion des participant·e·s. Nous recommandons à de futurs projets d'envisager plus de partenariats pour augmenter le nombre de points de collecte, ce qui facilitera l'accès des participant·e·s et sera donc susceptible de les garder motivé·e·s tout au long du projet.

Nous savions par avance que la majorité des participant·e·s ne pourrait pas se rendre disponible à chacune des collectes. Nous avons toutefois essayé de faciliter leur disponibilité en sélectionnant les événements en fonction des plages horaires auxquelles les iels pourraient installer et désinstaller les collecteurs. Nous avons fait en sorte que ces plages horaires soient suffisamment larges pour que cela convienne aux quelques

participant·e·s qui collectaient les échantillons depuis leur lieu de travail, et à celleux qui collectaient depuis leur domicile. Ainsi, l'installation et la désinstallation des collecteurs pouvaient être réalisées soit le matin avant de partir (d'arriver) au travail, soit le soir en rentrant (partant). Certain·e·s répondant·e·s (30 %) ont toutefois regretté de n'avoir pas pu être disponibles à chaque événement.

Suite à certains retours des participant·e·s en cours de projet, et dans le but d'évaluer la motivation à participer de publics de tous âges, nous avons également cherché à déterminer dans quelle mesure le protocole d'échantillonnage pouvait être perçu comme ludique et accessible à réaliser. En ce qui concerne le niveau d'amusement ressenti pendant les collectes, la plupart des répondant·e·s l'ont évalué comme *modéré* à *faible* (Figure 6.2b). Malgré ce manque d'aspect ludique, la majorité des participant·e·s a estimé que le protocole était globalement accessible à tous·tes (Figure 6.2c), ce qui témoigne de sa simplicité. Les aspects les plus appréciés ont été, d'une part, la possibilité de constater visuellement la quantité de pluie ou de neige recueillie dans les collecteurs après chaque événement (6 personnes ayant spontanément mentionné cet élément), et d'autre part, le fait de pouvoir mettre en valeur ou accéder à des endroits habituellement peu fréquentés autour de leur domicile ou de leur lieu de travail. Plusieurs répondant·e·s ont également souligné que l'installation suscitait la curiosité des passant·e·s et des invité·e·s.

Figure 6.2 : Participation aux collectes

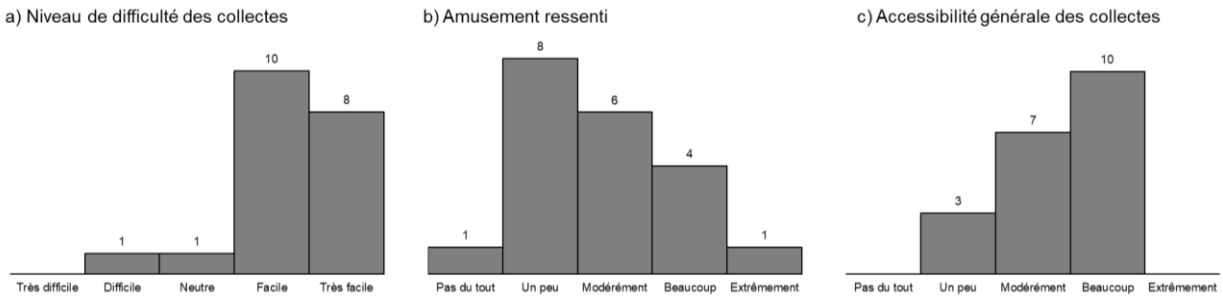

6.3.3 Sensibilisation des participant·e·s Collect'O

Nous avons observé qu'avant leur participation au projet, 65 % des répondant·e·s se déclaraient *pas du tout* à *modérément informé·e·s* quant à l'impact de l'urbanisation sur les précipitations urbaines et leurs conséquences (Figure 6.3a). Globalement, la totalité des répondant·e·s ont déclaré que leur compréhension du sujet avait été améliorée, dans des proportions allant d'*un peu* à *beaucoup*, la moitié d'entre eux déclarant une amélioration modérée (Figure 6.3b). Cette observation témoigne de l'efficacité des moyens de communication utilisés tout au long du projet. Bien que la majorité des répondant·e·s était liée, d'une façon ou d'une autre, au milieu universitaire (section 6.3.1), cela signifie qu'une part significative d'entre elleux

n'était pas familière avec la thématique de recherche spécifique du projet, et que nous sommes malgré tout parvenus à sensibiliser des individus y compris au sein même de l'université.

La totalité des répondant·e·s (100 %) a estimé que la fréquence des communications était suffisante, celles-ci intervenant principalement lorsque nous avions des informations pertinentes à partager. Il faut toutefois souligner que certaines périodes ont été marquées par une absence de communication de plusieurs mois, notamment lorsque l'équipe se consacrait à l'interprétation des données. Plusieurs répondant·e·s ont indiqué qu'iels trouvaient légitime que nous nous concentrions sur cet aspect. Certain·e·s ont même jugé qu'une fréquence de communication plus élevée aurait été intrusive.

Bien que plusieurs répondant·e·s aient souligné la complexité du sujet en question et que la notion même d'isotopes restait un peu abstraite, iels ont globalement estimé que les informations partagées étaient suffisamment vulgarisées (Figure 6.3c). Il est important de souligner que la compréhension du fonctionnement des isotopes nécessite un certain temps à acquérir, même pour les étudiant·e·s spécialisé·e·s dans ce domaine. Nous considérons donc ces réponses comme très positives.

Figure 6.3: Sensibilisation des participant·e·s Collect'O

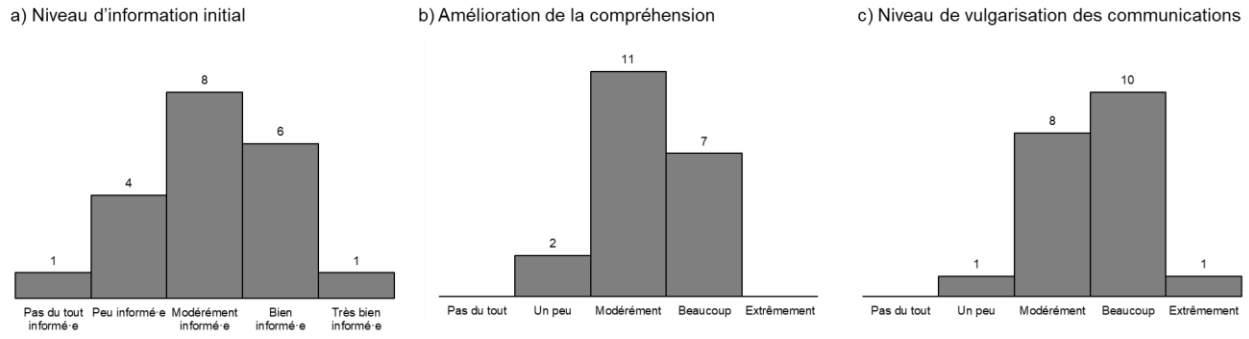

Cela souligne l'efficacité des formats de communication que nous avons utilisés, tels que les capsules vidéo, visites de laboratoire et réunion d'information, pour la diffusion des connaissances scientifiques issues du projet. Ces approches semblent avoir contribué à faciliter le dialogue entre les chercheur·euses et les citoyen·ne·s, et montrent qu'en plus de favoriser la collecte de données, ce projet a également joué un rôle de médiation scientifique. En vulgarisant un sujet complexe tel que les isotopes et leur lien avec la compréhension de l'impact de l'urbanisation, ce projet a permis à des participant·e·s non familier·e·s avec ce domaine de mieux comprendre les enjeux climatiques et environnementaux actuels. Ces retours positifs sur la communication expliquent notamment pourquoi 85 % des répondant·e·s estiment qu'iels seraient prêt·e·s à laisser leur contact afin de participer à des projets participatifs environnementaux futurs.

6.3.4 Sensibilisation de la communauté

Concernant la sensibilisation de la communauté, nous avons observé que la moitié des répondant·e·s a partagé de l'information autour d'eux. Parmi eux, 55 % l'ont fait par le biais de discussions informelles, notamment lorsque des passant·e·s remarquaient la présence de leur collecteur, tandis que 27 % ont utilisé les réseaux sociaux, et 18 % ont partagé les capsules vidéo (Figure 6.4a).

Parmi les répondant·e·s n'ayant pas diffusé d'information, la raison la plus fréquemment évoquée était simplement le fait de ne pas y avoir pensé. C'est pourquoi nous recommandons à de futurs projets environnementaux d'inciter explicitement les participant·e·s à partager l'information dans leur entourage.

En ce qui concerne l'impact perçu sur leur communauté, la majorité des répondant·e·s estime que celle-ci a été *un peu* sensibilisée aux enjeux de l'urbanisation sur les précipitations en milieu urbain (Figure 6.4b). Seuls 20 % des répondant·e·s jugent que leur entourage a été sensibilisé de manière *modérée* à *beaucoup*. Par ailleurs, presque aucun·e répondant·e n'a observé de changements concrets dans les comportements de son entourage. La seule personne ayant noté un effet estime que cela a rendu son entourage « plus conscient de l'environnement et de ses impacts ».

Le manque d'aspect ludique mentionné précédemment pourrait en partie expliquer pourquoi peu d'enfants étaient impliqué·e·s dans les collectes : seuls deux répondant·e·s ont mentionné que des enfants y avaient participé (respectivement 1 et 2 enfants). Nous aurions pu renforcer la dimension éducative du projet en adaptant par exemple le protocole en deux versions, dont l'une plus familiale, comme sous-entendu par l'un des participant·e·s. L'implication d'enfants aurait ainsi pu constituer une opportunité de leur faire découvrir concrètement les enjeux environnementaux et le monde de la recherche, leur permettant éventuellement d'avoir un impact fort sur le monde de demain. L'éducation de qualité est un enjeu fondamental dans le domaine des changements climatiques, et des activités de science participative adaptées à la jeunesse peuvent jouer un rôle clé dans l'atteinte de cet Objectif de Développement Durable (ODD).

Ces constats soulignent que bien que l'installation des collecteurs ait suscité de la curiosité et encouragé quelques partages informels, une stratégie de communication plus structurée aurait pu renforcer l'impact de sensibilisation communautaire. Parmi les suggestions formulées pour améliorer cet aspect, plusieurs répondant·e·s ont proposé de diffuser les résultats du projet et des recommandations de comportement via les médias publics et les réseaux sociaux, ainsi que d'impliquer les écoles et les communautés locales, ce qui fait écho à notre recommandation précédente d'impliquer davantage les enfants.

Enfin, un répondant a suggéré de créer un réseau entre participant·e·s afin de favoriser les échanges et le partage d'expériences. Bien que cette idée ait déjà été envisagée, nous avions fait le choix de préserver l'anonymat des participant·e·s. Ainsi, les participant·e·s volontaires ne se sont rencontré·e·s qu'à l'occasion de l'événement de partage des résultats et de la visite du laboratoire. Néanmoins, la création d'un groupe de discussion volontaire aurait pu contribuer à renforcer le sentiment d'appartenance communautaire, et pourrait être explorée dans de futures initiatives.

Figure 6.4: Sensibilisation communautaire

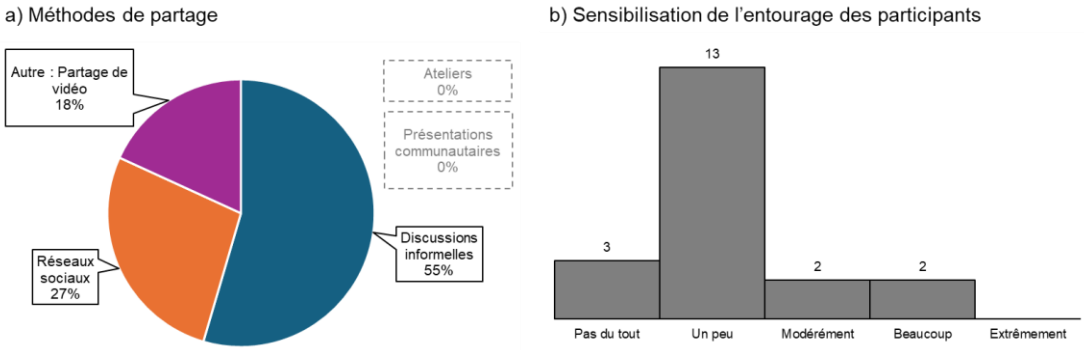

6.4 Conclusion

L'approche participative Collect'O a représenté une opportunité unique d'impliquer la communauté montréalaise dans la compréhension des changements climatiques urbains. Grâce à cette analyse, nous avons montré que ce projet a suscité une sensibilisation individuelle satisfaisante de ses participant·e·s. Ces retours suggèrent que valoriser le travail fourni par les participant·e·s, tout en intégrant une dimension éducative par des efforts simples tels que capsules vidéo et rencontres d'information, est efficace dans une démarche de partage des connaissances.

Cependant, la sensibilisation communautaire au-delà du monde académique est restée limitée. Pour pallier ce phénomène, nous recommandons d'adapter le protocole à la diversité des participant·e·s, et favoriser le contact avec les médias externes au milieu universitaire, ainsi que les partenariats avec des écoles ou des organismes communautaires, pour le recrutement des participant·e·s.

Dans notre cas, aucun des chercheur·euses à l'origine du projet ne possédait de formation spécifique en communication ou en sciences sociales. Avec un budget limité, nous avions fait le choix d'intégrer le développement de compétences en communication dans le cadre de ce doctorat. Selon les ressources disponibles (temps et budget) de futurs projets, il pourrait être judicieux de collaborer avec un·e spécialiste

avec plus d'expertise dans ce domaine. L'inclusion d'une stratégie de communication scientifique spécialement dédiée à cet aspect pourrait augmenter l'impact de sensibilisation sur la communauté.

Enfin, il est à noter que le nombre de répondant·e·s était limité, et que les personnes ayant répondu étaient peut-être déjà particulièrement engagées environnementalement, ou intéressées par la démarche scientifique. Cela a pu entraîner un biais de sélection. Néanmoins, ces réponses ont mis en lumière le rôle croissant que les chercheur·euses sont appelés à jouer dans la diffusion des connaissances scientifiques au-delà du milieu universitaire. Des projets similaires peuvent se révéler un excellent tremplin pour continuer cet effort de sensibilisation.

CONCLUSION GÉNÉRALE

Schéma de synthèse de la démarche et des principaux résultats

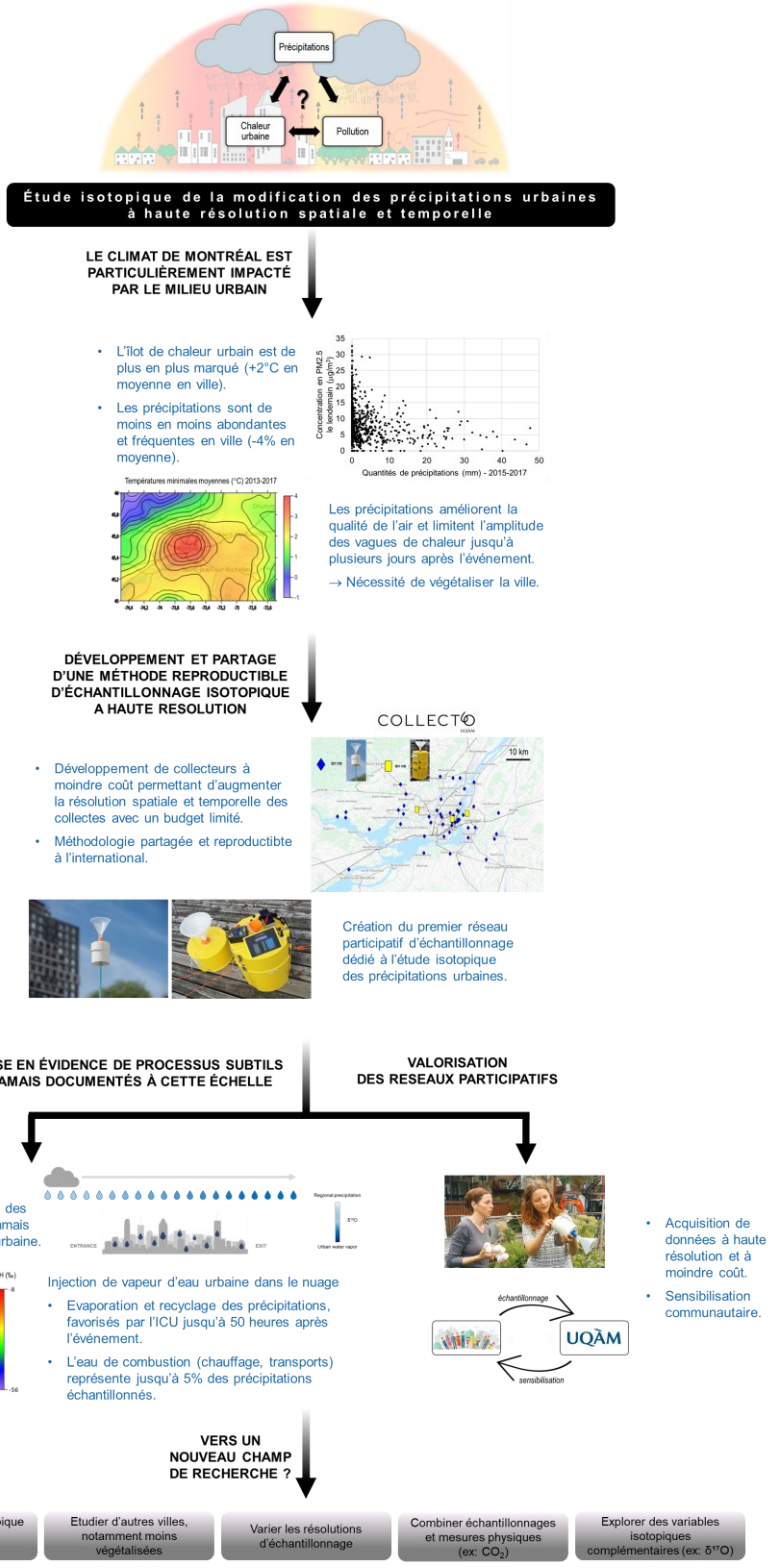

La modification des précipitations en milieu urbain est un sujet mal compris, car les outils météorologiques traditionnellement utilisés ne suffisent pas à capter l'hétérogénéité des villes, et ont jusqu'à présent amené des résultats très controversés. Des outils de traçage naturel tels que les isotopes stables de la molécule d'eau, bien qu'ayant un potentiel apparent dans un tel contexte, sont pourtant restés peu utilisés et discutés dans la recherche sur les climats urbains. L'objectif de cette thèse était d'évaluer comment l'étude isotopique des précipitations à haute résolution spatiale et temporelle en milieu urbain peut aider à améliorer la compréhension des processus modifiant les précipitations urbaines. Cette étude, réalisée à une échelle urbaine sans précédent, a nécessité un effort méthodologique important.

Premièrement, il était nécessaire de trouver un site d'étude approprié à cette investigation. Dans la première partie de cette thèse, l'étude climatologique des quatre plus grandes villes de l'Est canadien (Montréal, Toronto, Ottawa, Québec) sur la période 1988-2017 a mis en évidence que le climat de Montréal est particulièrement impacté par le milieu urbain. Sur cette période, les températures minimales journalières y étaient en effet de plus en plus élevées en moyenne que dans le paysage régional, jusqu'à avoisiner 2°C de plus en ville en moyenne. De plus, les précipitations y étaient de moins en moins fréquentes et abondantes en ville qu'aux alentours. Les conséquences sur la qualité de vie des citoyen·ne·s sont directes, comme mis en évidence par le fait que les épisodes de précipitations amélioraient la qualité de l'air grâce au lessivage de l'atmosphère, et limitaient l'amplitude des vagues de chaleur par évaporation jusqu'à plusieurs jours après l'événement. Ces résultats montrent que Montréal était donc un site d'étude adapté pour notre étude. Cela a également souligné l'importance de prévoir des techniques de stockage permettant de conserver l'eau en ville (telles que la végétalisation), afin qu'elle puisse être ré-évaporée durant les jours les plus secs et serve ainsi de climatisation naturelle de la ville.

Une fois le site d'étude validé, nous avons ensuite procédé à la création de collecteurs de pluie et de neige spécialement adaptés pour la conservation de la signature isotopique des échantillons, présentés dans la deuxième partie de cette thèse. Ces collecteurs ont la particularité de pouvoir être construits à un coût bien plus bas que ce qui peut habituellement être trouvé sur le marché, et permettent ainsi d'augmenter facilement la résolution spatiale des collectes tout en maintenant un budget limité. Nous avons partagé cette méthode avec la communauté scientifique, afin qu'elle puisse être appliquée à l'international.

En plus de ces collecteurs, nous avons également adapté des échantillonneurs automatiques d'eau de surface afin d'échantillonner la pluie à l'échelle intra-événementielle, à un pas de temps qui peut être spécifié avant l'événement. Nous avons testé différents designs afin que la signature isotopique de la pluie puisse être conservée après échantillonnage, tout en ce que l'échantillonneur puisse toujours être utilisé pour son

utilisation première, la collecte d'eau de surface. Cette méthodologie a également été partagée à la communauté scientifique dans un troisième article.

Une fois les échantillonneurs développés, collecter à nous seuls des précipitations à haute résolution spatiale et temporelle à l'échelle d'une ville restait un défi de taille. Pour y parvenir, nous avons créé Collect'O, le premier réseau participatif d'échantillonnage dédié à l'étude isotopique des précipitations urbaines. Ainsi, nous avons eu recours à la bonne volonté des citoyen·ne·s du Grand Montréal afin de nous aider à échantillonner des épisodes de pluie et de neige depuis leur domicile. Une cinquantaine de participant·e·s furent contactés à l'aide de l'équipe de communication de l'université et de différents médias, et les collecteurs ont ainsi pu être installés à leur domicile. Grâce à la mise en place de cette méthodologie à bas coût, l'échantillonnage de précipitations urbaines pour étude isotopique était maintenant réalisable à haute résolution.

Dans la troisième partie de cette thèse sont présentés les résultats de 19 événements météorologiques échantillonnés de septembre 2021 à octobre 2022, dont 14 événements pluvieux et 5 événements neigeux. Le premier résultat d'importance est la grande variabilité isotopique observée entre les différentes stations pour chaque événement échantillonné. À notre connaissance, une telle variabilité spatiale n'avait jamais été documentée à une telle échelle en ville. Grâce à cette approche à haute résolution, nous avons pu mettre en avant l'intérêt des signatures isotopiques des précipitations pour retracer la dynamique de processus subtils qui n'avaient jamais été observés à cette échelle dans de précédentes études isotopiques des précipitations urbaines, tels que l'injection de précipitations ré-évaporées ou de vapeur d'eau de combustion dans le nuage.

En effet, cette approche isotopique nous a permis de montrer que la variabilité du signal isotopique ne semblait pas être due à l'évaporation des précipitations sous le nuage, ce à quoi nous aurions pu nous attendre au vu de l'important îlot de chaleur urbain montré dans le chapitre 1. Nous avons pu cependant observer que l'îlot de chaleur urbain favorise le recyclage des précipitations urbaines sous forme de vapeur d'eau, qui augmente la variabilité isotopique mise en avant lors de certains événements, particulièrement après des épisodes de précipitations récents. La variabilité isotopique observée entre les stations lors d'un même événement apparaît ainsi corrélée avec le temps écoulé depuis les précipitations les plus récentes. Cela a notamment permis d'évaluer que dans la ville de Montréal, l'eau de pluie reste disponible à l'évaporation pendant un maximum de 2 jours suivant l'événement. Ce résultat est important pour le développement des infrastructures urbaines, notamment pour limiter l'amplitude des vagues de chaleur urbaines comme mentionné dans le premier article. D'autre part, nous avons pu évaluer la contribution potentielle de l'eau de combustion issue des transports et du chauffage résidentiel, qui s'élève à 5 % de la

vapeur d'eau précipitée dans certains des événements échantillonnés. C'est un point important à noter, car cette étude ne concernait qu'une seule ville. Il serait judicieux d'évaluer cette contribution et l'acidité des précipitations que cela entraîne si la trajectoire des précipitations passe au-dessus de plusieurs villes.

À travers la soumission de ces résultats au journal *Urban Climate*, nous espérons soulever l'intérêt de la communauté scientifique spécialisée dans les climats urbains à l'étude isotopique des précipitations urbaines à haute résolution spatiale et temporelle. Notre étude amène de premiers résultats prometteurs pour améliorer la compréhension de la modification des précipitations urbaines. Cependant, le volume important d'informations à traiter pour tous les événements échantillonnés, combiné à l'utilisation d'une étude statistique, a pu conduire à passer à côté de certains éléments plus fins du signal. De plus, en raison du caractère dynamique des processus en jeu, ces résultats ne peuvent être généralisés sans précaution. Pour aller plus loin, il serait notamment judicieux d'explorer la signature isotopique des précipitations dans d'autres villes moins végétalisées que Montréal, mais aussi d'explorer des résolutions variées, i.e. de l'échelle d'une rue à l'échelle régionale sur plusieurs villes. Le partage de la méthodologie à bas coût développée dans ce projet, facilement reproductible, est susceptible d'ouvrir un nouveau champ de recherche combinant climat urbain et approche isotopique à haute résolution, afin de multiplier les efforts en ce sens. De plus, combiner de tels échantillonnages avec la mesure en continu de différents paramètres physiques, et ouvrir l'analyse à des variables isotopiques complémentaires, sont des pistes à explorer afin d'enrichir la recherche dans ce domaine. En particulier, l'excès en $\delta^{17}O$, bien qu'encore peu exploré, constitue un traceur conservatif des variations d'humidité à l'origine de la vapeur et pourrait ainsi compléter les informations fournies par le d-excess. De plus, la corrélation entre le d-excess et le CO_2 atmosphérique avait déjà été mise en évidence dans la vapeur d'eau (Gorski *et al.*, 2015). Examiner si une telle relation se retrouve également dans les précipitations constituerait une étape importante pour mieux appréhender la dynamique des interactions entre précipitations et pollution.

Il va sans dire que coupler ces efforts à un travail de modélisation est également particulièrement recommandé, dans un contexte où les modèles climatiques sont de plus en plus performants et permettent de mieux prendre en compte l'hétérogénéité du milieu urbain. Intégrer des mesures isotopiques à haute résolution à la simulation de différents scénarios permettrait notamment la validation des hypothèses fournies par les mesures, mais aussi de mieux prédire et s'adapter à l'évolution climatique des milieux urbains, produite par la ville en elle-même mais également par les changements climatiques globaux.

Enfin, ce projet met en lumière la valeur ajoutée des réseaux participatifs pour l'acquisition de données pour les chercheur·euses. Nous avons également pu montrer que le réseau Collect'O a eu une certaine portée de

sensibilisation de la population montréalaise quant aux enjeux soulevés par la modification des précipitations urbaines. Dans un contexte où il est nécessaire d'adapter nos villes aux changements climatiques présents et futurs, la sensibilisation de la population apparaît en effet comme un tremplin important pour la prise de décisions et la mise en place de stratégies d'adaptation. Afin d'aider de futurs réseaux participatifs dans le domaine de l'environnement à parvenir à cet objectif, nous avons invité les participant·e·s du réseau à répondre à une enquête qui fait l'objet de la dernière partie de cette thèse. Grâce à leurs réponses, nous avons pu déterminer que la sensibilisation individuelle des participant·e·s reposait sur des retours visuels réguliers tels que des capsules vidéo et des rencontres d'information, mais aussi sur la valorisation de leur travail. Cette étude a néanmoins révélé que l'ouverture de la recherche participative au-delà du monde de la recherche est restée limitée. Adapter le protocole à la diversité des participant·e·s, et favoriser les partenariats avec des écoles ou des institutions communautaires hors milieux académiques, sont autant d'approches que nous suggérons afin de contourner ce problème.

Ce projet de thèse s'est ainsi révélé fondamentalement multidisciplinaire, entrecroisant climatologie urbaine, hydrologie isotopique et sciences sociales. Tout en soulignant l'intérêt d'approfondir l'étude isotopique des précipitations urbaines à haute résolution spatiale et temporelle, il met également en évidence la nécessité pour les recherches environnementales futures d'intégrer méthodes scientifiques innovantes et implication citoyenne. Alors que le 21ème siècle fait face à l'intensification de l'urbanisation et des changements climatiques, accentuant encore les interactions entre impacts environnementaux et activités humaines, la mise en place de telles démarches rassemblant chercheur·euses, citoyen·ne·s, et éventuellement urbanistes, apparait d'autant plus nécessaire pour soutenir la recherche, informer la décision publique, et adapter ensemble nos villes.

ANNEXE A

Materials and costs of an event-based and a monthly rain sampler (article B)

	Event-based sampler		Monthly sampler	
	Dimensions	**Price for 1 sampler (CAD)**	**Dimensions**	**Price for 1 sampler (CAD)**
Plastic funnel	12 cm top opening	2	9 cm top opening	1
3D printed piece	*See supplementary materials*	2	*See supplementary materials*	2
Outer PVC pipe	4 inches (100 mm) ∅ x 12 cm length	1	6 inches (150 mm) ∅ x 24 cm length	45
Inner PVC pipe	3 inches (75 mm) ∅ x 8 cm length	1	4 inches (100 mm) ∅ x 18 cm length	1
Outer PVC cap	4 inches (100 mm) ∅	2	6 inches (150 mm) ∅	13
Inner PVC cap	3 inches (75 mm) ∅	2	4 inches (100 mm) ∅	2
Outer polyurethane tube	1/8 inch (3.2 mm) inner ∅ x 5 m length	10	1/8 inch (3.2 mm) inner ∅ x 5 m length	10
Inner polypropylene tube	3/16 inch (4.8 mm) inner ∅ x 12 cm length	0.25	3/16 inch (4.8 mm) inner ∅ x 24 cm length	0.5
HDPE bottle	125 mL	1	1000 mL	3
Epoxy coated rebar	6 feet (1.8 m)	11	6 feet (1.8 m)	11
Hardware	/	2	/	2
TOTAL PRICE	**34 CAD**		**90 CAD**	

ANNEXE B

Evaporation rate experiment (article B)

Different volumes of water up to 40 mL were poured into the 125 mL bottles. Each bottle was weighed daily to measure the water loss compared to the previous day. After 3 days, the cumulated water loss is the highest for the largest volumes, which verifies the hypothesis that the humidity gradient between the water's surface and the atmosphere is stronger for smaller volumes.

Figure: a) Picture of the experiment, b) cumulated water loss for different sample volumes after 72 hours of experiment

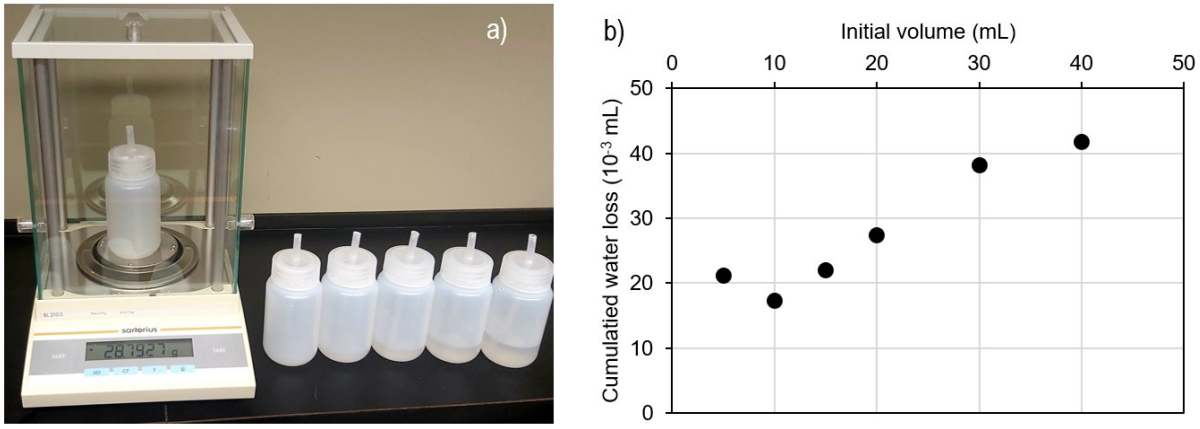

ANNEXE C

Evaporation tests (article C)

Figure: A) Top view for the design of the evaporation tests performed on each automatic rain sampler; B) Cross-sections of dry and saturated samplers, each centrifuge tube being filled with different volumes of water.

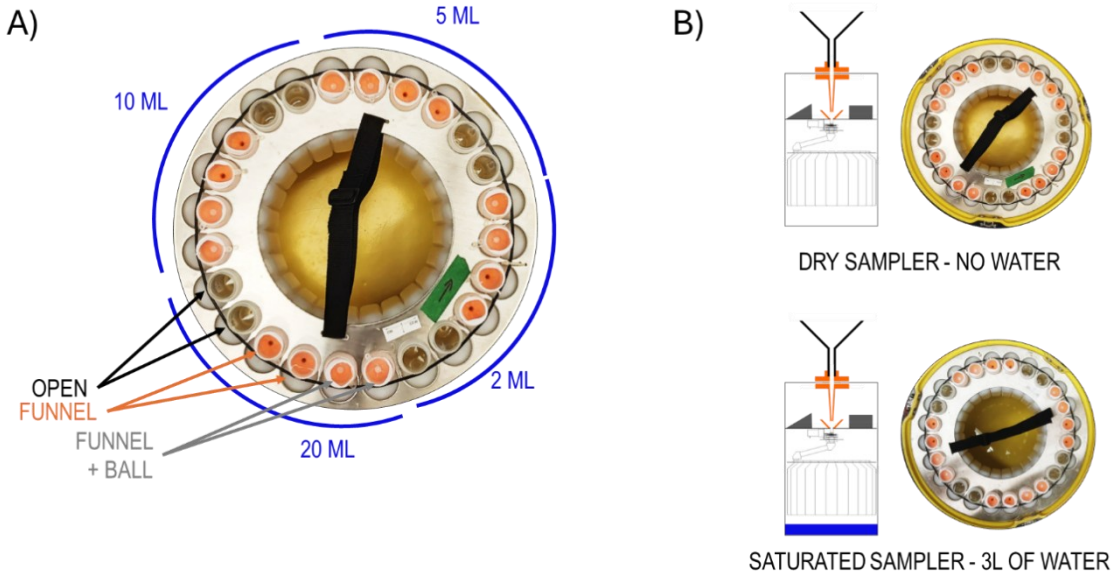

ANNEXE D

3D-printing material porosity (article C)

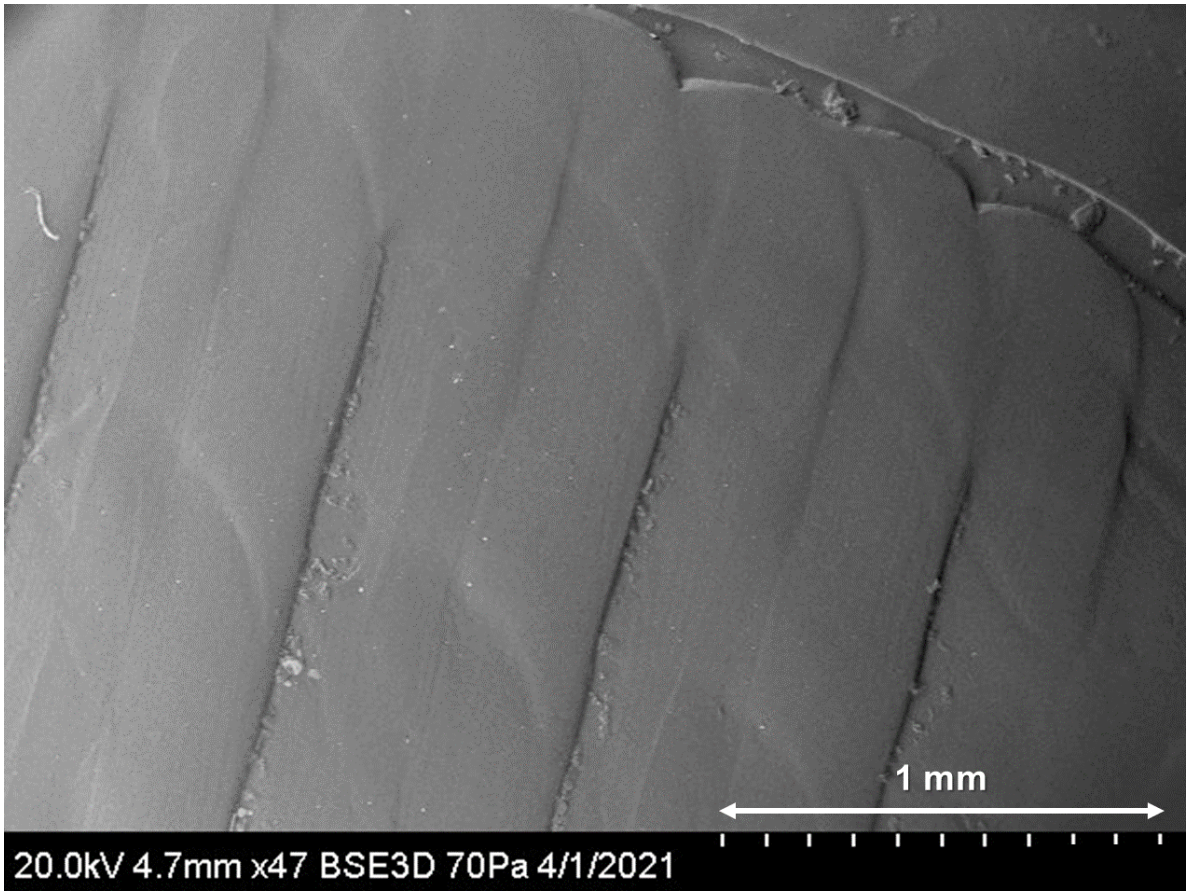

ANNEXE E

Separation factor determination (article C)

Figure: Determination of the $\delta^{18}O$ separation factor for the free atmosphere, the dry sampler, and the saturated sampler.

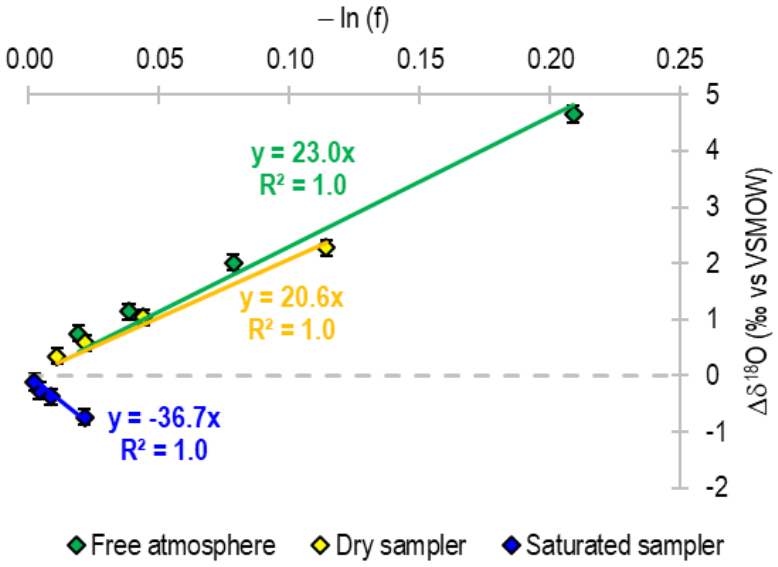

ANNEXE F

Maximum storage time in the saturated autosampler (article C)

Table: Order of magnitude of the maximum time (days) for open centrifuge tubes and centrifuge tubes modified with the funnel system to be left in the saturated automatic sampler before the equilibration between the sample and the autosampler starts to be significant compared to the overall analytical uncertainty. Different sample volumes from 2 to 40 mL, overall analytical uncertainties, and absolute differences in isotopic compositions between the sample and the water inserted in the bottom of the autosampler ($\Delta\delta_{bottom\text{-}sample}$) were investigated.

	$\Delta\delta_{bottom\text{-}sample}$ = 1 ‰				$\Delta\delta_{bottom\text{-}sample}$ = 4 ‰				$\Delta\delta_{bottom\text{-}sample}$ = 7 ‰			
	Open		Funnel		Open		Funnel		Open		Funnel	
V_{sample} (mL)	OAU = 0.1 ‰	OAU = 0.2 ‰	OAU = 0.1 ‰	OAU = 0.2 ‰	OAU = 0.1 ‰	OAU = 0.2 ‰	OAU = 0.1 ‰	OAU = 0.2 ‰	OAU = 0.1 ‰	OAU = 0.2 ‰	OAU = 0.1 ‰	OAU = 0.2 ‰
2	1	3	4	9	0	1	1	2	0	1	0	1
3	2	4	7	13	0	1	2	3	0	1	1	2
4	3	5	9	18	1	1	2	4	0	1	1	3
5	3	6	11	22	1	2	3	5	0	2	1	3
6	4	8	13	26	1	2	3	7	1	2	1	4
7	5	9	15	31	1	2	4	8	1	2	1	4
8	5	10	18	35	1	3	4	9	1	3	1	5
9	6	12	20	39	1	3	5	10	1	3	2	6
10	6	13	22	44	2	3	5	11	1	3	2	6
15	10	19	33	66	2	5	8	16	1	5	3	9
20	13	26	44	88	3	6	11	22	2	6	4	13
25	16	32	55	109	4	8	14	27	2	8	5	16
30	19	39	66	131	5	10	16	33	3	9	6	19
35	23	45	77	153	6	11	19	38	3	11	6	22
40	26	52	88	175	6	13	22	44	4	13	7	25

Figure: Representation of the order of magnitude of the maximum time (days) for open centrifuge tubes (black) and centrifuge tubes modified with the funnel system (orange) to be left in the saturated automatic sampler before the equilibration between the sample and the autosampler starts to be significant compared to the overall analytical uncertainty. Different sample volumes from 2 to 40 mL, overall analytical uncertainties, and absolute differences in isotopic compositions between the sample and the water inserted in the bottom of the autosampler ($\Delta\delta_{bottom\text{-}sample}$) were investigated.

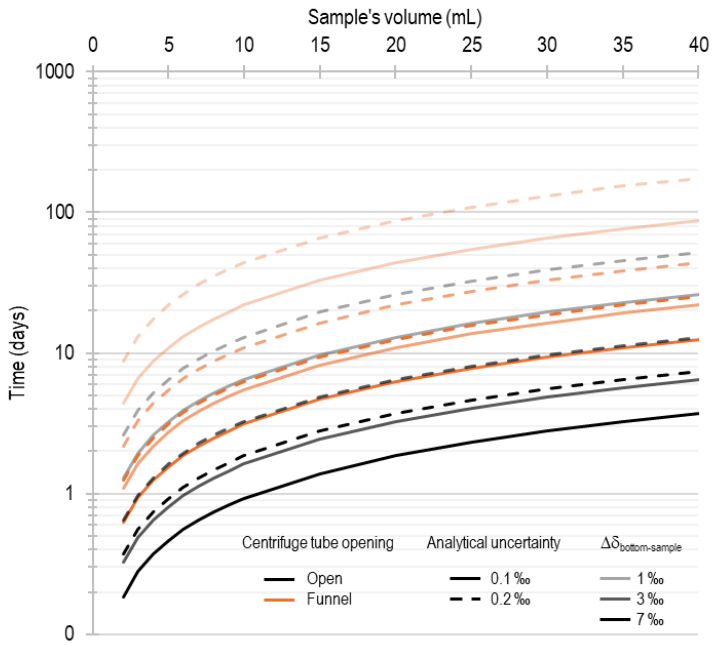

ANNEXE G

Sampling protocol (article C)

- Place a dry centrifuge tube with funnel + Tygon in each bottle in the rack

  /!\ Make sure the centrifuge tube does not protrude from the neck of the bottle.
- Optional step: Place a plastic ball in each small funnel

- At the preference of the user: Make sure there is no water at the bottom of the sampler OR pour 3L of water of known isotopic composition, as close to the expected rainfall isotopic composition as possible.
- Place the bottle rack in the sampler
- Connect the battery
- Program the sampling:

Programming of the sampling :

	“ *99 ” + Enter
Sampler setting?	**“2“ + Enter**
# of bottles?	**“24” + Enter**
Step to home?	**“0” + Enter**
Post draw?	**“0” + Enter**
Sample volume?	**Enter**
Tube length?	**Enter**
Draw height?	**Enter**
Rinses per simple?	**“0” + Enter**
Bot volume? Liters	**Enter**
Purge time?	**“03” + Enter**

Draw time?	**"004" + Enter**
Auto restart?	**"0" + Enter**
Test cycle mode?	**"0" + Enter**
Backlight mode?	**"1" + Enter**
Enter password	**"0000" + Enter**

Set-up of the sampling timestep (to be determined according to forecasts):

	TIME
Enter time interval	"**HH:MM" + Enter**

- At the scheduled time (determined on the day), take the sampler out to its sampling location and start sampling **START**
- Quickly check that the rotation arm is correctly positioned on the arrow
- Close all parts of the sampler securely

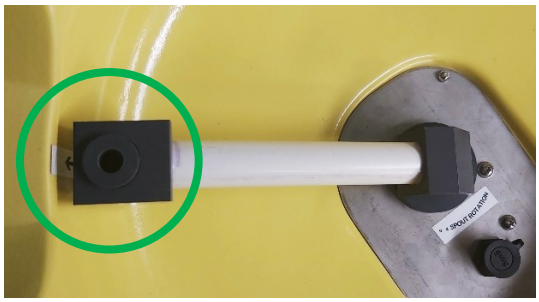

- At the end of the sampling, gently remove each centrifuge tube from each bottle. Take the Tygon and funnel system out of each centrifuge tube. Close the centrifuge tube with a cap and store it until isotopic analysis.

- Make sure to dry the funnel system before the following sampling.

ANNEXE H

Exemple de la page web dédiée à chaque collecte (chapitre 4)

Détails de l'événement

Un important système nous venant du Texas viendra affecter la région dès demain (*) ! Nous en profiterons pour collecter des échantillons de la neige reçue selon les horaires suivants :

Plage horaire d'installation du collecteur	Jeudi 10 mars, avant 22h
Plage horaire de récupération du collecteur	Dimanche 13 mars, entre 07h et 11h
Plage horaire d'embouteillage de la neige fondue	Dimanche 13 mars, entre 17h et 21h

Nous vous demandons de bien vouloir utiliser les **petites** bouteilles Collect'O qui sont à votre disposition.

(*) *Si vous souhaitez en apprendre plus sur ce système, nous vous conseillons la lecture de cet article de MétéoMédia.*

Protocole d'échantillonnage

Nous vous demandons également de bien vouloir suivre le protocole suivant afin de procéder à votre échantillonnage.

1. Durant la plage horaire d'installation du collecteur, retirez le capuchon de votre collecteur et installez-le sur son piquet.
2. Durant la plage horaire de récupération du collecteur, revissez bien le capuchon sur votre collecteur, puis rentrez-le à l'intérieur.
3. Placez votre collecteur sur une surface plane, éloignée de toute source de chaleur, pendant quelques heures.
4. Durant la plage horaire d'embouteillage de la neige fondue, retirez le capuchon, puis versez la neige fondue dans la bouteille Collect'O grâce à l'entonnoir qui vous a été fourni.
5. Veillez à **visser de toutes vos forces le bouchon de votre bouteille** *(très important pour éviter l'évaporation !)*, puis stockez-la à l'ombre, à température ambiante.
6. Rincez votre collecteur et votre entonnoir, puis laissez-les sécher pour la prochaine collecte.

Etape 1

Etape 2

Etape 3

Etape 4

Renseignements sur votre échantillonnage

Pour pouvoir communiquer plus facilement avec vous et obtenir plus de renseignements sur la façon dont votre échantillonnage s'est déroulé (ce qui nous aide grandement dans l'interprétation de nos résultats !), merci de bien vouloir remplir le formulaire suivant à la fin de votre collecte.

Fields marked with an * are required

Quel est votre numéro de station ? *

Ce numéro est inscrit sur votre collecteur.

Quelle est votre adresse courriel ? *

Merci de bien vouloir indiquer l'adresse avec laquelle nous communiquons avec vous, afin que nous puissions vérifier votre participation.

Horaire d'installation du collecteur *

00 00

Horaire de récupération du collecteur *

00 00

Horaire d'embouteillage de la neige fondue *

00 00

Avez-vous un commentaire à faire ?

Envoyer

ANNEXE I

Overview of stable water isotopes (article D)

Water molecules H_2O are composed of different combinations of hydrogen and oxygen isotopes. Lighter isotopes are the most abundant in nature (99.9 % for ^{1}H versus 0.1 % for ^{2}H, and 99.8 % for ^{16}O versus 0.2 % for ^{18}O).

H_2O molecules react differently to the physical and chemical processes they are subject to, depending on their isotopic combination. This makes water stable isotopes exceptional tracers of the source and trajectory of water in the hydrological cycle on various spatial and temporal scales (Leibundgut *et al.*, 2009b). In particular, they provide a good representation of the processes involved in droplet formation within the cloud itself, and of the various exchanges that take place as they fall to the ground (Clark et Fritz, 1997).

Because the natural variations in isotopic ratios R (Equation 1) remain very small, it is challenging to measure absolute isotopic ratios without a high degree of analytical uncertainty. Instead, the isotopic ratios of the samples are normalized against internal laboratory standards, traceable to an international reference scale known as the VSMOW-SLAP scale. This normalization allows for results comparison between laboratories.

Equation 1

$$R = \frac{[heavy\ isotope]}{[light\ isotope]}$$

The notation δ, expressed in per mil (‰), expresses the relative difference between the isotopic ratio of the sample and that of the Vienna Standard Mean Ocean Water (VSMOW) international standard (Equation 2).

Equation 2

$$\delta = \left(\frac{R_{sample}}{R_{VSMOW}} - 1\right)$$

Because heavy isotopes have much more affinity for high-bounded phases than light isotopes, molecules made of heavy isotopes preferentially condense and solidify, leading to precipitation isotopically heavier than the ambient water vapor. This partitioning is called fractionation. In a cloud, we consider that rain occurs when the cloud's relative humidity equals 100 %, and the hypothesis is made that the resulting precipitation is in isotopic equilibrium with the water vapor (Equation 3) (Clark et Fritz, 1997), meaning

that the isotopic partitioning between the liquid and vapor phases is governed by temperature. As the event progresses, precipitation removes heavy isotopes from the vapor phase, leaving the remaining water vapor progressively lighter. Consequently, both the isotopic composition of precipitation and that of water vapor gradually decrease over the course of the event (Clark et Fritz, 1997). This progressive distillation process can be described using the Rayleigh model (Equation 4).

Equation 3

$$\delta P_t = \delta V_t - \varepsilon_{V/W}$$

Equation 4

$$\delta V_t = \delta V_i - \varepsilon_{V/W} \times \ln(f)$$

where δP_t, δV_t, and δV_i are respectively the isotopic compositions (either $\delta^{18}O$ or $\delta^{2}H$) of the precipitation and the water vapor at time t and initial i stage, f the fraction of the remaining water vapor in the cloud, and $\varepsilon_{V/W}$ the separation factor of vapor over water, inversely proportional to temperature.

An $\delta^{18}O$-$\delta^{2}H$ diagram is particularly meaningful as it allows visualization of processes behind the formation and modification of precipitation (see Figure below). In this diagram, as the separation factor at equilibrium is 8 times more important for $\delta^{2}H$ than for $\delta^{18}O$, the Rayleigh distillation is represented by a line of slope 8.

Similarly to condensation, evaporation also implies equilibrium between liquid and vapor phases, with lighter isotopes evaporating preferentially. However, evaporation fractionation is more complex since it can also be subject to kinetic processes linked to meteorological parameters, such as the relative humidity and the wind (Clark et Fritz, 1997). Because $^{1}H^{1}H^{18}O$ is heavier than $^{1}H^{1}H^{16}O$ to a greater extent than $^{1}H^{2}H^{16}O$ is, kinetic fractionation during evaporation affects $\delta^{18}O$ more strongly than $\delta^{2}H$ (Clark et Fritz, 1997).

In an $\delta^{18}O$-$\delta^{2}H$ diagram, precipitation influenced by evaporation aligns along a characteristic line whose slope and intercept vary according to these kinetic processes. The d-excess (Dansgaard, 1964) (Equation 5) is a powerful index to trace them. The d-excess of evaporated water decreases (see Figure below), while the d-excess of produced water vapor increases.

Equation 5

$$d - excess = \delta\ ^{2}H - 8 \times \delta^{18}O$$

The linear regression of all δ^2H and δ^{18}O from 400 river, lake, and precipitation water samples from several continents defines the global meteoric water line (GMWL) (Craig *et al.*, 1963) (Equation 6).

Equation 6

$$\delta\ ^2H = 8 \times \delta^{18}O + 10$$

Figure: Evolution of the isotopic compositions of the water vapor and precipitation of a rain event from stages 0 to 1, followed by potential precipitation sub-cloud evaporation.

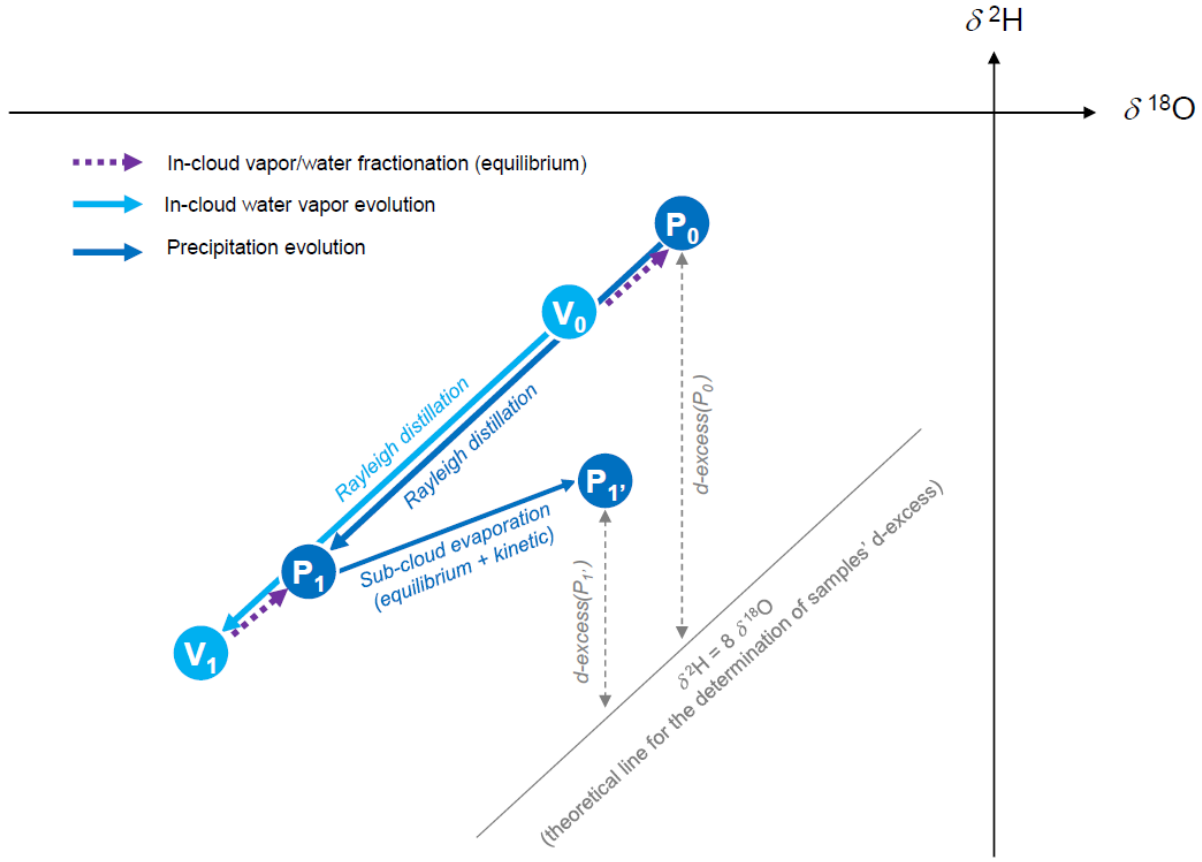

ANNEXE J

Protocol used by participants for rain and snow sampling (article D)

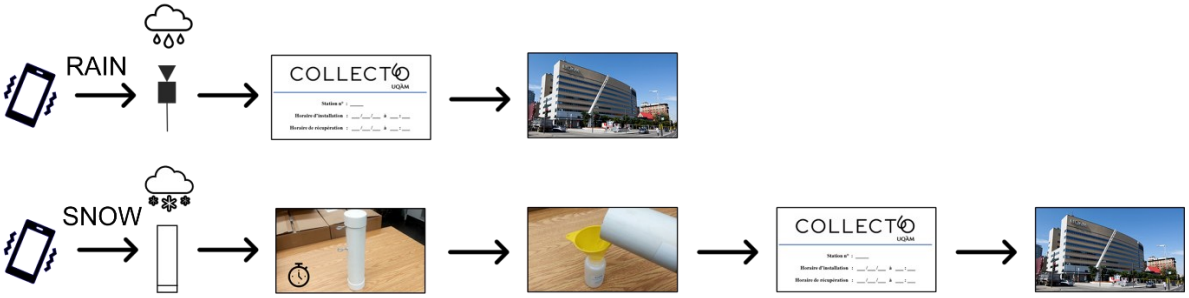

ANNEXE K

Precipitation events sampled and their analysis (article D)

Table: List of precipitation events sampled and instruments used for their isotopic analysis.

Event n°	Eastern Standard Time	Precipitation type	IRMS $\delta^{18}O$ and LGR $\delta^{2}H$	Picarro $\delta^{18}O$ and $\delta^{2}H$
1	4/9/21 7AM to 6/9/21 8AM	Rain	X	
2	6/9/21 6AM to 7/9/21 8AM	Rain	X	
3	21/9/21 8PM to 23/9/21 1PM	Rain	X	
4	23/9/21 2PM to 25/9/21 11AM	Rain	X	
5	20/10/21 9PM to 22/10/21 11AM	Rain		X
6	11/11/21 9PM to 13/11/21 12PM	Rain		X
7	8/1/22 9PM to 10/1/22 11AM	Snow		X
8	16/1/22 9PM to 18/1/22 10AM	Snow		X
9	1/2/22 9PM to 4/2/22 11AM	Snow		X
10	24/2/22 11PM to 26/2/22 11AM	Snow		X
11	10/3/22 10PM to 13/3/22 10AM	Snow		X
12	31/5/22 11PM to 2/6/22 2PM	Rain		X
13	2/6/22 3PM to 4/6/22 10AM	Rain		X
14	4/7/22 10PM to 6/7/22 8AM	Rain		X
16	22/8/22 4PM to 24/8/22 8AM	Rain		X
17	25/8/22 9PM to 27/8/22 11AM	Rain		X
18	29/8/22 7PM to 1/9/22 10AM	Rain		X
19	12/9/22 8PM to 15/9/22 10AM	Rain		X
20	21/9/22 6AM to 22/9/22 8PM	Rain		X

Figure: Correlation IRMS-LGR $\delta^{18}O$ values for Events 1 to 4

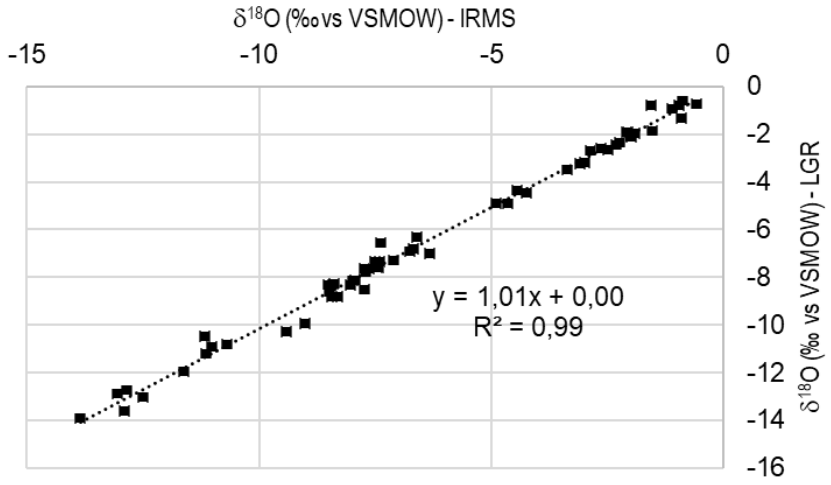

ANNEXE L

Distribution of the rain (red) and snow (blue) events compared to all events of the period (article D)

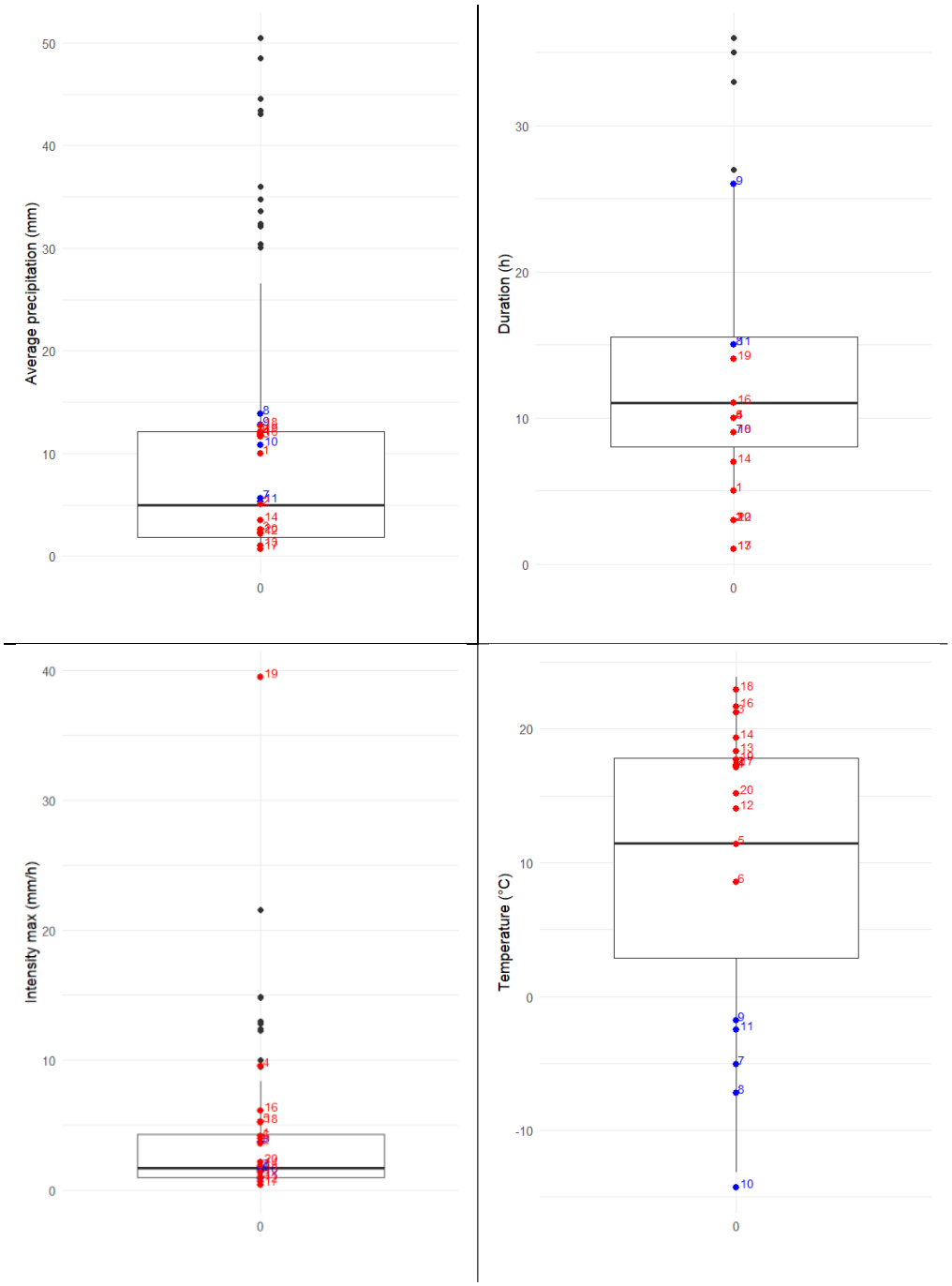

ANNEXE M

Data table used for the correlation matrix (article D)

Event n°	Convective/stratiform ratio	Average temperature (°C)	Minimum relative humidity (%)	Average relative humidity (%)	Maximum relative humidity (%)	Windspeed (km/h)	Maximum intensity (mm/h)	Duration (h)	Time since last precipitation (h)	Average precipitation amount (mm)	Precipitation standard deviation (mm)	Average $\delta^{18}O$ (‰)	$\delta^{18}O$ standard deviation (‰)	Average d-excess (‰)	d-excess standard deviation (‰)	Average electrical conductivity (µs/cm)	Electrical conductivity standard deviation (µs/cm)	Average particulate matter index	Particulate matter index evolution	Average proportion of combustion water vapor (%)	Maximum proportion of combustion water vapor (%)	Proportion of combustion water vapor standard deviation (%)
1	0.72	17	57	81	94	4	4.2	5	150	10.0	2.2	-7.4	0.4	12.6	1.0	15	8	11	5	0.4	1.5	0.6
2	0.74	17	74	83	90	5	3.6	3	14	5.0	3.9	-11.6	1.5	10.4	3.5	5	2	5	-7	2.0	4.7	1.5
3	0.56	21	45	71	93	6	1	3	186	2.6	1.5	-1.9	0.8	6.4	1.1	36	26	9	0	0.9	2.3	0.9
4	0.57	17	45	68	96	5	9.6	10	19	11.9	2.4	-6.9	1.8	14.3	1.7	8	10	7	3	0.7	2.6	0.9
5	0.63	11	72	88	97	4	5.3	10	112	11.6	2.1	-7.3	0.5	19.4	1.4	10	5	25	-15	0.8	2.2	0.9
6	0.26	9	50	75	95	5	4	10	224	12.0	1.2	-5.9	0.6	16.1	1.5	19	8	9	-3	1.0	2.5	1.0
7	0.19	-5	48	72	96	5	1.8	9	37	5.6	6.0	-7.9	0.4	21.3	1.8	87	63	11	-8	1.3	3.5	1.2
8	0.01	-7	75	88	93	10	3.7	15	81	13.9	5.8	-21.2	1.3	17.0	0.7	46	39	11	-19	0.5	1.3	0.7
9	0.00	-2	53	76	96	10	1.5	26	130	12.8	4.2	-22.7	1.2	14.4	0.9	54	19	11	-12	0.8	1.7	0.9
10	0.04	-14	52	72	86	12	1.4	9	12	10.9	7.1	-16.7	0.7	13.5	1.3	34	14	10	-10	0.4	2.3	0.7
11	0.03	-2	54	76	96	5	0.9	15	75	5.3	2.7	-16.0	0.8	14.4	2.4	38	21	10	-10	1.0	4.5	1.0
12	0.85	14	50	73	96	7	0.7	3	108	2.1	1.8	-4.5	0.6	12.2	1.9	37	21	6	-4	1.4	4.0	1.2
13	0.87	18	33	61	89	4	1.4	1	27	1.0	0.9	-6.2	1.4	11.7	2.1	14	5	8	0	1.7	4.2	1.4
14	0.50	19	54	76	95	6	1.9	7	67	3.5	1.9	-5.4	0.4	9.3	1.9	46	47	10	-3	1.4	4.9	1.2
16	0.75	22	53	88	98	4	6.1	11	11	11.8	2.0	-7.5	1.1	11.7	1.0	11	9	7	-6	0.8	1.6	0.9
17	0.48	17	56	78	93	6	0.4	1	84	0.7	0.8	-7.8	1.3	5.7	2.8	24	12	11	5	1.4	4.1	1.3
18	0.72	23	47	79	97	6	5.2	9	37	12.7	0.2	-7.0	1.8	12.3	1.6	8	7	6	-28	1.9	3.1	1.4
20	0.74	15	57	80	98	7	2.2	3	54	2.3	1.6	-7.7	2.5	11.2	2.6	28	23	10	-3	2.0	6.5	1.4

ANNEXE N

120-hour back trajectories of events 4, 5, 6, 7 using Hysplit with the model GFS, at mid-boundary level (article D)

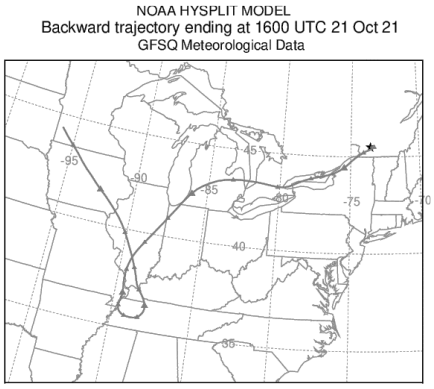

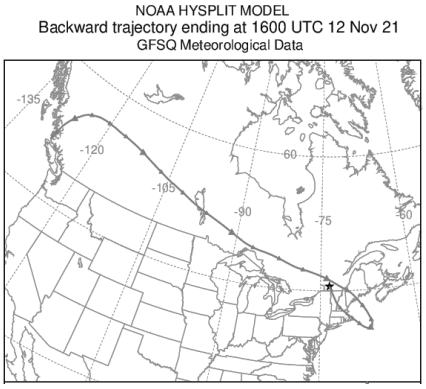

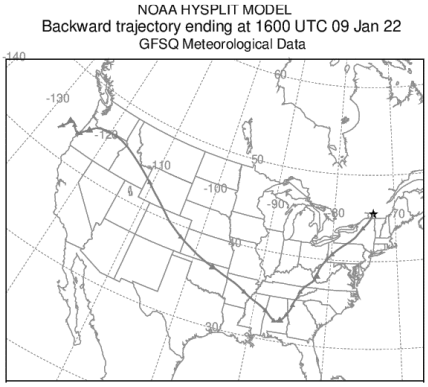

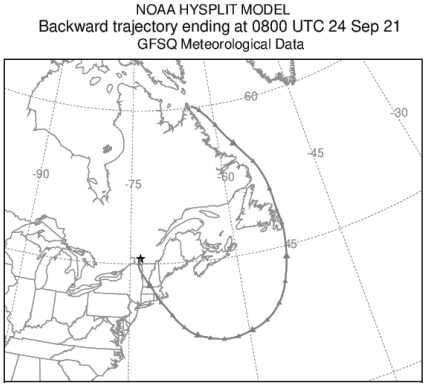

ANNEXE O

a) Particulate matter index evolution for rain (red) and snow (blue) events, and b) example of the effective PM reduction occurring during the snow Event 8 (article D)

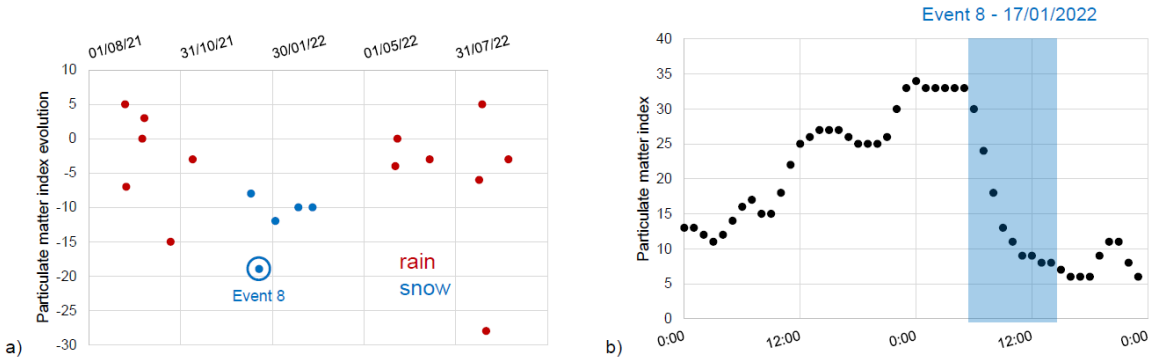

ANNEXE P

Protocol for high-resolution snow sampling for isotopic analysis (article D)

On the university rooftop, a tarpaulin was set up over a circular plastic structure with a surface area of approximately 1 m² to allow for snow accumulation during the event. Each hour, the accumulated snow was collected using a shovel and transferred into one of our cumulative snow samplers, which were then sealed with a cap to allow the snow to melt over a two-hour period. Once melted, the water was shaken to homogenize the sample, and a 30 mL HDPE bottle was filled with the resulting liquid. The amount of accumulated snow was estimated using data from a disdrometer already installed on the university rooftop (Lachapelle *et al.*, 2024).

ANNEXE Q

Questionnaire de l'enquête (chapitre 6)

Il est important que vous répondiez à toutes les questions en y **exprimant librement votre point de vue. Il n'y a pas de bonne ou de mauvaise réponse !** Merci de bien vouloir répondre à ce questionnaire **une seule fois**. Nous vous remercions pour votre participation à ce projet de recherche.

Fields marked with an * are required

Quelle est votre tranche d'âge ? *

- ○ Moins de 18 ans
- ○ 18-25 ans
- ○ 26-40 ans
- ○ 41-60 ans
- ○ Plus de 60 ans
- ○ Je préfère ne pas répondre

Quel est votre genre ? *

- ○ Homme
- ○ Femme
- ○ Autre
- ○ Je préfère ne pas répondre

Si vous avez répondu "Autre", précisez ici si vous le souhaitez

Quel est votre niveau de formation le plus élevé ? *

- ○ Education primaire
- ○ Education secondaire
- ○ Etudes universitaires
- ○ Etudes post-universitaires
- ○ Je préfère ne pas répondre

Comment avez-vous entendu parler du réseau Collect'O ? *

- ○ Lien professionnel ou personnel direct avec l'un des instigateurs du projet
- ○ Par le biais du centre de recherche Geotop (bouche-à-oreille, courriel…)
- ○ Média interne à l'UQAM (Actualités UQAM)
- ○ Médias externes à l'UQAM (MétéoMédia, Le Devoir, Les Années Lumière, etc…)
- ○ Bouche-à-oreille avec quelqu'un qui en avait entendu parler, externe au projet
- ○ Autre

Si vous avez répondu "Autre", précisez ici si vous le souhaitez

Quels facteurs vous ont incité·e à rejoindre Collect'O ? (cochez toutes les réponses pertinentes) *

- ☐ Intérêt pour la météorologie
- ☐ Préoccupations environnementales
- ☐ Volonté de contribuer à la recherche scientifique
- ☐ Engagement communautaire
- ☐ Autre

Si vous avez répondu "Autre", précisez ici si vous le souhaitez

Dans quelle mesure pensez-vous que votre participation à Collect'O a contribué à améliorer votre compréhension de ces impacts ? *

- ○ Pas du tout
- ○ Un peu
- ○ Modérément
- ○ Beaucoup
- ○ Extrêmement

Quel(s) avantage(s) percevez-vous dans la participation à un réseau participatif comme Collect'O ? *

Quel(s) inconvénient(s) ou défi(s) avez-vous rencontrés en participant à Collect'O, le cas échéant ? *

Dans quelle mesure avez-vous trouvé la collecte d'échantillons facile à réaliser ? *

- ○ Très facile
- ○ Facile
- ○ Neutre
- ○ Difficile
- ○ Très difficile

Des enfants étaient-ils impliqués dans la collecte des échantillons ? *

- ○ Oui
- ○ Non

Si oui, combien ?

0

Dans quelle mesure avez-vous trouvé le protocole ludique, amusant ? *

- ○ Pas du tout
- ○ Un peu
- ○ Modérément
- ○ Beaucoup
- ○ Extrêmement

Quel aspect a été le plus ludique, amusant ? *

Pensez-vous que la collecte de données au sein de Collect'O était accessible et compréhensible pour tous les participants ? *

- ○ Pas du tout
- ○ Un peu
- ○ Modérément
- ○ Beaucoup
- ○ Extrêmement

Si ce n'est pas le cas, pourquoi ?

Avant de rejoindre Collect'O, dans quelle mesure vous considériez-vous informé·e sur l'impact de l'urbanisation sur le climat urbain ? *

- ○ Pas du tout informé·e
- ○ Peu informé·e
- ○ Modérément informé·e
- ○ Bien informé·e
- ○ Très bien informé·e

Dans quelle mesure pensez-vous que votre participation à Collect'O a contribué à améliorer votre compréhension de ces impacts ? *

- ○ Pas du tout
- ○ Un peu
- ○ Modérément
- ○ Beaucoup
- ○ Extrêmement

Pensez-vous que nos communications avec vous sur l'avancement du projet étaient suffisamment fréquentes ? *

- ○ Oui
- ○ Non

Précisez *

Pensez-vous que nos communications étaient suffisamment vulgarisées ? *

- ○ Pas du tout
- ○ Un peu
- ○ Modérément
- ○ Beaucoup
- ○ Extrêmement

Expliquez *

Souhaitez-vous ajouter un commentaire à propos de nos communications ?

Le projet Collect'O s'achève. Aimeriez-vous que nous gardions votre contact pour de futurs projets semblables, en hydrologie et/ou environnement ? *

- ○ Oui
- ○ Non

Avez-vous pris des initiatives pour partager les résultats ou les informations de Collect'O avec d'autres membres de votre communauté ? *

- ○ Oui
- ○ Non

Si oui, comment avez-vous partagé ces informations ? (cochez toutes les réponses pertinentes)

- ☐ Discussions informelles
- ☐ Réseaux sociaux
- ☐ Présentations communautaires
- ☐ Ateliers
- ☐ Autre

Si vous avez répondu "Autre", précisez ici si vous le souhaitez

Dans quelle mesure pensez-vous que votre participation à Collect'O a contribué à sensibiliser votre communauté aux enjeux de l'urbanisation sur les précipitations en ville ? *

- ○ Pas du tout
- ○ Un peu
- ○ Modérément
- ○ Beaucoup
- ○ Extrêmement

Avez-vous remarqué des changements de comportement ou des actions concrètes de la part de votre entourage suite à la sensibilisation de Collect'O ? *

- ○ Oui
- ○ Non

Expliquez *

Avez-vous des suggestions pour améliorer la sensibilisation de la communauté via Collect'O ?

Envoyer

RÉFÉRENCES

Aggarwal, P. K., Romatschke, U., Araguas-Araguas, L., Belachew, D., Longstaffe, F. J., Berg, P., Schumacher, C. et Funk, A. (2016). Proportions of convective and stratiform precipitation revealed in water isotope ratios. *Nature Geoscience*, *9*(8), 624-629. https://doi.org/10.1038/ngeo2739

Ahrens, C. D. et Henson, R. (2019). *Meteorology today: an introduction to weather, climate, and the environment* (Twelfth edition). Cengage.

Angert, A., Cappa, C. D. et DePaolo, D. J. (2004). Kinetic 17O effects in the hydrologic cycle: Indirect evidence and implications. *Geochimica et Cosmochimica Acta*, *68*(17), 3487-3495. https://doi.org/10.1016/j.gca.2004.02.010

Arnfield, A. J. (2003). Two decades of urban climate research: a review of turbulence, exchanges of energy and water, and the urban heat island. *International Journal of Climatology*, *23*(1), 1-26. https://doi.org/10.1002/joc.859

Berenguer, M., Corral, C., Sánchez-Diezma, R. et Sempere-Torres, D. (2005). Hydrological Validation of a Radar-Based Nowcasting Technique. *Journal of Hydrometeorology*, *6*(4), 532-549. https://doi.org/10.1175/JHM433.1

Bergeron, O. (2016). Grilles climatiques quotidiennes du Programme de surveillance du climat du Québec, version 1.2. *Québec, ministère du Développement durable, de l'Environnement et de la Lutte contre les changements climatiques, Direction du suivi de l'état de l'environnement*, 33.

Bush et Lemmen. (2019). *Canada's changing climate report* (Government of Canada, Ottawa, ON). http://publications.gc.ca/collections/collection_2019/eccc/En4-368-2019-eng.pdf

Camin, F., Besic, D., Brewer, P. J., Allison, C. E., Coplen, T. B., Dunn, P. J. H., Gehre, M., Gröning, M., Meijer, H. A. J., Hélie, J., Iacumin, P., Kraft, R., Krajnc, B., Kümmel, S., Lee, S., Meija, J., Mester, Z., Mohn, J., Moossen, H., … Wielgosz, R. I. (2025). Stable Isotope Reference Materials and Scale Definitions—Outcomes of the 2024 IAEA Experts Meeting. *Rapid Communications in Mass Spectrometry*, *39*(14). https://doi.org/10.1002/rcm.10018

Carton, C., Barbecot, F., Birks, J. et Hélie, J.-F. (2024a). Improved understanding of the impact of urbanization on the temperature, precipitation, and air quality of major eastern Canadian cities. *Urban Climate*, *53*, 101781. https://doi.org/10.1016/j.uclim.2023.101781

Carton, C., Barbecot, F., Hélie, J., Horoi, V. et Birks, J. (2025). Adapting Automatic Water Samplers for the Isotopic Study of Rainfall at High Temporal Resolution. *Rapid Communications in Mass Spectrometry*, *39*(11), e10017. https://doi.org/10.1002/rcm.10017

Carton, C., Barbecot, F., Hélie, J., Horoi, V., Birks, J., Picard, A. et Mona, J. (2024b). Affordable event and monthly rain samplers: Improving isotopic datasets to understand meteorological processes. *Rapid Communications in Mass Spectrometry*, *38*(7), e9710. https://doi.org/10.1002/rcm.9710

Cavayas, F. et Baudouin, Y. (2008). Étude des biotopes urbains et périurbains de la CMM, Volets 1 et 2 : Évolution des occupations du sol, du couvert végétal et des îlots de chaleur sur le territoire de la

Communauté métropolitaine de Montréal (1984-2005). *Rapport destiné au Conseil Régional de l'Environnement de Laval*, 120.

Chartrand, J. et Pausata, F. S. R. (2020). Impacts of the North Atlantic Oscillation on winter precipitations and storm track variability in southeast Canada and the northeast United States. *Weather and Climate Dynamics*, *1*(2), 731-744. https://doi.org/10.5194/wcd-1-731-2020

Chen, L., Ng, E., An, X., Ren, C., Lee, M., Wang, U. et He, Z. (2012). Sky view factor analysis of street canyons and its implications for daytime intra-urban air temperature differentials in high-rise, high-density urban areas of Hong Kong: a GIS-based simulation approach: GIS-BASED SVF ANALYSIS AND APPLICATION IN HONG KONG. *International Journal of Climatology*, *32*(1), 121-136. https://doi.org/10.1002/joc.2243

Christen, A. et Vogt, R. (2004). Energy and radiation balance of a central European city. *International Journal of Climatology*, *24*(11), 1395-1421. https://doi.org/https://doi.org/10.1002/joc.1074

Clark, I. D. et Fritz, P. (1997). *Environmental isotopes in hydrogeology*. CRC Press/Lewis Publishers.

Climate Central. (2021, 14 juillet). *Hot zones: Urban Heat Islands*. https://assets.ctfassets.net/cxgxgstp8r5d/1XZZjkLYwtcmKL5k3wEinl/5f8c9b5b2d8dd56e1bda7f51278fc3d2/2021_UHI_Report.pdf

Cortecci, G., Dinelli, E. et Mussi, M. (2008). Isotopic composition and secondary evaporation effects on precipitation from the urban centre of Bologna, Italy. *Periodico di Mineralogia*, (77.1), 53-61. https://doi.org/10.2451/2008PM0004

Craig, H., Gordon, L. I. et Horibe, Y. (1963). Isotopic exchange effects in the evaporation of water: 1. Low-temperature experimental results. *Journal of Geophysical Research (1896-1977)*, *68*(17), 5079-5087. https://doi.org/10.1029/JZ068i017p05079

Dansgaard, W. (1964). Stable isotopes in precipitation. *Tellus*, *16*(4), 436-468. https://doi.org/10.1111/j.2153-3490.1964.tb00181.x

Dixon, P. G. et Mote, T. L. (2003). Patterns and Causes of Atlanta's Urban Heat Island–Initiated Precipitation. *JOURNAL OF APPLIED METEOROLOGY*, *42*, 12.

Gaur, A., Lacasse, M., Armstrong, M., Lu, H., Shu, C., Fields, A., Palou, F. S. et Zhang, Y. (2021). Effects of using different urban parametrization schemes and land-cover datasets on the accuracy of WRF model over the City of Ottawa. *Urban Climate*, *35*, 100737. https://doi.org/10.1016/j.uclim.2020.100737

Gorski, G., Strong, C., Good, S. P., Bares, R., Ehleringer, J. R. et Bowen, G. J. (2015). Vapor hydrogen and oxygen isotopes reflect water of combustion in the urban atmosphere. *Proceedings of the National Academy of Sciences*, *112*(11), 3247-3252. https://doi.org/10.1073/pnas.1424728112

Gröning, M., Lutz, H. O., Roller-Lutz, Z., Kralik, M., Gourcy, L. et Pöltenstein, L. (2012). A simple rain collector preventing water re-evaporation dedicated for δ18O and δ2H analysis of cumulative precipitation samples. *Journal of Hydrology*, *448-449*, 195-200. https://doi.org/10.1016/j.jhydrol.2012.04.041

Hardin, A. W., Liu, Y., Cao, G. et Vanos, J. K. (2018). Urban heat island intensity and spatial variability by synoptic weather type in the northeast U.S. *Urban Climate*, *24*, 747-762. https://doi.org/10.1016/j.uclim.2017.09.001

Hass, W. A., Hoecker, W. H., Pack, D. H. et Angell, J. K. (1967). Analysis of low-level, constant volume balloon (tetroon) flights over New York City. *Quarterly Journal of the Royal Meteorological Society*, *93*(398), 483-493. https://doi.org/https://doi.org/10.1002/qj.49709339807

Health Canada. (2021). *Health impacts of air pollution in Canada : estimates of premature deaths and nonfatal outcomes - 2021 report*. https://epe.lac-bac.gc.ca/100/201/301/weekly_acquisitions_list-ef/2021/21-21/publications.gc.ca/collections/collection_2021/sc-hc/H144-51-2021-eng.pdf

Heaviside, C., Macintyre, H. et Vardoulakis, S. (2017). The Urban Heat Island: Implications for Health in a Changing Environment. *Current Environmental Health Reports*, *4*(3), 296-305. https://doi.org/10.1007/s40572-017-0150-3

Holz, M., Heil, S. R. et Sacco, A. (2000). Temperature-dependent self-diffusion coefficients of water and six selected molecular liquids for calibration in accurate 1H NMR PFG measurements. *Physical Chemistry Chemical Physics*, *2*(20), 4740-4742. https://doi.org/10.1039/b005319h

Hurrell, J. W. (2003). CLIMATE VARIABILITY | North Atlantic and Arctic Oscillation. Dans *Encyclopedia of Atmospheric Sciences* (p. 439-445). Elsevier. https://doi.org/10.1016/B0-12-227090-8/00109-3

Kamsali, N., Prasad, B. S. N. et Datt, J. (2011). The Electrical Conductivity as an Index of Air Pollution in the Atmosphere. Dans F. Nejadkoorki (dir.), *Advanced Air Pollution*. InTech. https://doi.org/10.5772/17163

Kaseke, K. F., Wang, L., Wanke, H., Tian, C., Lanning, M. et Jiao, W. (2018). Precipitation Origins and Key Drivers of Precipitation Isotope (^{18}O, ^{2}H, and ^{17}O) Compositions Over Windhoek. *Journal of Geophysical Research: Atmospheres*, *123*(14), 7311-7330. https://doi.org/10.1029/2018JD028470

Kirchmeier-Young, M. C. et Zhang, X. (2020). Human influence has intensified extreme precipitation in North America. *Proceedings of the National Academy of Sciences*, *117*(24), 13308-13313. https://doi.org/10.1073/pnas.1921628117

Kottek, M., Grieser, J., Beck, C., Rudolf, B. et Rubel, F. (2006). World Map of the Köppen-Geiger climate classification updated. *Meteorologische Zeitschrift*, *15*(3), 259-263. https://doi.org/10.1127/0941-2948/2006/0130

Kuhlemann, L.-M., Tetzlaff, D. et Soulsby, C. (2020). Urban water systems under climate stress: An isotopic perspective from Berlin, Germany. *Hydrological Processes*, *34*(18), 3758-3776. https://doi.org/10.1002/hyp.13850

Lachapelle, M., Thompson, H. D., Leroux, N. R. et Thériault, J. M. (2024). Measuring Ice Pellets and Refrozen Wet Snow Using a Laser-Optical Disdrometer. *Journal of Applied Meteorology and Climatology*, *63*(1), 65-84. https://doi.org/10.1175/JAMC-D-22-0202.1

Lauer, A., Pausata, F. S. R., Leroyer, S. et Argueso, D. (2023). Effect of urban heat island mitigation strategies on precipitation and temperature in Montreal, Canada: Case studies. *PLOS Climate*, *2*(6), e0000196. https://doi.org/10.1371/journal.pclm.0000196

Leibundgut, C., Maloszewski, P. et Külls, C. (2009a). *Tracers in hydrology*. Wiley-Blackwell.

Leibundgut, Christian., Maloszewski, Piotr. et Külls, Christoph. (2009b). *Tracers in hydrology*. Wiley-Blackwell. [1 online resource (xiv, 415 pages, 8 unnumbered pages of plates) : color illustrations, maps]. https://doi.org/10.1002/9780470747148

Leroyer, S., Bélair, S., Souvanlasy, V., Vallée, M., Pellerin, S. et Sills, D. (2022). Summertime Assessment of an Urban-Scale Numerical Weather Prediction System for Toronto. *Atmosphere*, *13*(7), 1030. https://doi.org/10.3390/atmos13071030

Liu, J. et Niyogi, D. (2019). Meta-analysis of urbanization impact on rainfall modification. *Scientific Reports*, *9*(1), 7301. https://doi.org/10.1038/s41598-019-42494-2

Lorenz, J. M., Kronenberg, R., Bernhofer, C. et Niyogi, D. (2019). Urban Rainfall Modification: Observational Climatology Over Berlin, Germany. *Journal of Geophysical Research: Atmospheres*, *124*(2), 731-746. https://doi.org/https://doi.org/10.1029/2018JD028858

Lutgens, F. K., Tarbuck, E. J., Herman, R. L. 1972- et Tasa, D. (2019). *The atmosphere : an introduction to meteorology* (Fourteenth edition.). Pearson ;

Maier, R., Krebs, G., Pichler, M., Muschalla, D. et Gruber, G. (2020). Spatial Rainfall Variability in Urban Environments—High-Density Precipitation Measurements on a City-Scale. *Water*, *12*(4), 1157. https://doi.org/10.3390/w12041157

Majoube, Michel. (1971). Fractionnement en oxygène 18 et en deutérium entre l'eau et sa vapeur. *J. Chim. Phys.*, *68*, 1423-1436. https://doi.org/10.1051/jcp/1971681423

Matrosov, S. Y., Kingsmill, D. E., Martner, B. E. et Ralph, F. M. (2005). The Utility of X-Band Polarimetric Radar for Quantitative Estimates of Rainfall Parameters. *Journal of Hydrometeorology*, *6*(3), 248-262. https://doi.org/10.1175/JHM424.1

McDonald, R. I., Weber, K., Padowski, J., Flörke, M., Schneider, C., Green, P. A., Gleeson, T., Eckman, S., Lehner, B., Balk, D., Boucher, T., Grill, G. et Montgomery, M. (2014). Water on an urban planet: Urbanization and the reach of urban water infrastructure. *Global Environmental Change*, *27*, 96-105. https://doi.org/10.1016/j.gloenvcha.2014.04.022

McLeod, J., Shepherd, M. et Konrad, C. E. (2017). Spatio-temporal rainfall patterns around Atlanta, Georgia and possible relationships to urban land cover. *Urban Climate*, *21*, 27-42. https://doi.org/10.1016/j.uclim.2017.03.004

MELCCFP, M. de l'Environnement et de la L. contre les changements climatiques, de la Faune et des Parcs. (2022). *Données du Réseau de surveillance du climat du Québec*.

MELCCFP, M. de l'Environnement, de la Lutte contre les changements climatiques, de la Faune et des Parcs. (2023). *Banque de données sur la qualité de l'air ambiant*.

Merlivat, L. et Jouzel, J. (1979). Global climatic interpretation of the deuterium-oxygen 18 relationship for precipitation. *Journal of Geophysical Research*, *84*(C8), 5029. https://doi.org/10.1029/JC084iC08p05029

Michelsen, N., Laube, G., Friesen, J., Weise, S. M., Bait Said, A. B. A. et Müller, T. (2019). Technical note: A microcontroller-based automatic rain sampler for stable isotope studies. *Hydrology and Earth System Sciences*, *23*(6), 2637-2645. https://doi.org/10.5194/hess-23-2637-2019

Middel, A., Häb, K., Brazel, A. J., Martin, C. A. et Guhathakurta, S. (2014). Impact of urban form and design on mid-afternoon microclimate in Phoenix Local Climate Zones. *Landscape and Urban Planning*, *122*, 16-28. https://doi.org/10.1016/j.landurbplan.2013.11.004

Milrad, S. M., Atallah, E. H. et Gyakum, J. R. (2013). Precipitation Modulation by the Saint Lawrence River Valley in Association with Transitioning Tropical Cyclones*. *Weather and Forecasting*, *28*(2), 331-352. https://doi.org/10.1175/WAF-D-12-00071.1

Niyogi, D., Lei, M., Kishtawal, C., Schmid, P. et Shepherd, M. (2017). Urbanization Impacts on the Summer Heavy Rainfall Climatology over the Eastern United States. *Earth Interactions*, *21*(5), 1-17. https://doi.org/10.1175/EI-D-15-0045.1

Niyogi, D., Pyle, P., Lei, M., Arya, S. P., Kishtawal, C. M., Shepherd, M., Chen, F. et Wolfe, B. (2011). Urban Modification of Thunderstorms: An Observational Storm Climatology and Model Case Study for the Indianapolis Urban Region. *Journal of Applied Meteorology and Climatology*, *50*(5), 1129-1144. https://doi.org/10.1175/2010JAMC1836.1

Nogueira, M., Hurduc, A., Ermida, S., Lima, D. C. A., Soares, P. M. M., Johannsen, F. et Dutra, E. (2022, 28 janvier). *Assessment of the Paris urban heat island in ERA5 and offline SURFEX-TEB (v8.1) simulations using METEOSAT land surface temperature product* [preprint]. Climate and Earth system modeling. https://doi.org/10.5194/gmd-2021-431

Oke, T. R. (1982). The energetic basis of the urban heat island. *Quarterly Journal of the Royal Meteorological Society*, *108*(455), 1-24. https://doi.org/10.1002/qj.49710845502

Oke, T. R., Mills, G., Christen, A. et Voogt, J. A. (2017). *Urban Climates*. Cambridge University Press. https://doi.org/10.1017/9781139016476

Prechsl, U. E., Gilgen, A. K., Kahmen, A. et Buchmann, N. (2014). Reliability and quality of water isotope data collected with a low-budget rain collector. *Rapid Communications in Mass Spectrometry*, *28*, 879-885. https://doi.org/10.1002/rcm.6852

Rey, N., Rosa, E., Cloutier, V. et Lefebvre, R. (2018). Using water stable isotopes for tracing surface and groundwater flow systems in the Barlow-Ojibway Clay Belt, Quebec, Canada. *Canadian Water Resources Journal / Revue canadienne des ressources hydriques*, *43*(2), 173-194. https://doi.org/10.1080/07011784.2017.1403960

Roberge, F. et Sushama, L. (2018). Urban heat island in current and future climates for the island of Montreal. *Sustainable Cities and Society*, *40*, 501-512. https://doi.org/10.1016/j.scs.2018.04.033

Rosenfeld, D., Dai, J., Yu, X., Yao, Z., Xu, X., Yang, X. et Du, C. (2007). Inverse Relations Between Amounts of Air Pollution and Orographic Precipitation. *Science*, *315*(5817), 1396-1398. https://doi.org/10.1126/science.1137949

Rosenfeld, D., Lohmann, U., Raga, G. B., O'Dowd, C. D., Kulmala, M., Fuzzi, S., Reissell, A. et Andreae, M. O. (2008). Flood or Drought: How Do Aerosols Affect Precipitation? *Science*, *321*(5894), 1309-1313. https://doi.org/10.1126/science.1160606

Schatz, J. et Kucharik, C. J. (2014). Seasonality of the Urban Heat Island Effect in Madison, Wisconsin. *Journal of Applied Meteorology and Climatology*, *53*(10), 2371-2386. https://doi.org/10.1175/JAMC-D-14-0107.1

Seneviratne, S. I., Nicholls, N., Easterling, D., Goodess, C. M., Kanae, S., Kossin, J., Luo, Y., Marengo, J., McInnes, K., Rahimi, M., Reichstein, M., Sorteberg, A., Vera, C., Zhang, X., Rusticucci, M., Semenov, V., Alexander, L. V., Allen, S., Benito, G., … Zwiers, F. W. (2012). Changes in Climate Extremes and their Impacts on the Natural Physical Environment. Dans C. B. Field, V. Barros, T. F. Stocker et Q. Dahe (dir.), *Managing the Risks of Extreme Events and Disasters to Advance Climate Change Adaptation* (p. 109-230). Cambridge University Press. https://doi.org/10.1017/CBO9781139177245.006

Shu, C., Gaur, A., Wang, L. et Lacasse, M. A. (2023). Evolution of the local climate in Montreal and Ottawa before, during and after a heatwave and the effects on urban heat islands. *Science of The Total Environment*, *890*, 164497. https://doi.org/10.1016/j.scitotenv.2023.164497

Shu, C., Gaur, A., Wang, L. (Leon), Bartko, M., Laouadi, A., Ji, L. et Lacasse, M. (2022). Added value of convection permitting climate modelling in urban overheating assessments. *Building and Environment*, *207*, 108415. https://doi.org/10.1016/j.buildenv.2021.108415

Sinclair, K. E. et Marshall, S. J. (2009). Temperature and vapour-trajectory controls on the stable-isotope signal in Canadian Rocky Mountain snowpacks. *Journal of Glaciology*, *55*(191), 485-498. https://doi.org/10.3189/002214309788816687

Singh, J., Karmakar, S., PaiMazumder, D., Ghosh, S. et Niyogi, D. (2020). Urbanization alters rainfall extremes over the contiguous United States. *Environmental Research Letters*, *15*(7), 074033. https://doi.org/10.1088/1748-9326/ab8980

Starke, P., Göbel, P. et Coldewey, W. G. (2010). Urban evaporation rates for water-permeable pavements. *Water Science and Technology*, *62*(5), 1161-1169. https://doi.org/10.2166/wst.2010.390

Stein, A. F., Draxler, R. R., Rolph, G. D., Stunder, B. J. B., Cohen, M. D. et Ngan, F. (2015). NOAA's HYSPLIT Atmospheric Transport and Dispersion Modeling System. *Bulletin of the American Meteorological Society*, *96*(12), 2059-2077. https://doi.org/10.1175/BAMS-D-14-00110.1

Tabari, H. (2020). Climate change impact on flood and extreme precipitation increases with water availability. *Scientific Reports*, *10*(1), 13768. https://doi.org/10.1038/s41598-020-70816-2

Tabeaud, M. (2010). Climats urbains: Savoirs experts et pratiques sociales. *Ethnologie française*, *40*(4), 685. https://doi.org/10.3917/ethn.104.0685

Tang, Y., Li, H., Liao, A., Yang, L., Rinne-Garmston, K. T., Yao, D., Wang, W. et Song, X. (2023). What causes site-specific intra-event variations of stable isotopes in precipitation in Beijing? *Atmospheric Research*, *296*, 107052. https://doi.org/10.1016/j.atmosres.2023.107052

Tian, C., Wang, L., Kaseke, K. F. et Bird, B. W. (2018). Stable isotope compositions (δ2H, δ18O and δ17O) of rainfall and snowfall in the central United States. *Scientific Reports*, *8*(1), 6712. https://doi.org/10.1038/s41598-018-25102-7

Tiwari, A. et Rachlin, J. W. (2018). A Review of Road Salt Ecological Impacts. *Northeastern Naturalist*, *25*(1), 123-142. https://doi.org/10.1656/045.025.0110

Touchaei, A. G. et Wang, Y. (2015). Characterizing urban heat island in Montreal (Canada)—Effect of urban morphology. *Sustainable Cities and Society*, *19*, 395-402. https://doi.org/10.1016/j.scs.2015.03.005

Uchiyama, R., Okochi, H., Ogata, H., Katsumi, N., Asai, D. et Nakano, T. (2017). Geochemical and stable isotope characteristics of urban heavy rain in the downtown of Tokyo, Japan. *Atmospheric Research*, *194*, 109-118. https://doi.org/10.1016/j.atmosres.2017.04.029

United Nations, Department of Economic and Social Affairs, Population Division. (2019). *World urbanization prospects: the 2018 revision*. United Nations.

Villarini, G., Seo, B.-C., Serinaldi, F. et Krajewski, W. F. (2014). Spatial and temporal modeling of radar rainfall uncertainties. *Atmospheric Research*, *135-136*, 91-101. https://doi.org/10.1016/j.atmosres.2013.09.007

von Freyberg, J., Knapp, J. L. A., Rücker, A., Studer, B. et Kirchner, J. W. (2020). Technical note: Evaluation of a low-cost evaporation protection method for portable water samplers. *Hydrology and Earth System Sciences*, *24*(12), 5821-5834. https://doi.org/10.5194/hess-24-5821-2020

Walker, D. W., Smigaj, M. et Tani, M. (2021). The benefits and negative impacts of citizen science applications to water as experienced by participants and communities. *WIREs Water*, *8*(1), e1488. https://doi.org/10.1002/wat2.1488

Xi, X. (2014). A Review of Water Isotopes in Atmospheric General Circulation Models: Recent Advances and Future Prospects. *International Journal of Atmospheric Sciences*, *2014*, 1-16. https://doi.org/10.1155/2014/250920

Xing, M., Liu, W., Li, X., Zhou, W., Wang, Q., Tian, J., Li, X., Tie, X., Li, G., Cao, J., Bao, H. et An, Z. (2020). Vapor isotopic evidence for the worsening of winter air quality by anthropogenic combustion-derived water. *Proceedings of the National Academy of Sciences*, *117*(52), 33005-33010. https://doi.org/10.1073/pnas.1922840117

Yoo, J.-M., Lee, Y.-R., Kim, D., Jeong, M.-J., Stockwell, W. R., Kundu, P. K., Oh, S.-M., Shin, D.-B. et Lee, S.-J. (2014). New indices for wet scavenging of air pollutants (O3, CO, NO2, SO2, and PM10) by summertime rain. *Atmospheric Environment*, *82*, 226-237. https://doi.org/10.1016/j.atmosenv.2013.10.022

Yousif, E. et Hasan, A. (2015). Photostabilization of poly(vinyl chloride) – Still on the run. *Journal of Taibah University for Science*, *9*(4), 421-448. https://doi.org/10.1016/j.jtusci.2014.09.007

Zhao, P., Xia, C., Liu, G., Tang, J. et Zhou, M. (2023). Comparison of recycled vapor contribution to precipitation in urban vs. rural area—A case study in western China. *Frontiers in Ecology and Evolution*, *10*, 1012071. https://doi.org/10.3389/fevo.2022.1012071

Zhu, Y., Han, G., Zeng, J. et Wang, D. (2024). Determining hydrogen and oxygen isotopes to reflect the responses of rainfall process on urban activities: Insight from the extreme rainfall period in megacity. *Urban Climate*, *55*, 101994. https://doi.org/10.1016/j.uclim.2024.101994